The Agulhas Leakage: Role of Mesoscale Processes and Impact on the Atlantic Meridional Overturning Circulation

Arne Biastoch

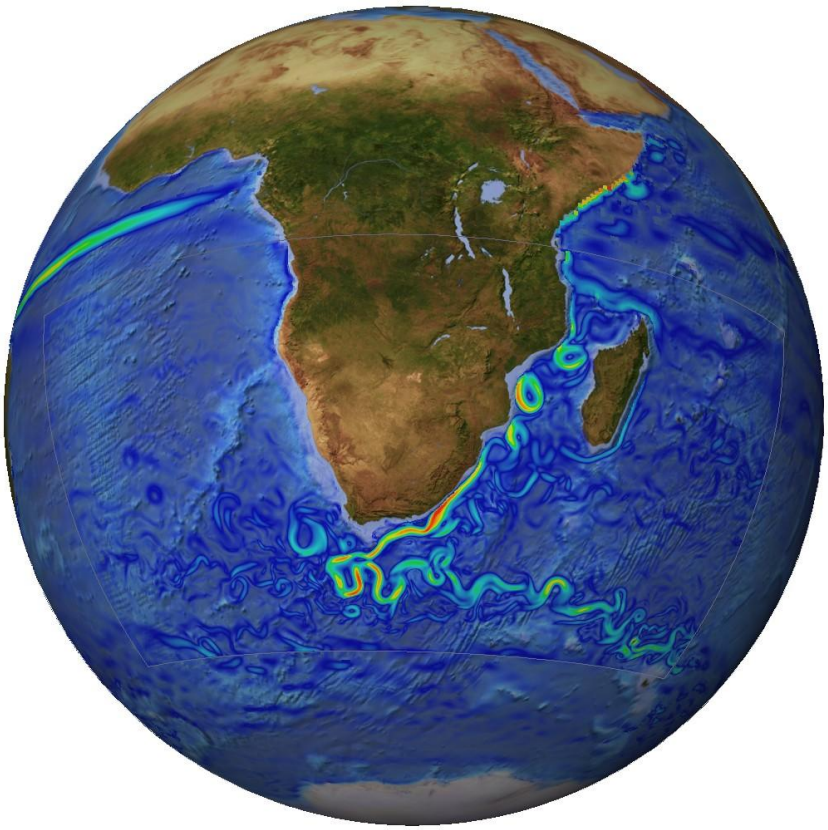

Habilitationsschrift

vorgelegt bei der Mathematisch-Naturwissenschaftlichen Fakultät der

Christian-Albrechts-Universität zu Kiel

Juni 2008

The figure on the title page shows a snapshot (5-day average, centered at 12-Oct-2001) of speed at 100 m depth in the high-resolution model, nested in the global coarse-resolution model. A moving version can be found at `http://biastoch.de/AG01/AG01_1995_2004.mpg`.

Contents

Abstract

The Agulhas region around South Africa is a key region of global climate and climate change. Under present climate conditions the Agulhas leakage from the Indian to the Atlantic Ocean feeds the bulk of the upper limb of the meridional overturning circulation (MOC) in the Atlantic Ocean, highly affected by the nonlinear constituents of the Agulhas Current system.

To examine the role of the mesoscale processes in the mean flow in the Agulhas system, particularly in regard to the Agulhas leakage and its effect on the Atlantic MOC, an innovative ocean modeling program has been set up that utilizes new global model components and methodologies developed in international cooperation (DRAKKAR) based on a framework of the European model system NEMO. The model configuration involves a high-resolution grid of the greater Agulhas region nested into a coarse-resolution global ocean – sea-ice model forced by atmospheric conditions of the period 1958 – 2004. Due to an effective "two-way" nesting approach this system for the first time allows to unravel, how the explicitly simulated mesoscale variability in the Agulhas dynamics feeds back to the global ocean.

There is vast range of mesoscale – mean flow interactions in the Agulhas region. In the South East Madagascar Current offshore eddies do lead to different modes of the current extension, one favoring cyclonic flow into the Mozambique Channel, the other anticyclonic eddies drifting towards southwest. Eddies generated in the central Mozambique Channel introduce strong perturbations into the western boundary current systems off the African coast by triggering Natal Pulses, causing offshore displacements of the Agulhas Current which then lead to strong changes in the volume transport of the Agulhas Current and eventually to upstream retroflections of the current back into the Indian Ocean. The barotropic nature of the interplay with Mozambique eddies and Natal Pulses also affects the Agulhas Undercurrent leading to strong fluctuations similar to observed ones, raising the question what portion of the Agulhas Undercurrent is a coherent flow throughout the South Indian Ocean and what portion is virtually generated by passing Natal Pulses.

The sequence of model experiments demonstrates that upstream perturbations have a vital effect on the mesoscale dynamics in the Agulhas retroflection area. A comparison of the reference model with a sensitivity experiment not including the Mozambique eddies shows that they are not only triggering the shedding of Agulhas rings but also lead to more realistic eddy structures in the Cape Basin and beyond. However, the presence of these upstream perturbations does not alter the mean Agulhas leakage, i.e, the net volume transport from the Indian to the Atlantic Ocean.

The magnitude of the Agulhas leakage is quantitatively strongly dependent on the representation of Agulhas rings and other associated mesoscale processes in the retroflection area; there is a strong difference in the interoceanic transport between the high-resolution, nested model and the coarser, non-eddying model, the latter leading to higher, unrealistic transport values. While in the time-mean the bulk of this difference is modifying the horizontal circulation of the subtropical super-gyre rather than the Atlantic MOC, the mesoscale dynamics of the Agulhas regime appear as an important source of decadal variability in the MOC: An isolation of the effect of the mesoscale demonstrated that the Agulhas leakage acts as the source of low-frequency undulations in thermocline depth, a signal carried across the South Atlantic by Rossby waves and into the North Atlantic by wave processes along the American continental slope. The resulting signal in MOC transport gradually diminishes from south to north, but has an amplitude in the tropical Atlantic of comparable magnitude to the effect of subarctic deep water formation processes discussed in previous studies. It is evident that a proper representation of the mesoscale processes it vital for the correct interpretation of variations of the upper ocean transport across the equator, and even at subtropical latitudes in the North Atlantic where current monitoring efforts aim at a quantification of inter-annual MOC variations.

Zusammenfassung

Die Agulhasregion vor Südafrika ist eine Schlüsselregion für das globale Klima. Unter gegenwärtigen Klimabedingungen stellt der Einstrom vom Indischen in den Atlantischen Ozean den Hauptanteil des oberen Astes der meridionalen Umwälzbewegung (MOC) im Atlantik dar. Er wird dabei stark durch die nichtlinearen Bestandteile des Agulhasstromsystems beeinflusst.

Zur Untersuchung der Rolle mesoskaliger Prozesse auf die mittlere Strömung im Agulhassystem, speziell bezogen auf deren Rolle im interozeanischen Transport und dessen Auswirkung auf die Atlantische MOC, wurde ein innovatives Modell aufgesetzt. Dieses ist eingebettet in ein neues globales Modellkonzept, das in internationaler Kooperation (DRAKKAR) auf Basis des europäischen Modellsystem NEMO entwickelt wurde. Die Modellkonfiguration beinhaltet ein hochauflösendes Gitter in der Agulhasregion, genestet in ein grobauflösendes globales Ozean – Meereismodell, das für die Jahre 1958 – 2004 durch vorgegebene Atmosphärenbedingungen angetrieben wird. Ein effektiver „Zwei-Wege“ Nestingansatz ermöglicht damit zum ersten Mal die Untersuchung der Rückkopplung der explizit modellierten mesoskaligen Variabilität auf den globalen Ozean.

Die Agulhasregion ist geprägt von vielzähligen Interaktionen zwischen der Mesoskala und der mittleren Strömung. Im Südostmadagaskarstrom führen seewärtige Wirbel zu verschiedenen Moden, wovon einer den zyklonalen Einstrom in den Mozambiquekanal favorisiert, der andere zu antizyklonalen, nach Südwesten driftenden Wirbeln führt. In Verbindung mit der Auslösung von Natalpulsen prägen im zentralen Mozambiquekanal erzeugte Wirbel dem westlichen Randstromsystem vor der afrikanischen Küste starke Störungen auf. Diese seewärtigen Verlagerungen des Agulhasstroms führen zu starken Transportschwankungen und führen teilweise zu frühen, stromaufwärtigeren Retroflexionen des Agulhasstroms zurück in den Indischen Ozean. Die barotrope Struktur dieses Zusammenspiels von Mozambiquewirbeln und Natalpulsen beeinflusst auch den Agulhasunterstrom, der im Modell die beobachteten starken Fluktuationen reproduziert. Sein Verhalten wirft die Frage auf, welcher Anteil des Agulhasunterstroms ein kohärenter Strom im südlichen Indischen Ozean ist und welcher virtuell durch passierende Natalpulse erzeugt wird.

Die Sequenz von Modellexperimenten zeigt, dass die Störungen in den Quellregionen des Agulhasstroms eine zentrale Rolle für die mesoskalige Dynamik in der Retroflexionsregion südlich von Afrika spielen. Ein Vergleich des Referenzmodells mit einem Sensitivitätsexperiment ohne Mozambiquewirbel verdeutlicht, dass diese nicht nur einen auslösenden Effekt auf die Bildung von Agulhasringen haben, sondern auch zu realistischeren Wirbelstrukturen im Kapbecken und darüber hinaus haben. Im Gegensatz dazu verändert die Existenz der Störungen aber nicht den mittleren interozeanischen Transport vom Indischen in den Atlantischen Ozean.

Der genaue Betrag des interozeanischen Transportes ist stark abhängig von der Repräsentierung der Agulhasringe und anderer mesoskaliger Strukturen in der Retroflexionsregion. Es gibt dabei einen großen Unterschied zwischen dem hochauflösenden, genesteten und dem grobaufgelösten Modell, wobei das letztere höhere, unrealistische Transporte aufweist. Im langzeitlichen Mittel führt dieser Unterschied im interozeanischen Transport allerdings nicht zu einer Veränderung der MOC, sondern zu Verlagerungen der Horizontalzirkulation im subtropischen „Supergyre“. Erst im zeitlichen Verlauf zeigt sich die mesoskalige Variabilität im Agulhasregime als Quelle dekadischer Variabilität in der MOC: Eine Isolation dieses Effektes verdeutlicht, dass der Einstrom aus der Agulhasregion zu niederfrequenten Schwankungen in der Thermoklinenstruktur führt – ein Signal, dass durch Rossbywellen über den Südatlantik und mit Hilfe von Wellenprozessen entlang des amerikanischen Kontinentalanhangs bis in den Nordatlantik transportiert wird. Das resultierende Signal in der MOC wird nach Norden zwar langsam schwächer, hat aber im tropischen Atlantik eine Größenordnung, die mit dem Effekt von Tiefenwasserbildungsprozessen aus dem subpolaren Nordatlantik gleichzusetzen ist. Es ist offenkundig, dass eine angemessene Repräsentierung der mesoskaligen Prozesse entscheidend ist für die korrekte

Interpretation der Transportvariationen oberer Wassermassen über den Äquator. Dieses gilt sogar für die Subtropen im Nordatlantik, wo gegenwärtige Beobachtungssysteme zur Quantifizierung der MOC auf interannualen Zeitskalen etabliert wurden.

1. Introduction

The flow of warm and salty waters from the Indian Ocean to the Atlantic Ocean around the southern tip of Africa is an important element of the global ocean circulation (Fig. 1.1) [*Gordon*, 2003]. Under present climate conditions this interoceanic flux provides the bulk [*Speich et al.*, 2001, *Friocourt et al.*, 2005] of the upper limb of the meridional overturning circulation (MOC) in the Atlantic Ocean, highly affected by the nonlinear constituents of the Agulhas Current system [*Lutjeharms*, 2006].

Paleo observations and model studies have linked variations in the MOC to changes in the Agulhas leakage [*Martnez-Méndez et al.*, 2007, *Knorr and Lohmann*, 2003]. Similar arguments have been advanced for future climate trends, so that the Agulhas region is acknowledged to play a key role in global climate and climate change [*Stocker et al.*, 2001]. Factors causing changes in the Agulhas leakage are still under investigation. Variations in the wind fields, such as latitudinal shifts of the southern hemisphere mid-westerlies [*Cai*, 2006], would directly impact on the retroflection of the Agulhas Current and in consequence the interoceanic transport of heat and salt. Especially the supply of salt has repercussions for the large-scale global ocean circulation by its influence on the deep water formation in the subpolar North Atlantic (and therefore the lower limb of the MOC) via advective processes [*Weijer et al.*, 1999]; in consequence this feeds also back to climate [*Marsh et al.*, 2007].

What factors determine the intensity of the Agulhas leakage? How will it react on changes in the atmospheric conditions, in particular a southward shift of the westerlies as projected by some climate scenario calculations for the recent IPCC report [*Meehl et al.*, 2007]? Addressing such questions does require an improved quantitative understanding of the dynamics of the Agulhas region and its interplay with the global circulation. The goal of this thesis is to significantly advance this understanding by a sequence of model studies based on a newly developed "nested" model configuration which combines the global ocean circulation with a high-resolution representation of the Agulhas leakage. The studies focus on some key

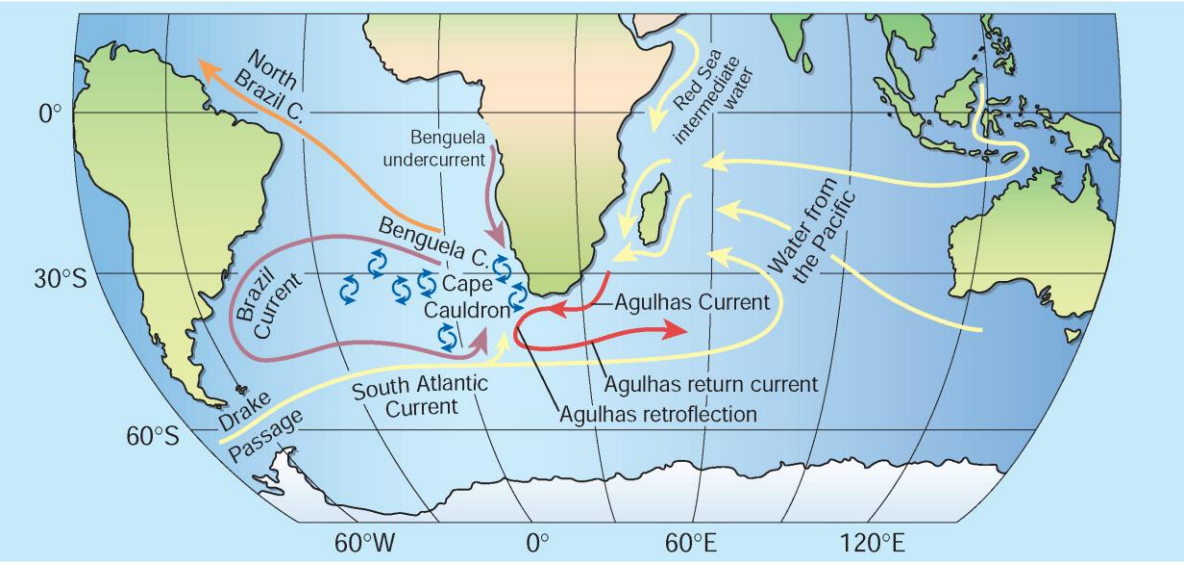

Fig. 1.1: Embedding of the Agulhas system into the large-scale circulation. [Adopted from ***Gordon*, 2003**]

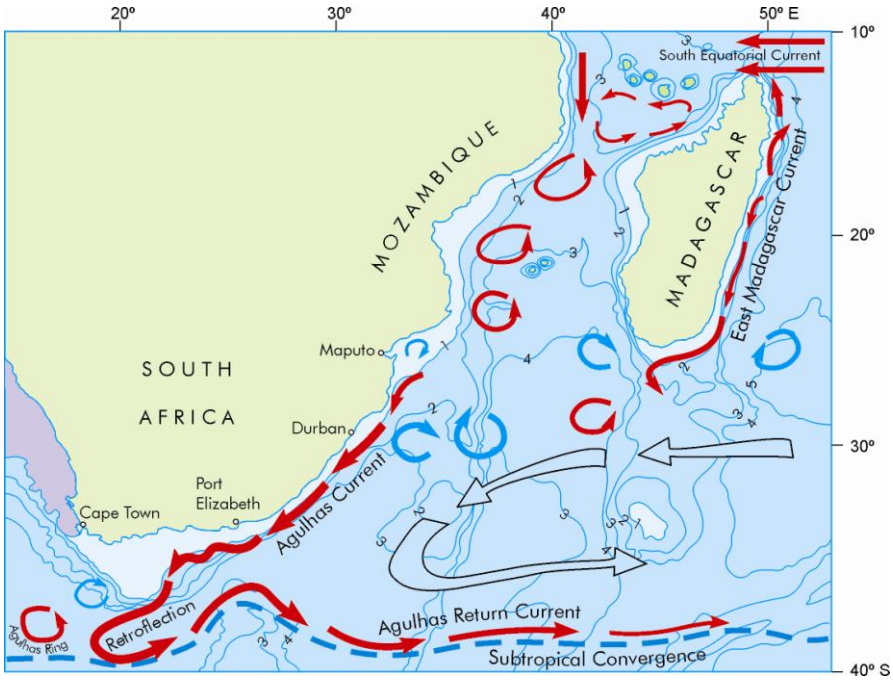

Fig. 1.2: Conceptual portrayal of the flow patterns in the greater Agulhas system. [Adopted from ***Ansorge and Lutjeharms*, 2007**]

aspects of the Agulhas regime: the role mesoscale dynamics around South Africa, their interplay with the mean current system and their effect on the interocean exchange and the large-scale circulation.

The Agulhas system (Fig. 1.2) is not a simple conveyor of heat and salt from the Indian to the Atlantic Ocean. It consists of a strong western boundary current, the Agulhas Current [*Lutjeharms*, 2006], which flows southward along the African Coast. After shooting over the southern tip of the continent it abruptly retroflects back into the Indian Ocean, forming the Agulhas Return Current, which then gradually closes the return flow of the subtropical gyre in the South Indian Ocean. The retroflecting Agulhas Current intermittently sheds the largest mesoscale eddies in the World Ocean [*Olson and Evans*, 1986]. These Agulhas rings are the dominating vehicles transporting and gradually releasing the Indian Ocean waters into the Atlantic. However, they are only one constituent in a vast range of mesoscale features in the "Cape Cauldron" [*Boebel et al.*, 2003], complicating the exact quantification of the interocean exchange [*de Ruijter et al.*, 1999a].

The retroflection process appears affected by mesoscale perturbations upstream of the Agulhas Current. For the first time described by results from a numerical model [*Biastoch and Krauss*, 1999], later verified by analyses from satellite observations [*Schouten et al.*, 2003], these eddies are being formed in the Mozambique Channel and drift pole-ward. Further south the Mozambique eddies do strongly interact with the Agulhas Current, possibly in combination with offshore displacements of the Agulhas Current, called Natal Pulses [*Lutjeharms and Roberts*, 1988]. Observationally this interplay [*de Ruijter et al.*, 1999b] has only been verified for a single instance [*Schouten et al.*, 2002]. Eddies that appear east of Madagascar [*de Ruijter et al.*, 2004] are even more under debate since there are contradicting theories on the question

wether the South East Madagascar Current is retroflecting [*Lutjeharms*, 1988] or not [*Quartly et al.*, 2006], which then has also consequences for its feeding of the Agulhas Current.

What governs the variability of the interocean exchange south of Africa? It is quite clear that largest variations [*de Ruijter et al.*, 1999a] are caused by mesoscale processes [*Reason et al.*, 2003], such as Agulhas rings. Their shedding might be related to some extent to inter-annual changes in the wind fields [*Witter and Gordon*, 1999], but it is more likely that upstream perturbations have a triggering effect on the formation of Agulhas rings [*Schouten et al.*, 2002]. Natal Pulses have also been implicated in the upstream retroflection of the Agulhas Current [*Lutjeharms and van Ballegooyen*, 1988a] through which all the water in the Agulhas Current is siphoned off to the Agulhas Return Current at an early stage with no normal inter-ocean exchange being feasible for a while. However, no quantitative effect has been estimated to date. There is evidence that the Agulhas leakage is highly variable on paleo time scales [*Howard and Prell*, 1992, *Flores et al.*, 1999] due to the shift of the subtropical and subpolar frontal structures; however, it was possibly never completely broken [*Rau et al.*, 2002]. Quite opposite, it is thought that a strong Agulhas leakage was always linked to a strong input of North Atlantic Deep Water (NADW) into the Southern Ocean, and hence a strong MOC [*Peeters et al.*, 2004].

A quantitative understanding of the dynamics that govern low-frequency fluctuations of the MOC is a prerequisite for the predicting the evolution of climate, especially in Europe and North America, over decadal time scales [*Keenlyside et al.*, 2008]. This task is complicated due to the overall dominance of mesoscale eddies in the global ocean [*Wunsch*, 2008]. Attempts to quantify the MOC have been or are currently being undertaken, sometimes making use of the fact that the important parts of the flow have to pass through certain choke points, such as the flow of dense water across the Greenland-Scotland Ridge [*Käse et al.*, 2003]. Due its character as a key region similar attempts exist in the Agulhas region (GoodHOPE) [*Ansorge et al.*, 2005]. In addition monitoring programs have been established building on historic observations; its most prominent example, the RAPID array at 26°N in the North Atlantic where possible declines [*Bryden et al.*, 2005b] have been recently controversially discussed [*Latif et al.*, 2006], is also subject to strong variability on intra-seasonal to inter-annual time scales [*Kanzow et al.*, 2007].

Decadal changes of the MOC at 26°N have mainly been attributed to atmospheric fluxes causing variations of the deep flow. Model studies have been linked those to deep water formation processes in the sub-arctic Atlantic, particularly to the renewal rate of Labrador Sea Water (LSW) [*Eden and Willebrand*, 2001, *Böning et al.*, 2006] that reverberates in the mid-latitude MOC with typical amplitudes of ± 1.5 - 3 Sv ($1\ Sv = 1 \times 10^6\ m^3\ s^{-1}$) on decadal time scales, whereby changes in the dense overflow from the Nordic Seas appeared to have comparatively minor effects in the last decades [*Beismann and Barnier*, 2004, *Latif et al.*, 2006]. It is unclear at the current stage if the Agulhas leakage, which acts on the upper limb of the MOC, could have the potential to also cause decadal changes.

Due to the mesoscale nature of the flow, modeling the Agulhas system is not straightforward. Early models simulated and attributed the main element of the system, the abrupt retroflection, to dynamical causes such as inertia due to the overshooting the African continent [*de Ruijter*, 1982], vortex stretching [*Boudra and de Ruijter*, 1986], topographic

features [*Matano*, 1996] or the large-scale structure of the wind field [*de Ruijter*, 1982]; the latter led to the formulation of a "super-gyre" covering both Atlantic and Indian Ocean, possibly also the Pacific Ocean [*Speich et al.*, 2002, *Meijers et al.*, 2007]. But, if it gets beyond the conceptual modeling it becomes clear that simulations have to include the mesoscale dynamics for a more realistic representation of all processes. In those cases an adequate resolution is stringent since Agulhas rings cannot adequately be parameterized by current numerical eddy parameterizations [*Gent and McWilliams*, 1990]; the assumption for such a parameterization, a classical distinction into mean flow and mesoscale, does not hold in the case of large Agulhas rings where one rather has to consider trapped volumes of water [*Treguier et al.*, 2003]. The lack of a proper representation of the Agulhas dynamics in coarse-resolution models leads to questions regarding its effect on the large-scale flow [*Weijer et al.*, 1999, *Marsh et al.*, 2007]; it also contributes to deficits in the representation of South Atlantic intermediate waters further downstream (via salt advection) affecting the North Atlantic subpolar deep water formation in current IPCC-type coupled models [*Russell et al.*, 2006, *Banks et al.*, 2007].

Eddy-permitting models with typical horizontal resolutions of 1/4° - 1/3° touch the mesoscale part of the spectrum (for a detailed description see Chapter 2) and are in principle able to simulate the process of ring shedding at the Agulhas retroflection [*Lutjeharms and Webb*, 1995, *Matano and Beier*, 2003]. However, the resulting Agulhas rings are typically too regular to represent the full range of variability in the interocean exchange. One possible cause is the crude representation of Mozambique eddies at this resolution and the fact that Natal Pulses are completely lacking [*Biastoch and Krauss*, 1999]. Results of eddy-permitting models have thus to be used with care, but are able to demonstrate certain connections of the Agulhas regime with the global circulation, e.g. the influence of the Indonesian Throughflow on the circulation in the Mozambique Channel [*Matano et al.*, 2008]. Global high-resolution (1/10° - 1/12°) models such as recent, first simulations obtained with POP [*Maltrud and McClean*, 2005], OCCAM [*Coward and de Cuevas*, 2005] and OFES [*Matsumoto et al.*, 2004] do capture the upstream perturbations [*Chapman et al.*, 2003] and do therefore contain the most important ingredient; but even here a high resolution alone is no guarantee for a successful simulation, e.g. to avoid too regular Agulhas ring paths [*Barnier et al.*, 2006]. In addition, it appears that not only the upper ocean is affected by resolution issues but also the deeper flow. It was noted that with shifting from eddy-permitting to high resolution an Agulhas Undercurrent emerged in the solution [*Maltrud and McClean*, 2005], but it was too weak compared to observations [*Beal and Bryden*, 1999].

A solution for a systematic testing of numerical choices needed for a proper simulation of the Agulhas regime is the setup of regional models that allow high resolutions but are still effective enough to be integrated in several sensitivity experiments. Successful applications have been demonstrated [*Penven et al.*, 2001, *Speich et al.*, 2006, *Backeberg et al.*, 2008] and applied to individual questions such as the role of topographic features [*Penven et al.*, 2006, *Speich et al.*, 2006]. However, due to the regulatory use of open boundary conditions [*Stevens*, 1990] which are necessary to connect the regional models with the global ocean, the simulated interocean fluxes are constrained by the prescribed data along the lateral boundaries and are not part of the solution [*Reason et al.*, 2003, *Speich et al.*, 2006].

In this study a new high-resolution model of the Agulhas region was devised and used for a series of studies of the dynamics of the Agulhas regime and its interaction with the large-scale circulation. The main questions being addressed are:

1. How do mesoscale dynamics and mean flow interfere in the greater Agulhas system? More specifically,
   - What is the effect of Mozambique eddies on the Agulhas Current system?
   - What is the role of eddies in the retroflection of the East Madagascar Current?

2. Which processes determine the net volume transport from the Indian to the Atlantic Ocean? Specifically,
   - What is the role of Agulhas rings?
   - How important are upstream perturbations for the interoceanic exchange?
   - Can one derive an index to monitor the interocean exchange?

3. What is the effect of the Agulhas mesoscale on the large-scale circulation? Specifically,
   - How does the Atlantic MOC react on decadal variability internally induced in the Agulhas regime?
   - What is the relative contribution of "Agulhas-induced" MOC variability compared to deep water related events emerging from the sub-arctic North Atlantic?

The outline of this thesis is as follows. Chapter 2 provides a discussion of the important aspects of modeling the Agulhas region and a detailed model description and its nesting technique. The following chapters (3 - 5) provide summary discussions pertaining to the main questions outline above. Chapter 6 summarizes and gives an outlook into future work.

Major parts of this thesis appeared in or are submitted to international journals. Since most were accepted after June 2008 the reader is referred for the latest status to the following references (status of December 2008):

- Biastoch, A., C.W. Böning, J. Getzlaff, J.-M. Molines, and G. Madec, 2008: Causes of inter-annual - decadal variability in the meridional overturning circulation of the mid-latitude North Atlantic Ocean, *J. Clim*., **21**, 6599-6615. [*Biastoch et al.*, 2008b].

- Biastoch, A., J.R.E. Lutjeharms, and C.W. Böning, and M. Scheinert, 2008: Mesoscale perturbations control inter-ocean exchange south of Africa, *Geophys. Res. Lett.,**35**,* L20602, doi: 10.1029/2008GL035132 . [*Biastoch et al.*, 2007].

- Biastoch, A., C.W. Böning, and J.R.E. Lutjeharms, 2008: Agulhas leakage dynamics affects decadal variability in Atlantic overturning circulation, *Nature*, **456**, doi: 10.1038/nature07426, 489-492. [*Biastoch et al.*, 2008c].

- Biastoch, A., L. Beal, T.G.D. Casal, and J.R.E. Lutjeharms, 2008: Variability and coherence of the Agulhas Undercurrent in a High-resolution Ocean General Circulation Model, submitted to *J. Phys. Oceanogr.* [*Biastoch et al.*, 2008a].

...

- Siedler, G., M. Rouault, A. Biastoch, B. Backeberg, C.J.C. Reason, and J.R.E. Lutjeharms, 2008: Modes of the southern extension of the East Madagascar Current, *J. Geophys. Res*, in press. [*Siedler et al.*, 2008].
- Van Sebille, E., C. N. Barron, A. Biastoch, P.J. van Leeuwen, C. Vossepoel, and W.P.M. de Ruijter, 2008: An Index for the inter-annual variability in Agulhas leakage, submitted to *J. Geophys. Res*. [*van Sebille et al.*, 2008].

2. A Nested Model of the Agulhas Region

The model used in this study is based on the "Nucleus for European Modelling of the Ocean" (NEMO, v.2.3) [*Madec*, 2006], consisting of the C-grid primitive equation ocean model OPA [*Madec et al.*, 1999] and the LIM2 sea-ice model [*Fichefet and Morales Maqueda*, 1999]. The global ORCA version used here is part of a model hierarchy developed by the European model collaboration DRAKKAR [*The DRAKKAR Group*, 2007]. Before the explicit setup will be described some specific requirements on a model of the Agulhas region will be discussed.

General Aspects of Model Configuration

Horizontal grid resolution is certainly the most crucial parameters for a correct simulation of the Agulhas region. At coarse resolution (Fig. 2.1a), typically used for current climate simulations, the Agulhas Current is consisted of a (quite unrealistically) continuous flow through the Mozambique Channel, following the African Coast as a western boundary current. Its most prominent circulation feature, the abrupt turn south of Africa and the return flow back into the Indian Ocean, the Agulhas Return Current [*Lutjeharms and Ansorge*, 1997],

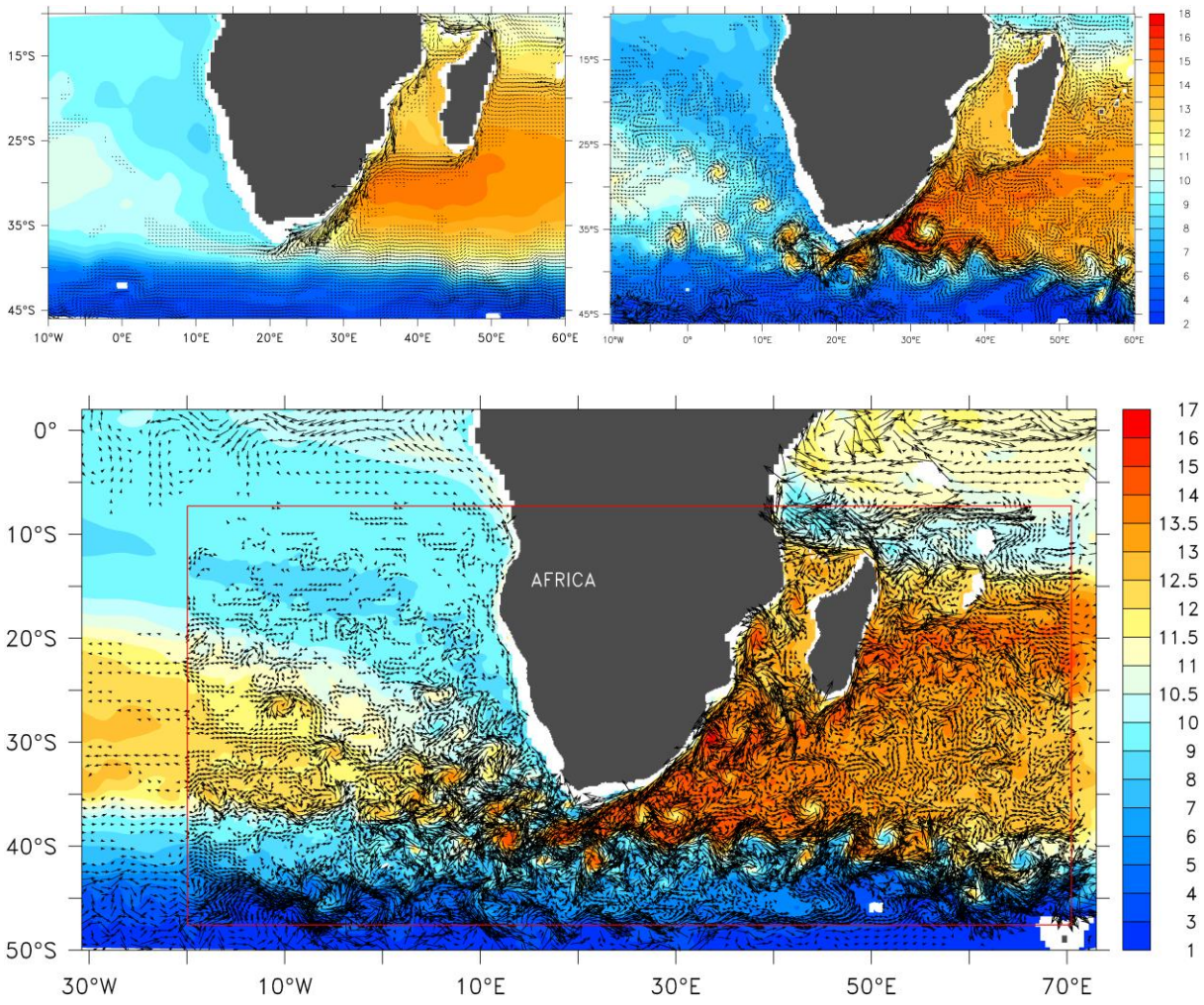

Fig. 2.1: Influence of horizontal resolution on the numerical simulation of the Agulhas regime. Shown are 5-day averages of temperature and velocity at 450 m depth for a model with **(a)** 1/2° (ORCA05), **(b)** 1/4° (ORCA025) and **(c)** 1/10° (AG01) nominal resolution (note that for ORCA025 every 2nd vector is shown, for AG01 every 4th).

is already visible at this resolution, although as a rather broad flow. At eddy-permitting resolution (Fig. 2.1b) a part of the mesoscale spectrum is resolved and Agulhas rings begin to form at the retroflection [*Gordon et al.*, 1987]; however, in contrast to observations [*Gordon and Haxby*, 1990, *Byrne et al.*, 1995, *Schouten et al.*, 2000, *Boebel et al.*, 2003] these do follow too regular paths and have too uniform dimensions (like "pearls on a chain"). Apart from those mesoscale circulation features the western boundary and frontal structures begin to sharpen, the Agulhas Return Current is meandering along its paths into the Indian Ocean. Only at high, eddy-resolving grid size (Fig. 2.1c) ,with an average grid cell of 9.1 km at 35°S now resolving the baroclinic Rossby radius of 30 km in this region [*Chelton et al.*, 1998], a wider range of mesoscale circulation characteristics appear: the Agulhas rings do, more realistically, cover a large range in ring paths and dimensions. Also visible are eddies in Mozambique Channel and east of Madagascar [*Biastoch and Krauss*, 1999, *Schouten et al.*, 2003]. This is especially important since it has been assumed that those eddies, due to their interplay with the formation of Natal Pulses, would have a significant impact on the triggering of Agulhas rings [*de Ruijter et al.*, 1999b, *van Leeuwen and Lutjeharms*, 2000, *Schouten et al.*, 2002]. Therefore, a high resolution is stringent to properly simulate all important large-scale features in the greater Agulhas system.

How can this high-resolution be achieved? In principle, two alternatives exist: Firstly, setting up a regional model. Although this has been proven to work for the Agulhas region [*Matano*, 1996, *Biastoch and Krauss*, 1999, *Penven et al.*, 2001, *Speich et al.*, 2006] a proper connection to the outside world is needed. A number of open boundaries are typically needed

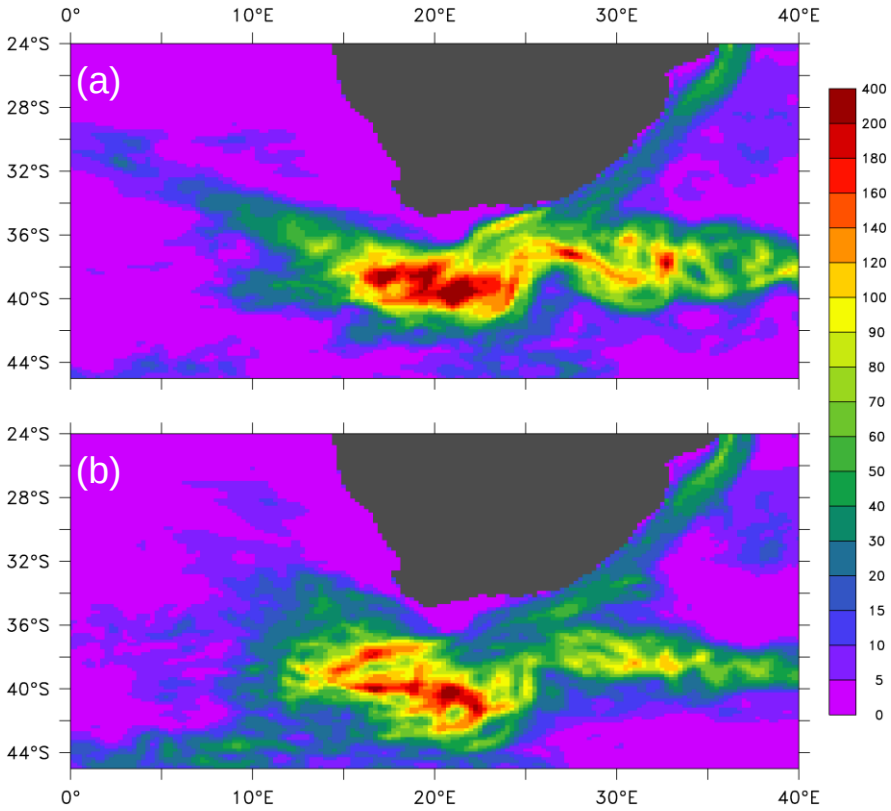

Fig. 2.2: Influence of the sea surface salinity restoring time scale on the mesoscale variability. Eddy kinetic energy density (in $cm^2\ s^{-2}$, averaged over the upper 100 m) in two eddy-permitting ORCA experiments at 1/4° resolution [***The DRAKKAR Group*, 2007**] using different SSS restoring time scales: **(a)** 300 days, **(b)** 60 days.

since the Agulhas region itself is not bounded by any continents and rather cuts through the subtropical gyres in the South Atlantic and Indian Ocean, touches the Antarctic Circumpolar Current (ACC) in the Southern Ocean. The formulation of open boundary conditions [*Stevens*, 1990] usually puts constraints on the interior solution, e.g. by determining the strength of the ACC and the gyre circulation [*Biastoch*, 1998], and does not allow for a feedback of the Agulhas dynamics on the outside ocean, and thus, the open boundary conditions. To overcome the regulatory use of open boundaries, a second choice could be to use a relatively large basin-scale, if not global, setup. Global models do exist [*Matsumoto et al.*, 2004, *Maltrud and McClean*, 2005] that properly simulate the Agulhas dynamics [*Matano et al.*, 2002, *Barnier et al.*, 2006]; however, apart from being too costly to run long-term sensitivity experiments that are typically needed for a proper understanding of the dynamical causes of the circulation, global high-resolution models do not allow for an isolation of the effect of mesoscale dynamics in the Agulhas regime (see below), i.e., an understanding of the individual role of Agulhas rings on the meridional overturning circulation.

Beside the pure resolution the choices of advection schemes (for both tracer and momentum) are other key factors for a good representation of the Agulhas retroflection and its associated mesoscale variability. It has been shown that serious numerical noise (especially in the high dynamical Agulhas Current) could be avoided by using improved advection schemes [*Webb et al.*, 1998]. It has also shown that especially the combination of the partial bottom cell formulation and the new momentum advection scheme conserving energy and enstrophy (see "Global Base Model" below) in NEMO led to remarkable improvements in the retroflection and ring dynamics, in some cases with a better performance even in an eddy-permitting resolution using this advection scheme than a high-resolution version without [*Barnier et al.*, 2006].

Sometimes even choices appearing minor may have significant impact on the modeled solution. A common approach for ocean-only models to overcome the large uncertainties in the reanalysis products [*Large and Yeager*, 2004] is an additional restoring of sea surface salinities towards climatological conditions derived from observations [*Conkright et al.*, 2002]. However, this does not only imply a correction on the resulting salinity distribution, in consequence leading to unrealistic fluxes [*Killworth et al.*, 2000], but might also put an additional constraint on the circulation. An example is given in Fig. 2.2 where a relatively strong (but commonly used, c.f. Tab. 2.1) restoring time scale leads to serious modifications in the mesoscale field. A significant reduction of the restoring resulted in higher eddy kinetic energy levels, allowed an improved meandering of the Agulhas Return Current and implied a well developed Agulhas ring path (Fig. 2.2a). Note that this is also mapped onto greater depths (here not shown), so that the whole barotropic structure is affected. Tab. 2.1 summarizes some of the described key parameters used in currently used global high-resolution models.

	nominal resolution (lon × lat)	Δx at 35°S	vertical levels	bottom cells	momentum advection	SSS-restoring
OCCAM	1/12° × 1/12°	9.3 km	66	partial	flux form	30 days
POP	1/10° × 1/10° cos (ϕ)	9.1 km	40	full	flux form	18 days
OFES	1/10° × 1/10°	11.1 km	54	partial	flux form	6 days
AG01	1/10° × 1/10° cos (ϕ)	9.1 km	46	partial	vector invariant, EEN	> 365 days

Tab. 2.1: Key parameters in global high-resolution z-coordinate ocean models OCCAM [***Coward and de Cuevas*, 2005**], POP [***Maltrud and McClean*, 2005**], OFES [***Matsumoto et al.*, 2004**] and this study (AG01).

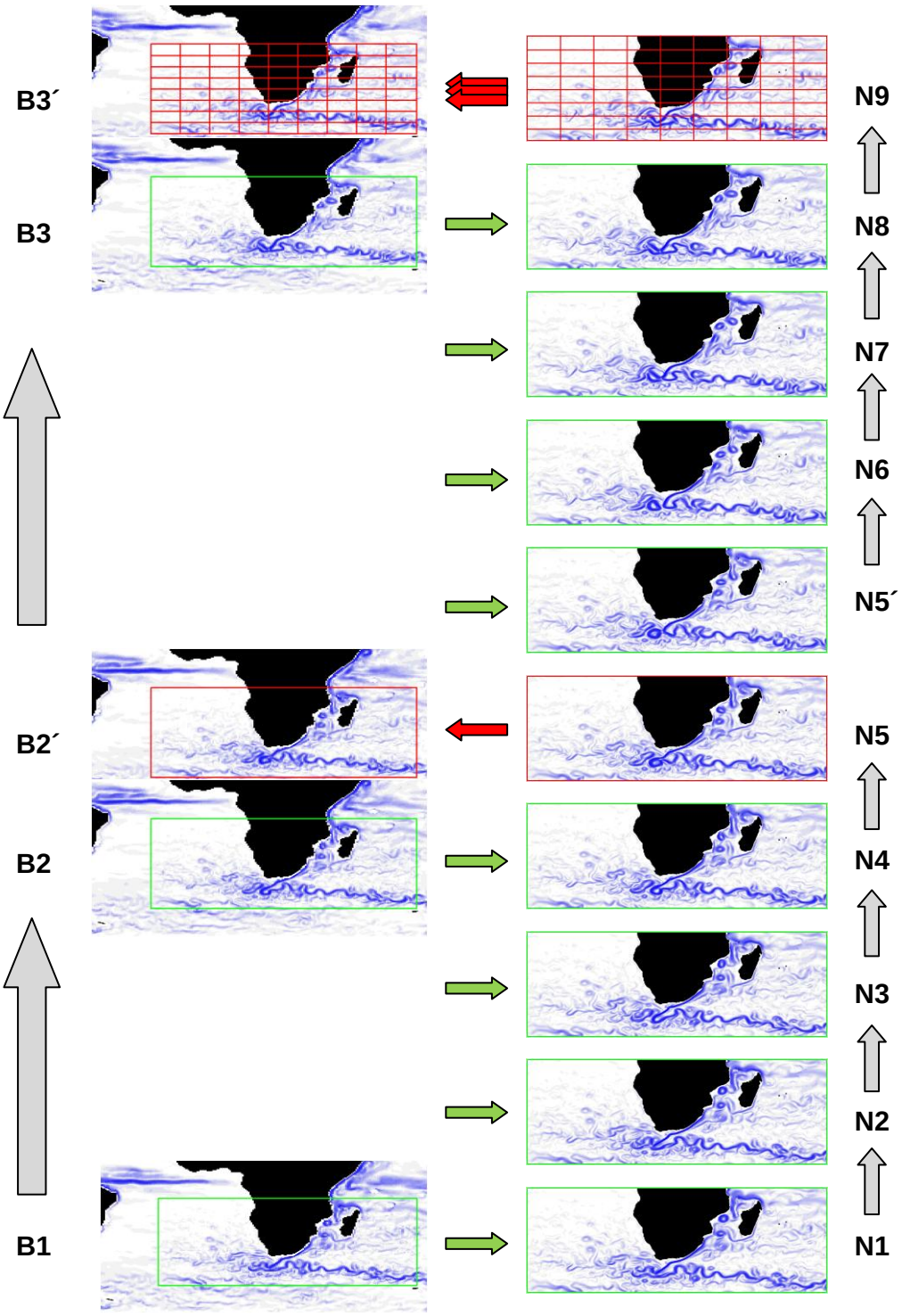

Fig. 2.3: Time-stepping of the base (left) and nested (right) grids. The green boxes and arrows indicate an interpolation from the base grid onto the outer boundaries of the nest, the red ones an averaging of the outer and surface boundaries of the nest onto the base grid; the mesh indicates an averaging of the whole nest onto its base grid points in the Agulhas region. Gray arrows and numbers indicate the timesteps of base (Bn) and nest (Nn) and their respective updates (Bn', Nn'). (Note that this is a schematic representation, the actual circulation will not evolve so fast within one timestep.)

Nesting Approach

The approach used here is to host a high-resolution Agulhas grid into a global coarse-resolution base model via a "two-way" nesting. This effectively combines the two alternatives mentioned in the preceding section: the high resolution nest captures all important circulation features from the large-scale to the mesoscale in the Agulhas region but (with the base model) explicitly simulates the rest of the world ocean without the usual constraints of open boundary conditions; due to reasonable numerical costs it allows to perform run several O(50 years) sensitivity experiments. In addition to the prescribed advantages and most important for the embedding of the Agulhas region is the fact that this choice is not only a computational compromise: the two-way nesting also provides an effective means to study the feedback of the mesoscale dynamics in the Agulhas region onto the large-scale base model. Away from the Agulhas region one can (by comparing with a global simulation without an Agulhas nest) isolate the effect of the mesoscale dynamics in the nest from local effects that would otherwise appear in a fully global high-resolution model.

The nesting approach is based on the "Adaptive Grid Refinement in Fortran" (AGRIF, [*Debreu et al.*, 2008]) coupling both model grids at every baroclinic time step of the base model (2160 s in this case). At any given timestep the base grid provides its prognostic data along the boundary of the nest (green box in Fig. 2.3), interpolated in time between two base model time steps, e.g. *B1* and *B2*. Then the nest is integrated some time steps (4 times in this configuration, each 540 s, *N1* to *N5*), afterwards all data are averaged onto the base grid along the boundary of the nest (red box in Fig. 2.3); in addition all coarse-resolution grid points in the Agulhas region are updated with the sea surface height from the nest. Both averaging processes feed the baroclinic and barotropic states back to the base model. Using this updated time step *B2'* the

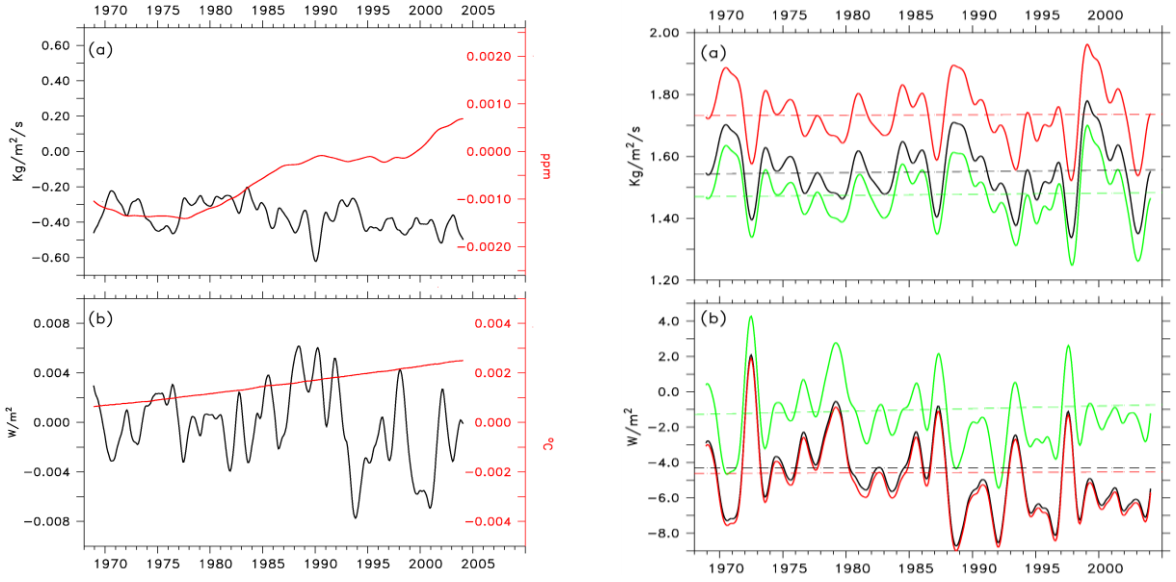

Fig. 2.4: Drifts associated with the AGRIF interpolation and averaging. Left: Globally averaged difference in **(a)** surface freshwater flux (black) and salinity (red) and **(b)** heat fluxes (black) and temperature (red) between the model with Agulhas nest (AG01) minus the one without (ORCA05). **Right:** Area averaged **(a)** surface freshwater and **(b)** surface heat fluxes in the region covered by the Agulhas nest (20°W-70°E, 47°S-7°S) for the AG01 base model (black), AG01 nest (red) and ORCA05 without Agulhas nest (green). [Adopted from ***Biastoch et al.*, 2007**]

base model is integrated for another timestep and the cycle starts again. Every few timesteps (3 in this configuration) the full three-dimensional, baroclinic state vector of the nest is averaged onto the base model grid points and fed back to the base model (red mesh in Fig. 2.3). The interpolation and averaging between both grids is conservative, so that mean model fields are almost maintained during the full length of integration (the drift in global mean temperatures and salinities due to the nesting approach are less than 0.02 °C and 0.02 psu, Fig. 2.4). This is a significant improvement over earlier attempts [*Fox and Maskell*, 1996] where hydrodynamic conditions in base and nest diverged after a few model weeks. Due to its success the AGRIF technique embedded in OPA has been used in applications of the Labrador Sea [*Chanut et al.*, 2008] and in the Caribbean [*Jouanno et al.*, 2008].

Global Base Model

The base model utilizes the ORCA configuration simulating ocean and sea-ice, widely used for physical and geochemical purposes [*Latif et al.*, 2006, *DeBoyer Montegut et al.*, 2007, *Lachkar et al.*, 2007, *Biastoch et al.*, 2008b]. Its layout of the variables is on a tripolar grid [*Madec and Imbard*, 1996], avoiding the North Pole singularity by mapping two poles over Canada and Russia; south of 20°N (and therefore in the Agulhas region) it is a Mercator grid. The present configuration uses a quasi-isotropic grid size with a nominal resolution of 1/2° (ORCA05); its cell size of 45 - 50 km in the Agulhas region is not resolving the mesoscale, simulating just some single, relatively large and unrealistic Agulhas rings (in contrast to Fig. 2.1a an eddy parameterization [*Gent and McWilliams*, 1990] was not used here, which would otherwise further damp the explicit simulation of those large eddies).

In the vertical 46 levels (with 10 levels in the upper 100 m and 250 m resolution at the maximum depth of 5750 m) are used, whereby the bottom cells are allowed to be partially filled (up to a minimum thickness of 25 m or 20% of its associated full cell thickness). This improved representation of topographic slopes in combination with a refined, energy and enstrophy conserving advection scheme (EEN, an adaptation of [*Arakawa and Hsu*, 1990] onto spherical coordinates [*Arakawa and Lamb*, 1981]) were found to lead to marked improvements in various circulation features [*Barnier et al.*, 2006, *Le Sommer et al.*, 2008]. It especially led to an improvement of the Agulhas retroflection area in an eddy-permitting version ORCA025 [*Barnier et al.*, 2006].

The subgrid-scale mixing parameterizations include a representation of mixed layer dynamics by a 1.5-level turbulent kinetic energy closure [*Blanke and Delecluise*, 1993, *Madec et al.*, 1998] model (in addition to the original NEMO v2.3 this version includes the effects of surface waves, Langmuir cells, and the vertical penetration of inertial and internal waves, to be appear in v3.0), static instabilities are removed by enhanced vertical diffusion. Viscosity is discretized for momentum by a bilaplacian scheme (for parameters see Tab. 2.2), diffusion by an iso-neutral laplacian scheme. For tracer advection a total variance dissipation scheme (TVD) [*Zalesak*, 1979] is used, which is a second-order, two-step monotonic scheme with moderate numerical diffusion avoiding spurious extremes [*Kantha and Clayson*, 2000]. Lateral boundary conditions are free-slip; the bottom friction is nonlinear ($C_D = 10^{-3}$, $e_b = 2.5 \times 10^{-3}$ $m^2\ s^{-2}$) [*Tréguier*, 1992].

	Base model	Nested Model
Nominal horizontal grid resolution	1/2°	1/10°
Horizontal momentum diffusivity (A_{hm})	$-8.5 \times 10^{11}\ m^4\ s^{-1}$	$-2.125 \times 10^{10}\ m^4\ s^{-1}$
Horizontal tracer diffusivity (A_{ht})	$2000\ m^2\ s^{-1}$	$200\ m^2\ s^{-1}$
Vertical momentum diffusivity (A_{vm})	$10^{-4}\ m^2\ s^{-1}$	$10^{-4}\ m^2\ s^{-1}$
Vertical tracer diffusivity (A_{vt})	$10^{-5}\ m^2\ s^{-1}$	$10^{-5}\ m^2\ s^{-1}$
Tracer diffusion, bottom boundary layer	$6000\ m^2\ s^{-1}$	$500\ m^2\ s^{-1}$
Timestep	$2160\ s$	$540\ s$

Tab. 2.2: Resolution-dependent parameters of the base and nested model.

CORE Forcing

The surface boundary conditions used for the present ORCA simulations are based on the atmospheric data sets and formulations developed [*Large and Yeager*, 2004] for the use in global ocean – sea-ice models; these have been suggested as a basic choice for the design of "Coordinated Ocean-ice Reference Experiments (COREs)" [*Griffies et al.*, 2007, *Large and Yeager*, 2007]. The forcing data set (Tab. 2.3) is based on a combination of the NCEP/NCAR reanalysis product [*Kalnay et al.*, 1996] for the years 1958 - 2004 with various observational data (e.g. satellite products for the last 15 years, TOGA/TAO arrays, rain climatologies), used to correct and to remove known biases, involving adjustments that remove global imbalances (e.g., to produce near zero global mean heat and freshwater fluxes when used in combination with observed SSTs). Turbulent fluxes are computed from bulk formulae (every 5 time steps or 3 hours, twice within the highest, 6-hourly, temporal resolution of the forcing fields) as a function of the prescribed atmospheric state and the simulated ocean surface state (SST and surface currents). Wind components were modified along the coast of Antarctica to parameterize the effect of katabatic winds [*Mathiot*, 2005]. To complete the freshwater fluxes a climatology of the global river run-off [*Dai and Trenberth*, 2002] is used which was combined with the general coastal runoff required to globally balance the CORE forcing.

Variable	Data Set	Interpolation	Resolution	Inter-annual
Wind at 10m height (U_{10}, V_{10})	CORE	bicubic	6-hourly	1958 – 2004
Atmospheric temperature (T_{10})	CORE	bicubic	6-hourly	1958 – 2004
Humidity (Q_{10})	CORE	bicubic	6-hourly	1958 – 2004
Longwave radiation (QLW)	CORE	bicubic	daily	1984 – 2004
Shortwave radiation (QSW)	CORE	bilinear	daily	1984 – 2004
Total precipitation (rain)	DFS3	bilinear	monthly	1979 – 2004
Solid precipitation (snow)	DFS3	bilinear	monthly	1979 - 2004

Tab. 2.3: Variables of the used atmospheric forcing (DFS3 stands for "Drakkar Forcing Data Set #3" [***Brodeau et al.*, 2007**]).

With the existing CORE data set ("cnyf/ciaf_1po", provided on a 2° × 2° Mercator grid by the Geophysical Fluid Dynamics Laboratory) it was found in ORCA05 that a relatively high freshwater supply to the North Atlantic caused a collapse of the MOC [*Griffies et al.*, 2007, *Biastoch et al.*, 2008b] which could only be avoided by a constraining the polar oceans, i.e., by applying a restoring towards the climatology [*Conkright et al.*, 2002, *Steele et al.*, 2001] over the full water depth. After identifying an excess of freshwater in the rain component as being

responsible for the artificial drift the precipitation field was reduced blending observational values [*Béranger et al.*, 2006] north of 30°N with the CORE data [*Brodeau et al.*, 2007]. However, since even small errors in the freshwater budget are prone to lead to unacceptable drifts in (uncoupled) global model integrations [*Griffies et al.*, 2007] the common practice has been followed by damping sea surface salinity (SSS) towards monthly-mean climatological values with a piston velocity of 50 m × (300 days)$^{-1}$ (about one month timescale) north of 70°N and south of 50°S. Equator-ward of these latitudes a weak damping (more than one year timescale) was used leaving the evolution within the Agulhas area almost unaffected. The use of bulk formulae cannot be globally balanced per se; therefore, due to the volume conserving formulation of the linear free surface [*Roullet and Madec*, 2000] the remaining small freshwater imbalances cause a heave of the sea surface height (~2 cm/year). Its global offset does not affect the dynamics of the circulation and was removed before working with the sea surface height data.

This ORCA05 DRAKKAR version under CORE forcing (although with sometimes different parameterizations and using three-dimensional Arctic restoring) has been used in a series of large-scale studies, such as the variability of the MOC [*Latif et al.*, 2006, *Latif et al.*, 2007, *Alvarez-Garcia et al.*, 2008, *Biastoch et al.*, 2008b], the freshwater budget in the subpolar North Atlantic [*Scheinert*, 2008] or on the variability of the Pacific subtropical cells [*Lübbecke et al.*, 2008]. It has been demonstrated that it reasonably simulates the large-scale circulation including the heat and freshwater driven components of the meridional overturning.

Agulhas Nest

The nested model covers the greater Agulhas region (20°W - 70°E, 47°S - 7°S, Fig. 2.5), cutting right through the subtropical gyres in the south-west Indian Ocean and in the South Atlantic. As a prerequisite of AGRIF it shares the same ORCA grid (which is basically a Mercator grid in this region), but has a refinement factor of 5 compared to ORCA05; it therefore resolves the major spectrum of the mesoscale (see discussion at the beginning of this chapter). With 909 × 474 grid points it is 17% larger than the ORCA05 base grid; however,

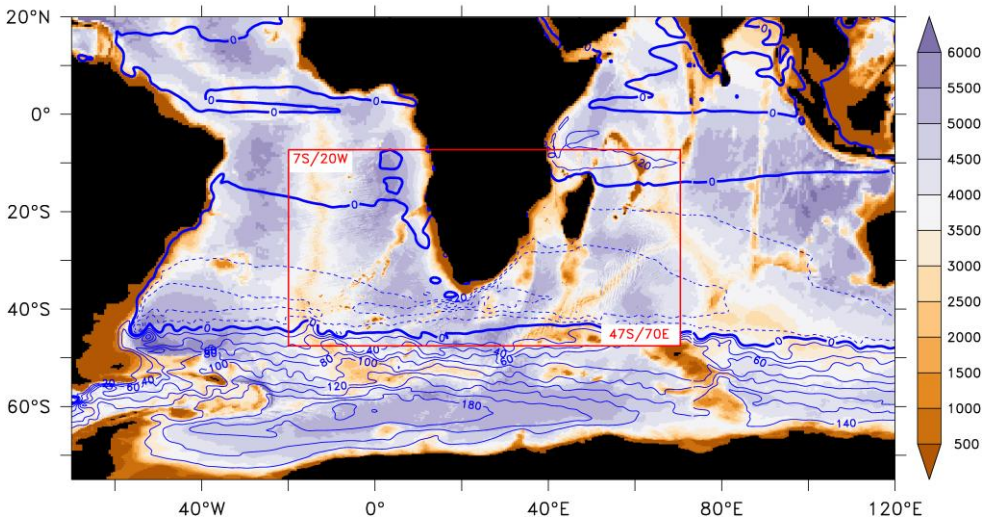

Fig. 2.5: Embedding of the Agulhas nest. Bathymetry (in m) of (a part of) the global base model (ORCA05) and the high-resolution nest (red box). The blue contour lines show the barotopic streamfunction of ORCA05 in Sv.

since it uses a time step refinement factor of 4 (which is reasonable to match the numerical stability criteria), most of the computation takes place in the nest. Therefore, apart from the AGRIF interpolation itself, the base model is a 20% overhead compared to the nest alone. It is self-evident that the use of the sea-ice model is omitted in the Agulhas nest.

The bottom topography has been interpolated from the 2-minute resolution ETOPO2, a combination of a satellite-based topography [*Smith and Sandwell*, 1997] and the "International Bathymetric Chart of the Arctic Ocean" [*Jakobsson et al.*, 2000], taking the median average and applying an additional smoothing up to a maximum slope of $\nabla h/h = 0.75$ to avoid too much numerical noise due to topography [*Penduff et al.*, 2002]. Apart from some resolution-dependent parameters which are scaled to give a similar nominal value (Tab. 2.2) the same parameterizations have been used. All CORE forcing data were interpolated onto the high-resolution grid, keeping its original time resolution.

Integration Strategy

The global base model alone (ORCA05) was started from rest, initialized by temperatures and salinities from a global climatology [*Conkright et al.*, 2002, *Steele et al.*, 2001] and integrated for 20 years using the climatological CORE forcing (Fig. 2.6). After the spin-up of the dynamical fields all restart data were interpolated onto the high-resolution nest to avoid further spin-up effects. Starting with an Euler forward timestep the combined model (AG01[1]), consisting of the base model and nest, was then integrated for 47 years using the CORE forcing of the years 1958 - 2004. In parallel ORCA05 (without the high-resolution nest) was also integrated over the same period to provide a coarse-resolution reference case.

To test the influence of mesoscale perturbations in the source regions of the Agulhas Current, the Mozambique eddies, a sensitivity experiment (AG01-S) was performed where the northern boundary of the high-resolution nest ended at 26°S, leaving the Mozambique Channel and the Indian Ocean east of Madagascar at base model resolution, therefore without the explicit simulation of upstream perturbations. Only used as a sensitivity case this configuration was only integrated until model year 1978.

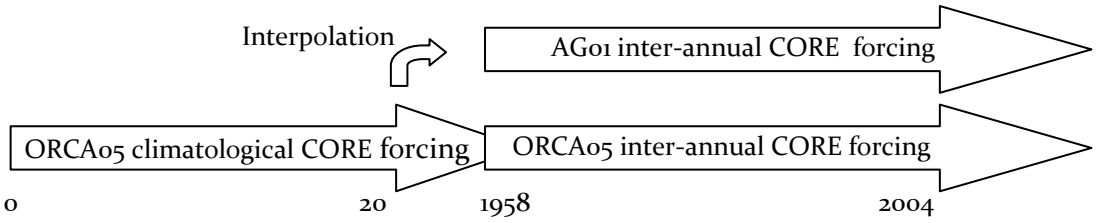

Fig. 2.6: Integration Strategy of the coarse-resolution model without Agulhas nest (ORCA05) and the AGRIF configuration (AG01) consisting of base grid and nest.

[1] This experiment is sometimes also called AG01-R to distinguish it from sensitivity experiments.

While the standalone ORCA05 runs were performed on 4 processors of a NEC SX-8 at the Computing Centre of the Kiel University, the nested AG01 runs needed to be parallelized over significantly more processors. These runs took place at the High Performance Computing Center Stuttgart (HLRS) using 16 processors (2 nodes) of a NEC SX-8. All prognostic state variables plus the (via bulk formulae) derived atmospheric fluxes were stored as 5-daily averages for both base model and nest, resulting in a total data volume of 5 Terabytes.

Quantification with Lagrangian Particles

To follow the path of the Agulhas Undercurrent (Chapter 3) and to quantify the inter-oceanic exchange between Indian Ocean and Atlantic (Chapter 4), an offline Lagrangian diagnostic (ARIANE, http://www.univ-brest.fr/lpo/ariane [*Blanke et al.*, 1999]) was used. Typically O(3×10^6) floats, each representing a small amount (max. 10^{-2} Sv in most cases) of water, were seeded over a current (e.g. the southward flowing Agulhas Current at 32°S) and advected using the 5-daily velocity output of the model. The particles were measured when crossing control sections (further downstream) and summed up again to give a transport number in Sv. Such a diagnostic has been shown to give reasonable estimates, e.g. on the amount of Agulhas waters entering the Atlantic [*Speich et al.*, 2006]. Particles were continuously seeded over a certain period (typically 7 - 10 years) to capture almost all temporal variability and to get a representative statistics; after stopping the seeding all particles were further integrated for an additional period of some years. At the end of this period typically only 1 - 2% had still not crossed one of the control sections.

General Verification

How successful is this model configuration in providing simulations with a high degree of verisimilitude? A first inspection shows that all the major elements of the greater Agulhas

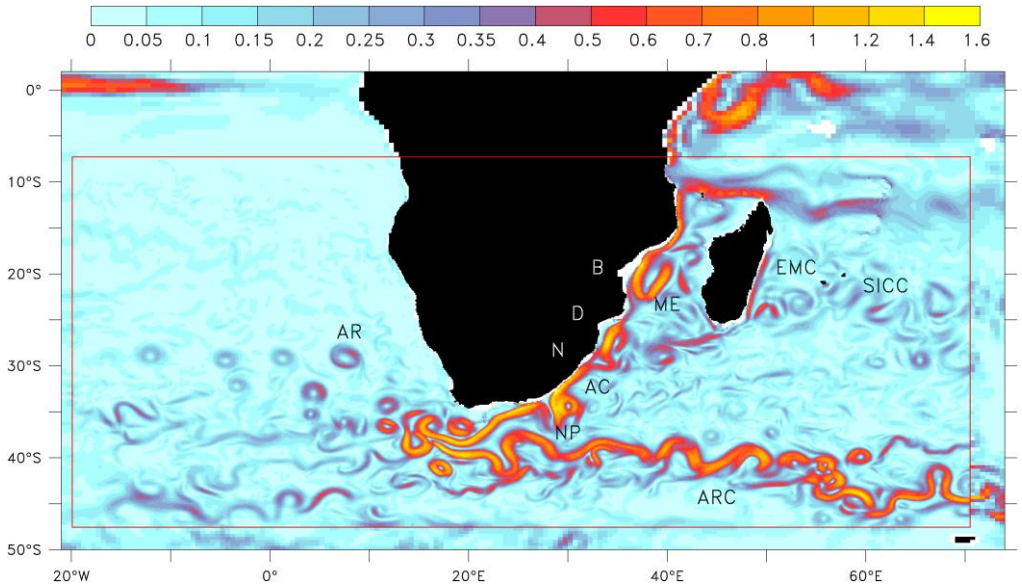

Fig. 2.7: Snapshot of the high-resolution model nested in the global, coarse resolution model. Shown are speeds (5-day average around 12 Feb 1969) at 100 m depth (in m s^{-1}). The geographic locations of the bights of Beira (B), Delagoa (D) and Natal (N) are shown as are the circulation features Agulhas Current (AC), Agulhas Ring (AR), Agulhas Return Current (ARC), East Madagascar Current (EMC), eddies of the South Indian Countercurrent (SICC), Mozambique Eddy (ME) and Natal Pulse (NP). [Adopted from ***Biastoch et al.*, 2007**]

Current are represented in a highly realistic way (Fig. 2.7). These include the Agulhas Current with a realistic transport of 71 ± 16.4 Sv at 32°S (concurring with estimates based on hydrographic sections [*Beal and Bryden*, 1999, *Donohue and Toole*, 2003] as well as on moored current meter records [*Bryden et al.*, 2005a]) characteristically hugging the shelf edge and extending 200 km offshore; a highly variable [*Bryden et al.*, 2005a] Agulhas Undercurrent of 4.8 ± 3.8 Sv; a narrow southern branch of the East Madagascar Current ending in a retroflection at 25°S, shedding the occasional ring and most of its waters subsequently being carried eastward in the eddying South Indian Counter Current [*Siedler et al.*, 2006]; Agulhas rings with a diameter of 360 ± 40 km rapidly spinning down in the Cape Basin and then moving off into the South Atlantic with a translation speed of about 24 km/week and an Agulhas Return Current with a faithful representation [*de Ruijter et al.*, 1999a, *Olson and Evans*, 1986] of its average location, variability and shedding of eddies to either side. About 5 ± 1 anti-cyclonic Mozambique eddies, realistic in size and frequency [*Schouten et al.*, 2002], are formed per year with average diameters of 270 ± 45 km and extending to the sea floor. Natal Pulses are evident on the landward border of the Agulhas Current at least 2 ± 1 times per year and move downstream with an average rate of about 22 km/day. Upstream retroflections [*Lutjeharms and van Ballegooyen*, 1988a] are seen in the expected location south of Port Elizabeth at 26 ± 1 °E. The observed distribution of different water masses in the south-west Indian Ocean is reproduced accurately [*Donohue and Toole*, 2003], so that all the salient elements of the large-scale circulation are also well captured.

A statistical picture is obtained in comparison with satellite data covering the region in time and space (Fig. 2.8). The reference model shows variability comparable in shape and value with observations (taking into account the blurring due to the objective mapping of the Aviso data[2]). It has to be noted that even some global models at similar or better resolution do show more confined, unrealistic paths [*Barnier et al.*, 2006], again underlining the correct choice of the advection scheme. Small differences occur southwest of Madagascar, possibly due to the lack of eddies shed from the Leeuwin Current [*Fang and Morrow*, 2003] outside the high-resolution nest and therefore not properly represented. Inspection of a global 1/10° ORCA model (R. Bourdallé-Badie, pers. comm.) indicated that those rings would drift into the region south-east of Madagascar. The sensitivity model, as intended by the choice of the setup, completely lacks the variability from the source regions and has a more regular path of the Agulhas rings in the Cape Basin (for detailed discussion see Chapter 4).

The distinct authenticity of every one of the features mentioned above gives considerable confidence in the reliability of the model and its ability to simulate interactions between the various circulation elements. However, additional verification is certainly needed before examining individual circulation features; this is done in the following (e.g. the Agulhas Current and Undercurrent in Chapter 3).

[2] The altimeter products were produced by Ssalto/Duacs and distributed by Aviso, with support from Cnes.

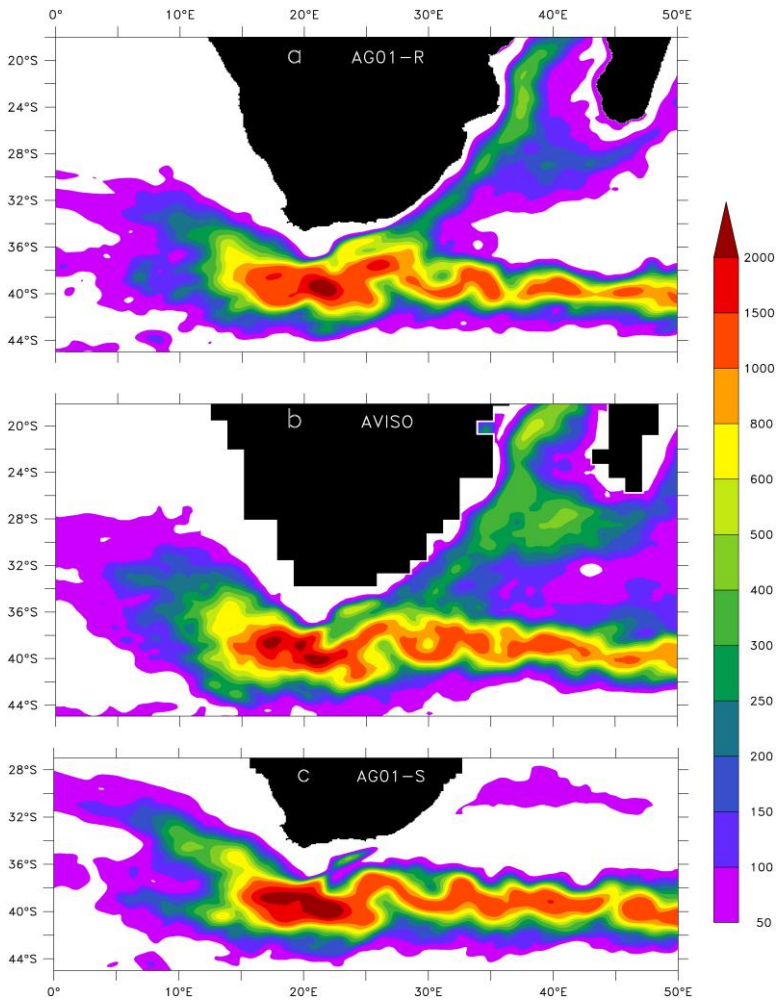

Fig. 2.8: Comparison of the mesoscale eddy statistics in comparison with observations. Variance of sea surface height (in cm²) in **(a)** the reference model (AG01-R, 1970 - 1979), **(b)** Aviso satellite data (1991 - 1999), and **(c)** the sensitivity model (AG01-S). [Adopted from ***Biastoch et al.*, 2007**]

3. Mesoscale – Mean Flow Interactions in the Greater Agulhas System

Before the Agulhas Current leaves the African Coast and retroflects back into the Indian Ocean mesoscale eddies originating from the Mozambique Channel and east of Madagascar are the dominant signature of variability, interfering with the western boundary currents, the East Madagascar Current and the Agulhas Current. This chapter will examine to what extent the upstream perturbations have an effect on the structure and transport of those currents.

Chapter 2 has demonstrated the general performance of the high-resolution model with respect to the gross circulation features. Before stepping into a detailed description on the interplay between upstream perturbations and the mean flow along the African coast,

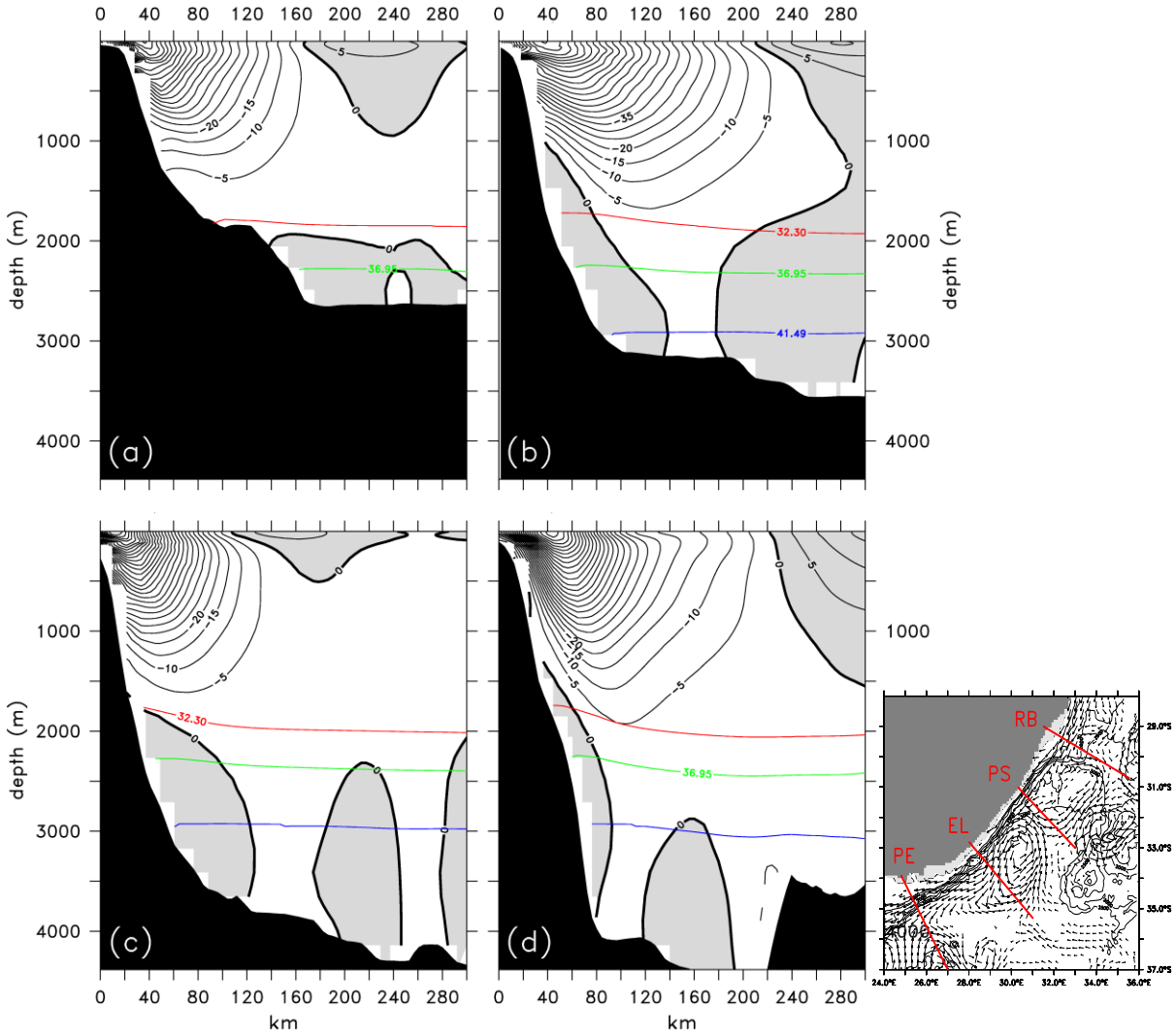

Fig. 3.1: Western boundary current structure along the African Coast. Sections across the Agulhas Current from north to south: off **(a)** Richards Bay (RB), **(b)** Port Shepstone (PS), **(c)** East London (EL), **(d)** Port Elizabeth (PE), showing along-shore velocity in cm s^{-1} (north-eastward velocities are shaded grey). Data are averaged over the period 1995 - 2004. Also shown are isopycnals marking upper bounds of uNADW (σ_1 = 32.30), mNADW (σ_2 = 36.95) and lNADW (σ_3 = 41.49). All model sections are rotated perpendicular to the stream axis. The inlet figure shows a snapshot of 100 m velocity (every 3rd vector) and locations of the sections.

additional verification of the western boundary current regime is required. Fig. 3.1 works its way along the African Coast: off Richards Bay (~29°S, Fig. 3.1a) the Agulhas Current is already fully developed, covering the upper 1500 m and extending 150 km offshore. On its way to the south it increases in speed, depth and lateral extensions; off Port Elizabeth (~34°S, Fig. 3.1d), just before leaving the shelf, it is more than 250 km wide and extends over full depth. The comparison off Port Shepstone (~31°S, Fig. 3.1b) with a composite mean section of seven observational cruises between 1995 and 2003 (Fig. 3.2) reveals a similar v-type shape of the current extending down to the bottom; its width, however, is significantly wider in the model. Differences might occur due to the bias in the observational ensemble towards Austral fall and winter. But the more likely causes are in the numerical simulation, e.g. due to the still limited horizontal resolution or due to the choice of physical parameterization and its associated values (Tab. 2.2). In this respect it should also be noted that the vertical axis in this model is represented in z-coordinates, traditionally, despite the enhanced representation of topography by partially filled bottom cells, not optimally suited to represent flow along topographic slopes.

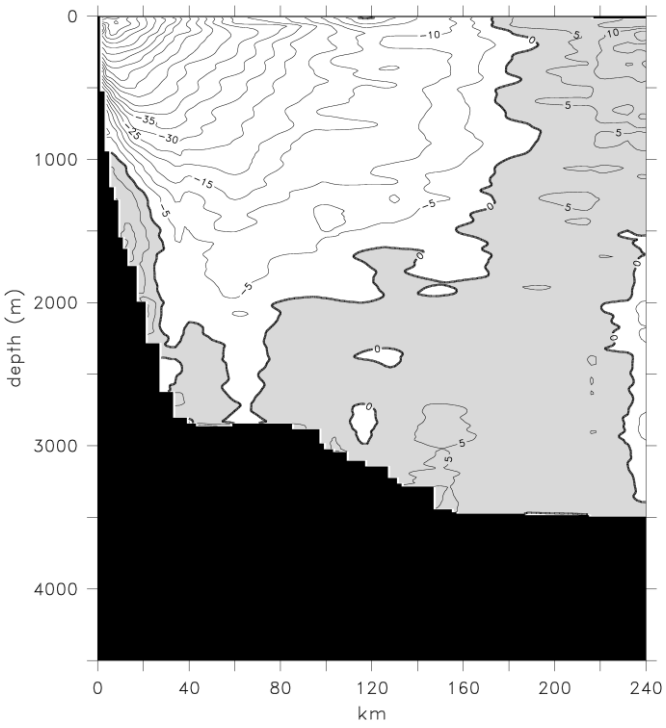

Fig. 3.2: Observational western boundary current structure. As **Fig. 3.1**b but composite section of 7 cruises off Port Shepstone (processed by L. Beal).

[*Beal and Bryden*, 1997] gave first clear evidence for a northward flowing Agulhas Undercurrent, constrained between the continental slope and the Agulhas Current, with a core at about 1200 m depth. Since then additional observations [*Donohue et al.*, 2000, *Bryden et al.*, 2005a, *Beal et al.*, 2006] further supported strongly varying transports which exists at the other Agulhas locations as well. The model also simulates such an Agulhas Undercurrent: Off Port Elizabeth (Fig. 3.1d) it characteristically hugs the continental slope, extending from about 1500 m down to the bottom; at least the inner core is not extending more than 50 km off the slope. On its way to the north it begins to widen and, more important, to be cut off from greater depth by shallower bottom topography. Off Richards Bay only its upper portion continues, underlined by tracing some representative water masses showing the upper bounds of upper,

middle and lower North Atlantic Deep Water (NADW) in this region [*Arhan et al.*, 2003, *Beal et al.*, 2006]. Especially the lower portion of the deep water is effectively cut off by bathymetry shallower than 3000 m. In addition, the other isopycnals, e.g., the σ_2 = 36.95 are subject to a downward shift of 200 m from Port Elizabeth to Richards Bay, indicating an erosion of deep water with Atlantic origin due to mixing along its northward way in the Indian Ocean.

	AG01-R		AG01-S		Bryden et al. (2005)	
	AC	AUC	AC	AUC	AC	AUC
1968 - 1978	71.2 ± 16.9	5.0 ± 3.1	69.7 ± 7.8	2.6 ± 1.6		
5/3 - 26/11/1995	68.3 ± 8.2	4.7 ± 2.7			69.7 ± 21.5	4.2 ± 2.9
1995 - 2004	68.0 ± 15.7	5.4 ± 3.9				

Tab. 3.1: Transports of the Agulhas Current (AC) and Undercurrent (AUC) at 31°S (in Sv) in comparison with [***Bryden et al.*, 2005a**]. For the calculation model velocities are integrated between the coast and 33°E and over the upper 2400 m (AC) or below 1000 m (AUC). Standard deviations for the model values are calculated from 5-daily averages. Note that standard deviations for the observations are based on daily timeseries.

Tab. 3.1 compares transport numbers for the Agulhas Current and the Agulhas Undercurrent at 31°S with estimates from a mooring array [*Bryden et al.*, 2005a], indicting a good overall performance of the model in both mean values and standard deviations. A revisit of the data [*Bryden et al.*, 2005a] in respect to the calculated Agulhas Undercurrent (Tab. 3.2) demonstrates that the inshore portion of the current is somewhat underrepresented and that a one-by-one comparison of the similar time frame is not possible; this is not surprising considering the different timing of individual Natal Pulses in both model and observations. Nevertheless, the total northward flowing Agulhas Undercurrent, measured over a longer timeframe, is with 9.8 ± 7.4 Sv in good agreement with the observations. This now enables the model to put the individual measurements of the Agulhas Undercurrent in a wider context. Especially the high fluctuations, its origin and a possible coherence of the flow are still open questions in the current literature.

	AG01-R				[*Bryden et al.*, 2005a]		
	5/3/1995 - 26/11/1995		1/1/1995 - 31/12/2004		5/3/1995 – 26/11/1995		
	mean	5d std.dev	mean	5d std.dev	mean	5d-	1d-std.dev
all	8.6 ± 4.8 Sv		9.8 ± 7.4 Sv		9.8 ± 7.1 Sv		(± 8.6 Sv)
below 1000 m	4.9 ± 3.0 Sv		5.7 ± 4.6 Sv		5.9 ± 3.6 Sv		(± 3.9 Sv)
inshore	2.1 ± 2.1 Sv		2.8 ± 4.1 Sv		3.5 ± 3.6 Sv		(± 3.9 Sv)
inshore / below 1000 m	2.1 ± 2.1 Sv		2.6 ± 3.3 Sv		2.9 ± 2.1 Sv		(± 2.3 Sv)

Tab. 3.2: Transport calculations of the Agulhas Undercurrent off Port Shepstone (rotated section, see **Fig. 3.1**b) in comparison with revisited [***Bryden et al.*, 2005a**] data. For the calculation only north-eastward velocities are taken, integrated over the first 205 km ("all") or 100 km ("inshore"). Model data are calculated over the last 20 years or covering the same period (5-Mar – 26-Nov-1995), but extend further offshore (270 km for "all", 135 km for "inshore") to match a similar dynamical regime. Standard deviations for the observational values are calculated both based on 5-daily or 1-daily averages.

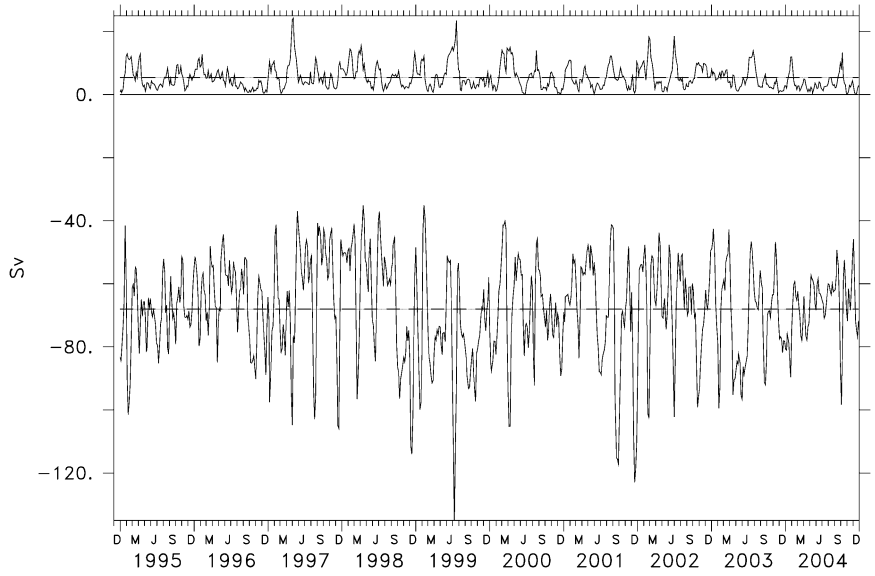

Fig. 3.3: Transports of the Agulhas Current (AC) and Undercurrent (AUC). Shown are 5-daily time series (in Sv) for the AC (negative/southward values) and AUC (positive/northward values). Velocities are integrated between 30 - 33°E, 0 – 2400 m (AC), 1000 - bottom (AUC). Note that the transport calculations have been performed along longitude at 31°S for accuracy reasons. The dashed lines show the mean values.

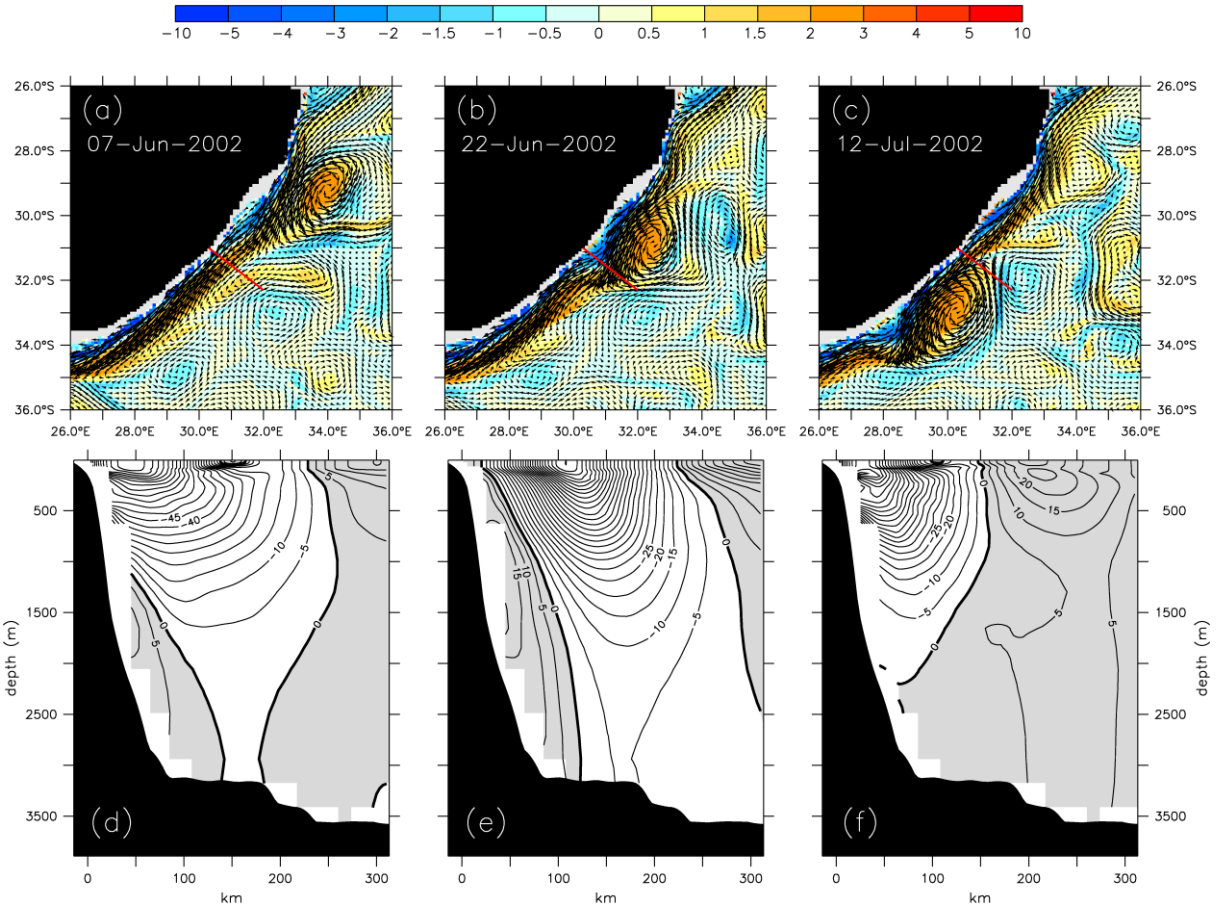

Fig. 3.4: Example snapshots before, during and after the transition of a Natal Pulse. Shown are 5-day averages of **(a-c)** vorticity (color, in 10^{-5} s^{-1}, blue = cyclonic, red = anticyclonic) and velocity (every 2nd vector) at 100 m depth, **(d-f)** the section off Port Shepstone (similar to **Fig. 3.1**b).

Already quantified by the large standard deviations (Tab. 3.1) the transport time series at 31°S (Fig. 3.3) shows enormous fluctuations of the Agulhas Current ranging from a maximal southward transport of 136 Sv to a minimal transport of 35 Sv; the Agulhas Undercurrent has maxima of more than 20 Sv (strongly dependent up to which longitude and depth velocities are integrated) but there are also phases with a disrupted northward flow. Both transports have a (significant) variability around 70 days, similar to the observations [*Bryden et al.*, 2005a] and indicating an active interplay with Mozambique eddies and Natal Pulses.

How does such interplay between upstream perturbations and both constituents of the Agulhas Current system take place? There is observational evidence that the Agulhas Current at 32°S at some times reaches down to the bottom, at other times covers only the upper 2300 m [*Donohue et al.*, 2000]. Fig. 3.4 gives an explanation for such a behavior by showing an exemplary series of snapshots before, during and after the transition of an upstream perturbation, consisting of a Mozambique Eddy and the generated Natal Pulse. Prior to the arrival of the eddy (Fig. 3.4a and d) the Agulhas Current is with relatively stable with a transport of 75 Sv (Fig. 3.5) and has a maximum speed of about 105 cm s^{-1} close to the coast (~ 45 km offshore). The Natal Pulse, generated as a cyclonic anomaly in the Natal Bight (~29°S) by the Mozambique eddy arriving from the north, causes a barotropic, northward velocity anomaly at the inshore side and a southward anomaly further offshore (Fig. 3.4b and e). This then leads to an offshore displacement of the Agulhas Current by 60 - 70 km and an increase in speed (to 130 cm s^{-1}) and transport (110 Sv). Consequently the extent of the Undercurrent increases, reaching up to the surface at the inshore side of the displaced Agulhas Current. Its core transport (limited to the first 135 km) peaks at 11.7 Sv. Such intermittent peaks in the Agulhas Undercurrent transport that are associated with passing Natal Pulses are also clearly evident in the temporal record shown in Fig. 3.5. The Mozambique eddy, directly following the Natal Pulse, reverses anomalies (southward inshore and northward offshore), putting the Agulhas Current back in place and further increasing it to 130 Sv. Due to the southward anomaly inshore of the Agulhas Current the Undercurrent is completely removed, instead a

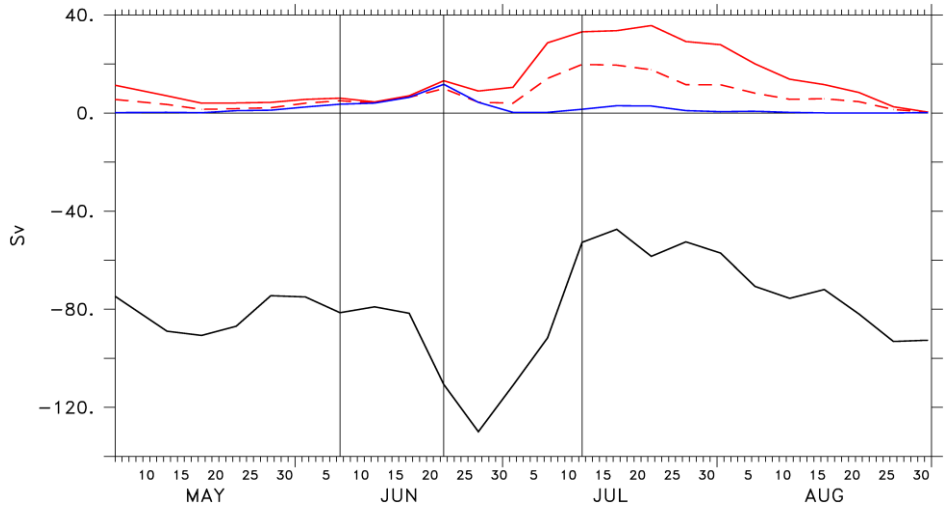

Fig. 3.5: Evolution of the transports during the transition of a Natal Pulse. Shown are transport of the Agulhas Current (black, averaged over the whole section) and the Undercurrent within the first 135 km (blue) and over the whole section including the offshore countercurrent (red) and below 1000 m (red dashed). The vertical lines display the centers of the averaging window of the 5-day averages shown in **Fig. 3.4**.

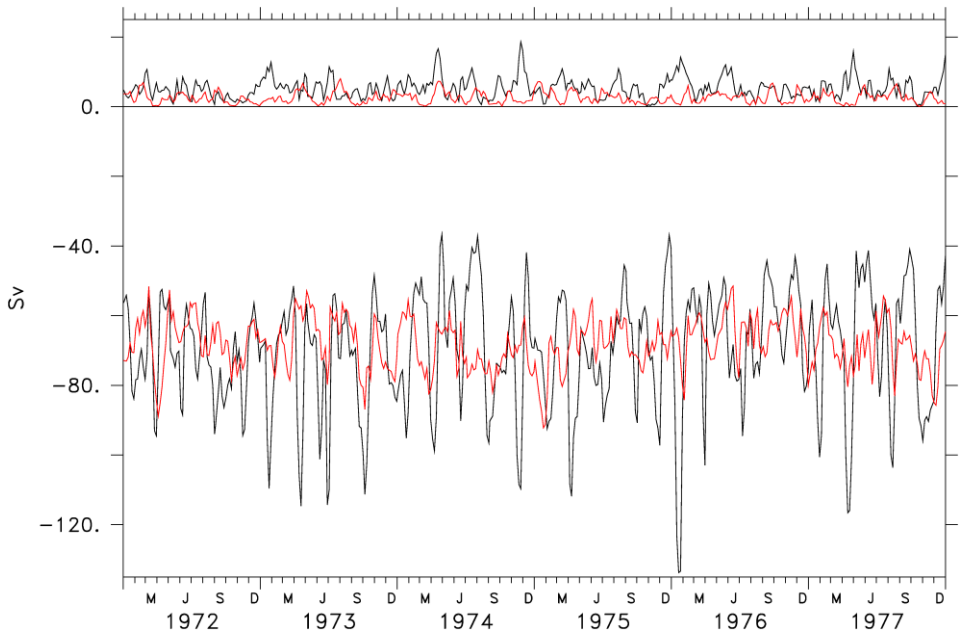

Fig. 3.6: Influence of upstream perturbations on the transports. As **Fig. 3.4** but AG01-R (black), AG01-S (red).

strong northward countercurrent exists at the offshore side (Fig. 3.4c and f) peaking 35 Sv (Fig. 3.5).

Proof and a quantification of the strong influence of the upstream perturbations on the Agulhas Current and Agulhas Undercurrent can only be tested by artificially omitting the perturbations from the modeled solution. Exp. AG01-S (see Chapter 2) reduces the high-resolution nest to areas south of the Mozambique Channel, thus effectively preventing Mozambique eddies and Natal Pulses being formed. Fig. 3.6 shows that variations for both components are significantly reduced without upstream perturbations; the strong extreme values are much more reduced and the variability in general is just half of the reference case (Tab. 3.1). It is especially noteworthy that the mean transport for the Agulhas Undercurrent is reduced from 5.0 to 2.6 Sv if upstream perturbations are no longer part of the solution (which is not the case for the Agulhas Current). Does that imply that the undercurrent is (at least partially) driven by the mesoscale perturbations arriving from the North?

Undercurrents have not only been observed under the Agulhas Current but also in the Mozambique Channel [*de Ruijter et al.*, 2002] and east of Madagascar [*Nauw et al.*, 2008]. Both do exist in the model as well (here not shown) in similar strengths compared to the sparse observations. This has raised a question on the coherence of the Agulhas Undercurrent along the African shelf, and whether it connects and supplies the west and east of Madagascar with deep water of Atlantic origin. An inspection of the time-mean flow (Fig. 3.7) does not support such a connection. Is this due to the small currents involved or is there no coherent flow throughout the deep southwestern Indian Ocean? To examine a possible connection of the undercurrents a Lagrangian analysis is better suited than a simple Eulerian mean since it actively follows all individual pathways that may arise due to the existence of mesoscale eddies.

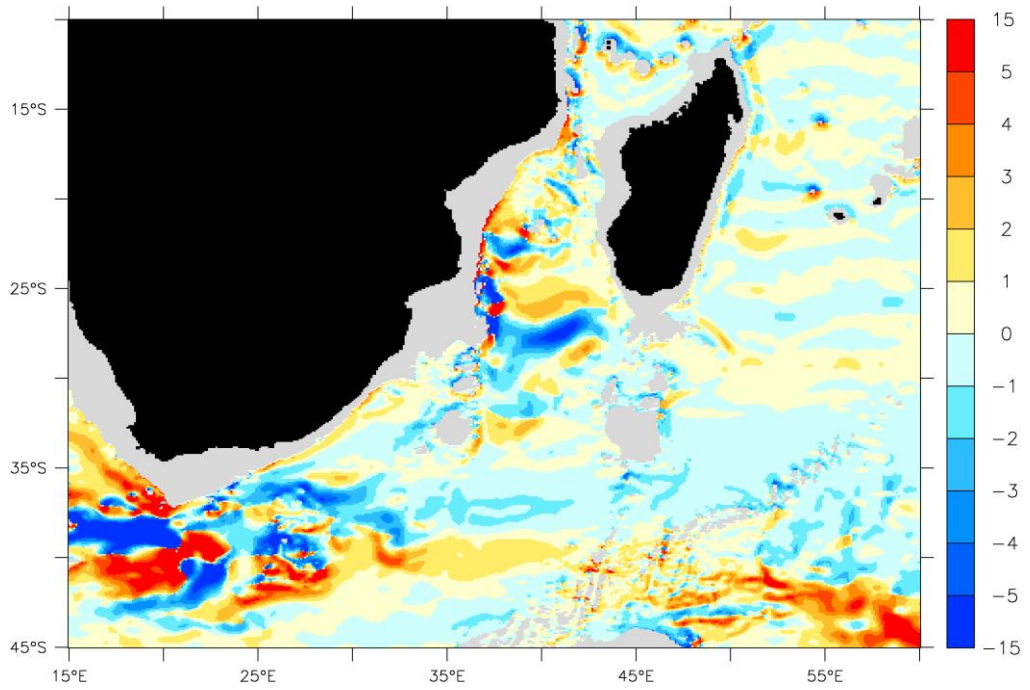

Fig. 3.7: Deep flow in the southwest Indian Ocean. Model speed (1995 – 2004 mean, in cm s^{-1}) averaged between 2000 and 3000 m depth. To indicate the direction of the flow southward velocities are negative.

A quantitative assessment has been made using different sets of virtual floats in the model (ARIANE, see Chapter 2). In a first series about 500,000 floats have been released at 26°E, restricted to eastward flows and densities $\sigma_1 \geq 32.30$, thus representing only the Agulhas Undercurrent portion of the flow. Examples of float trajectories are shown in Fig. 3.8; the full statistics (Tab. 3.3) has been performed over 20 years of integration. About 7 Sv does enter the northern Agulhas Basin between the African continent and the Agulhas Plateau, but almost 70% directly leaves westward across the same section. Since the software only releases floats for inflow conditions (spanned by the bold box in Fig. 3.8) it covers a significant portion of the passing Natal Pulses. This again indicates the strong barotropic influence of the upstream perturbation covering the full water column. About 10% (less than a Sv) of the remaining volume flux of the undercurrent finds its way across 33.5°S and 32°S, mainly directly under the southward flowing Agulhas Current. North of ~29°S float movement is entirely blocked by shallower topography, and only few floats (4% representing 0.3 Sv) do cross some narrow topographic gaps in the Mozambique Ridge (35°E) into the Natal Basin. Virtually no float (less than 0.1 Sv) enters the southern entrance of the Mozambique Channel.

	AUC	
26°E (INI)	4.76	69%
36°S	2.06	30%
45°E	0.00	0%
16°S	0.01	0%
INTERIOR	0.10	1%
TOTAL	6.93	100%

Additional Control Sections		
33.5°S (AC)	0.64	9%
33.5°S	0.04	1%
32.0°S (AC)	0.60	9%
32.0°S	0.02	0%
28.0°S	0.01	0%
36.6°E	0.15	2%
36.6°E (> 33.5S)	0.15	2%
24°S	0.07	1%

Tab. 3.3: Quantitative float calculations, released in the eastward flowing AUC at 26°E (1980 - 1984), marked by the density range $\sigma_1 \geq 32.30$ and integrated for another 20 years (1985 - 2004). Colors correspond to **Fig. 3.8** (The left table spans the control volume indicated by the bold lines in **Fig. 3.8**, additional control sections are marked by thin lines). All numbers are in Sv or relative to the total transport at 26°E.

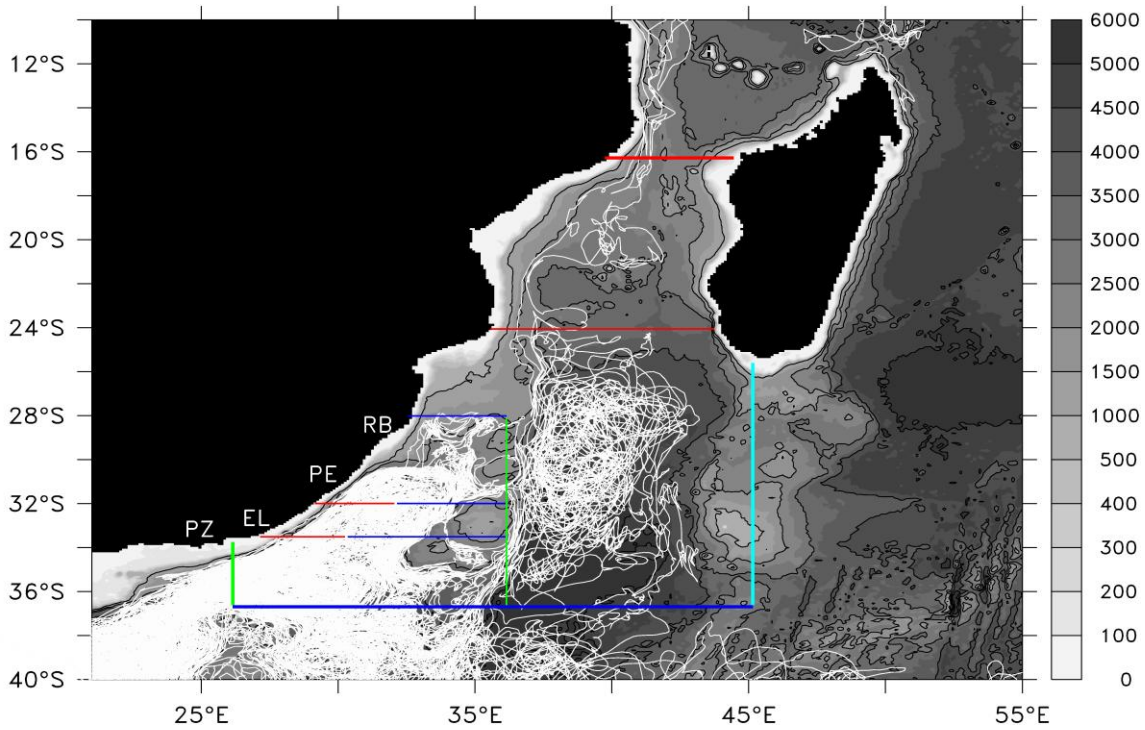

Fig. 3.8: Example floats released continuously over year 1980 in the AUC ($\sigma_1 \geq 32.30$) at 26°E (green line) and integrated until year 2000. Shaded in grey is bathymetry in m, contour lines are drawn with an interval of 1000 m. Colored sections correspond to **Tab. 3.3**. (Note that the full quantification uses much more floats and spans a longer time range). Marked are locations of Richards Bay (RB), Port Edward (PE), East London (EL), and Port Elizabeth (PZ).

To further examine the meridional coherence of the Agulhas Undercurrent along the African coast an additional experiment has been performed where floats have been released at 33.5°S (here not shown). Here, 37% (1 Sv) do form a continuous flow under the Agulhas Current up to 32°S. But again, 60% do directly leave southward across 33.5°S by the Agulhas Current or its associated upstream perturbations. However, it must be stated that a small number of those floats do escape the cull de sac and go round the Mozambique Ridge into the

Natal Basin. A third experiment has been performed in which floats were released at 24°S in the Mozambique Channel and integrated backwards in time to establish from where this water mass came. In this case more than 60% of the floats (11 Sv in total) crossing 24°S northward do enter from the north, i.e. are therefore part of the (re-) circulation in the Mozambique Channel or arrive via Mozambique eddies. About 28% enter the channel from the east (45°E). Just 5% enter from the south and virtually no float (1% or 0.08 Sv) were previously in the Agulhas Undercurrent at 32°S.

All three float experiments draw a similar picture: The continuous flow of the Agulhas Undercurrent along the African shelf is just 1 Sv, sometimes less. Most of the flow is blocked by topography; just a minor portion is able to enter the Natal Basin. A connection between deep floats in the Agulhas Undercurrent and those in the Mozambique Channel is almost absent, tested both forward and backward in time. The same naturally holds for the East Madagascar Undercurrent. There is a natural risk that the model might not capture the correct basic flow of the undercurrent in the southwest Indian Ocean. Water mass structures, especially in combination with topographic slopes, are not a typical strength of z-coordinate models [*Legg et al.*, 2006]. Deficits would also arise if the source regions of the undercurrent would be outside the high-resolution nest, not properly represented at coarse-resolution. However, this might not be reason, since an existent but too low Agulhas Undercurrent was also reported in a global high-resolution model [*Maltrud and McClean*, 2005]. On the other hand this model shows a good reproducibility of the Agulhas Current and Undercurrent transports at 31°S, so it might capture the flow properly. Anyhow, the model clearly demonstrates that mesoscale eddies do interact with deeper levels, which does have important consequences on the observability of the undercurrent structures in time-limited observations.

Another region where eddy – mean flow interactions are suspected to be a main element of the dynamics is in the western boundary current structure east of Madagascar. Although the level of variability is somewhat underrepresented compared to observations there is a clear path of mesoscale features in the model (Fig. 2.8). The western boundary current in that regime, the South East Madagascar Current (SEMC), is fed by the southern core of the South

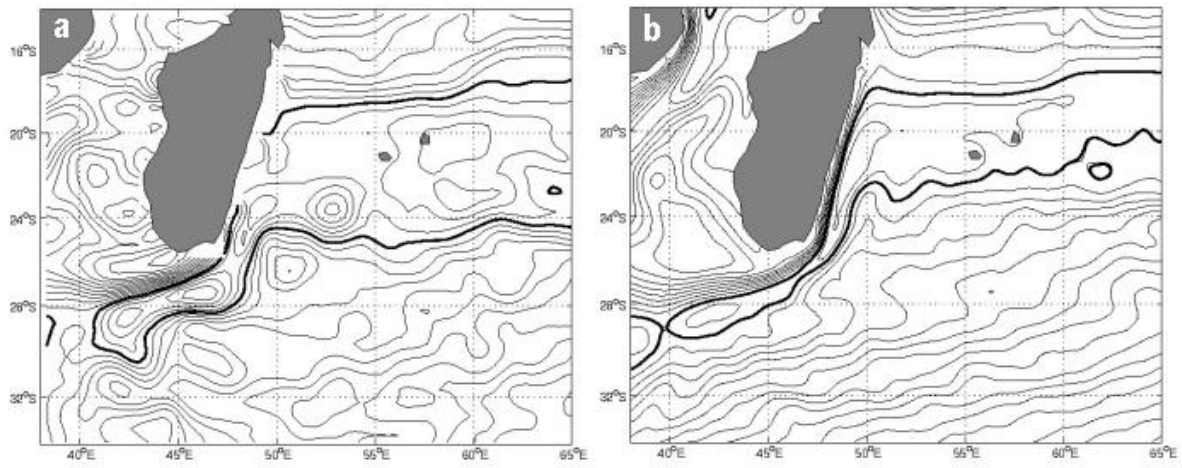

Fig. 3.9: Sea surface height maps indicating the retroflection of the South East Madagascar Current, averaged over 3 years (2001 – 2003): **(a)** Aviso altimeter data, **(b)** model data. The thick lines indicate the 225 cm contour line in **(a)** and the 220.1 cm contour line in **(b)**. [Adopted from ***Siedler et al.*, 2008**]

Equatorial Current [*New et al.*, 2007]. Controversial theories exist about its behavior after shooting over the southern tip of Madagascar, one hypothesis favors a retroflection of the SEMC similar to the Agulhas Current [*Lutjeharms et al.*, 1981, *Lutjeharms*, 1988] another denounces such a dynamical feature due to an apparent lack of long-term eastward flow at 25° - 30°S [*Quartly et al.*, 2006]. However, recent studies have documented the existence of such an eastward South Indian Ocean Countercurrent (SICC) near 25°S from satellite observations [*Siedler et al.*, 2006] and idealized models [*Palastanga et al.*, 2007].

The objective of our study [*Siedler et al.*, 2008] was to document a possible influence of the mesoscale eddies on such a retroflection. For comparison absolute geostrophic currents were used derived from absolute sea surface heights constructed from a combination of satellite altimetry with an improved geoid model from GRACE satellite measurements and an in situ dataset with drifter and hydrographic observations [*Rio et al.*, 2005]. We used the resulting data set Aviso CMDT RIO05, version DT-MADT[3].

Time-averaged sea surface height maps of this observational product and the model solution (Fig. 3.9) clearly indicates a retroflection of the SEMC south of Madagascar and a continuation into the eastward flowing SICC. The model does not produce such a distinct retroflection as in the observational data, but nevertheless shows a similar behavior. More in-depth comparison of the time-dependent flow behavior in this region supported by inspection of eddy tracking analyses [*Chelton et al.*, 2007] expose two basic modes of the SEMC extension (Fig. 3.10): Cyclonic retroflection takes place in the northern Mozambique Basin when the extension is in a south-westerly direction, anticyclonic retroflection occurs in the case of the

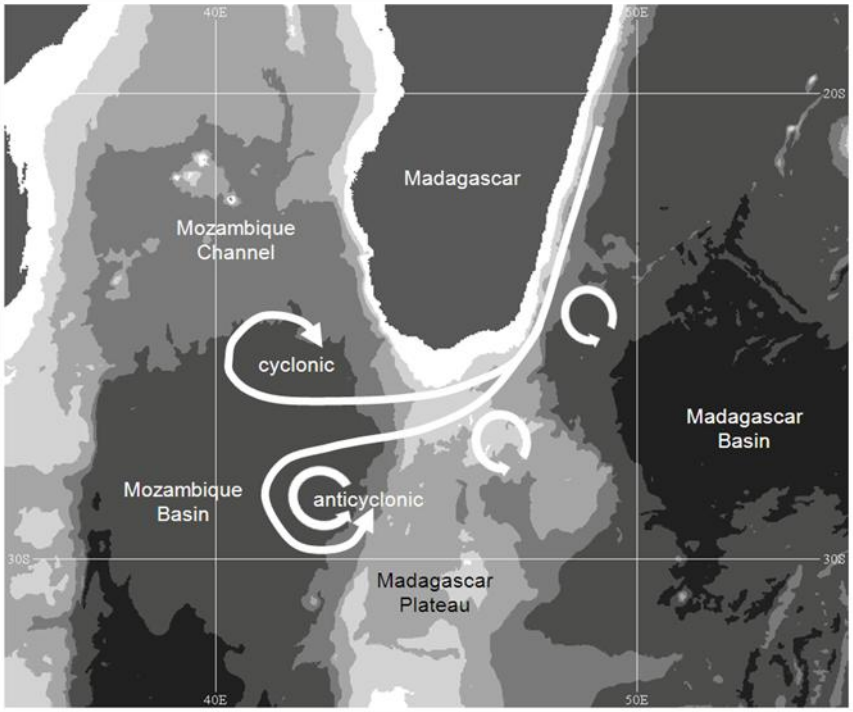

Fig. 3.10: Schematic representation describing the modes of the SEMC extension. The shading indicates isobaths with 1000 m separation. [Adopted from ***Siedler et al.*, 2008**]

[3] The altimeter products used in this study were produced by Ssalto/Duacs and distributed by Aviso with support from Cnes. Rio05 was produced by CLS Space Oceanography Division.

SEMC flowing westward along the southern Madagascar slope.

Quantitative float analyses, similar to those performed for the Agulhas Undercurrent, revealed (in a forward integration) that almost half of the total SEMC volume transport (16 ± 4.5 Sv) contributes to the Agulhas system, most of the remaining flows back into the central Indian Ocean. A backward integration showed that about 40% of SICC water originates from the north, clearly demonstrating the SEMC as a main contributor and supporting the theory of a retroflecting SEMC.

This chapter confirmed a good performance of the model representing the western boundary current structures. The analyses inevitably demonstrated that the prominent mesoscale dynamics arising in the source regions of the Agulhas Current cannot be seen isolated but strongly interacts with the main currents. Due to the barotropic nature of the eddies this interaction is not limited to the upper ocean but also dominates the deep flow. In the case of the Agulhas Undercurrent the mesoscale perturbations might cause a significant portion of the time-mean flow. The next chapter will illustrate the interactions of the upstream perturbations with the Agulhas retroflection and its effect on the Agulhas leakage.

4. The Role of Mesoscale Dynamics in the Interoceanic Transport

The interoceanic transport between the Indian and the Atlantic Ocean is an important element of the global circulation. However, due to the highly non-linear dynamics in the Agulhas system its quantification is extremely difficult as reviews of numbers of direct inflow from geostrophic calculations, complemented by interocean volume transports due to ring translation have shown [*de Ruijter et al.*, 1999a]. Large spreads in both quantifications suggested not only large uncertainties in the assumptions for the calculation but also strong variations in time, a behavior that was demonstrated in previous model results [*Biastoch and Krauss*, 1999, *Reason et al.*, 2003]. In this section it will be demonstrated that the mesoscale processes do have a limiting effect on the interocean exchange, causing more realistic values comparing to a coarse-resolution model that does not explicitly simulate those processes.

What is the role of the host of mesoscale processes interacting with the Agulhas Current in the net volume transfer between the Indian and Atlantic Ocean? This question is addressed by comparing the reference simulation (AG01-R) with an experiment in which the same global model (ORCA05) was integrated without the high-resolution nest in the Agulhas regime. The solution of this non-eddying model portrays the inter-oceanic exchange as a continuation of parts of the Agulhas Current as a smooth current, reminiscent of coarse resolution models typically used for climate studies.

For assessing the portion of the Agulhas water flowing into the South Atlantic analyzing the Eulerian model field is not an optimal choice since mesoscale eddies would lead to enormous fluctuations in the east- and westward velocities (with a small net transport actually representing the leakage). Strong variations of the retroflection longitude [*Lutjeharms and van Ballegooyen*, 1988b] across a transport line would furthermore complicate the assessment

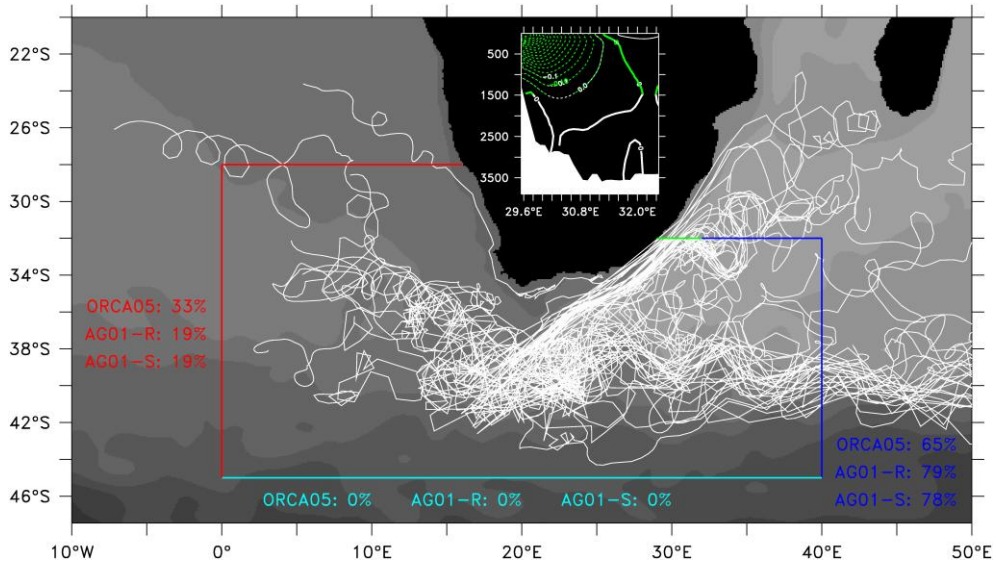

Fig. 4.1: Example float trajectories (model year 1968). The floats have been seeded over the Agulhas Current at 32°S (marked as green line and in the inserted figure), numbers on the control sections (red, light blue, blue) show the fractional amounts of particles crossing the lines during 11 years of integration. Numbers (**Tab. 4.1**) are given for the standard (AG01-R) and sensitivity (AG01-S) experiments as well for the base experiment (ORCA05), the latter without a high-resolution Agulhas nest. [Adopted from ***Biastoch et al.*, 2007**]

which portion of the westward flowing Agulhas Current actually leaks into the Atlantic Ocean and what portion returns (with a certain time delay) back into the Indian Ocean. In this respect a Lagrangian measure based on tracking a number of artificial "fluid" particles (see model section) was used. A large number of particles (each representing an infinitesimal volume element) were seeded continuously over a time span of 4 years into the modeled Agulhas Current at 32°S. The particles are advected by the time-dependent flow field and end up at specified control sections in the Atlantic and Indian Ocean (Fig. 4.1), where they are added up to an average transport. In the reference simulation (AG01-R), with the eddy-resolving Agulhas nest, about 12 Sv (about one fifth of the Agulhas transport of 63 Sv at 32°S, Tab. 4.1) do reach the northern and western sections in the Atlantic, representing the portion of upper water masses of the inter-oceanic exchange south of Africa, consistent with the range of observational estimations [*de Ruijter et al.*, 1999a] based on hydrographical sections (2 - 10 Sv) and Agulhas rings (6 per year × 0.5 - 1.5 Sv). It is to note, however, that this number is lower than a recent estimate (15 Sv) by surface drifters and deep floats [*Richardson*, 2007].

The interocean flux in the high-resolution model is in marked contrast to the coarse-resolution model ORCA05. Without the eddy-resolving nest a much higher fraction (one third) of the Agulhas water enters the Atlantic. The pronounced contrast clearly demonstrates that the supply of Indian Ocean water to the South Atlantic, and thus, the warm water path of the global thermohaline circulation, is not determined by large-scale dynamics alone, but significantly influenced by the regional, mesoscale dynamics of the Agulhas regime.

	AG01-R		AG01-S		ORCA05	
INI	3,02	5%	1,16	2%	3,28	5%
AUC	0,01	0%	0,00	0%	0,00	0%
NORTH_IND	3,39	5%	0,89	1%	2,46	4%
EAST	43,21	68%	45,25	74%	36,05	56%
SOUTH	0,72	1%	1,40	2%	0,00	0%
WEST	5,76	9%	4,96	8%	14,51	22%
NORTH_ATL	6,11	10%	6,47	11%	6,95	11%
SURFACE	0,06	0%	0,07	0%	0,06	0%
INTERIOR	0,83	1%	0,72	1%	1,32	2%
TOTAL	63,12	100%	60,92	100%	64,62	100%
Σ INDIAN	49,62	79%	47,30	78%	41,79	65%
Σ ATLANTIC	11,88	19%	11,43	19%	21,45	33%

Tab. 4.1: Statistics of ARIANE floats for high-resolution reference (AG01-R) and sensitivity experiment without Mozambique Channel (AG01-S), in comparison with the coarse resolution base model without Agulhas nest (ORCA05). Floats are released over years 1968 - 1971 and further integrated until the end of 1978. The interior number gives the amount of floats that have not reached one of the control sections at the end of the integration, usually 1 - 2%. Values are given in Sv and relative to the total transport of the Agulhas Current at 32°S. The red and blue colors correspond to the sections in **Fig. 4.1**. The total transports differ somewhat from the Eulerian transports in the previous chapter due a large sensitivity due to the offshore longitude used for the integration.

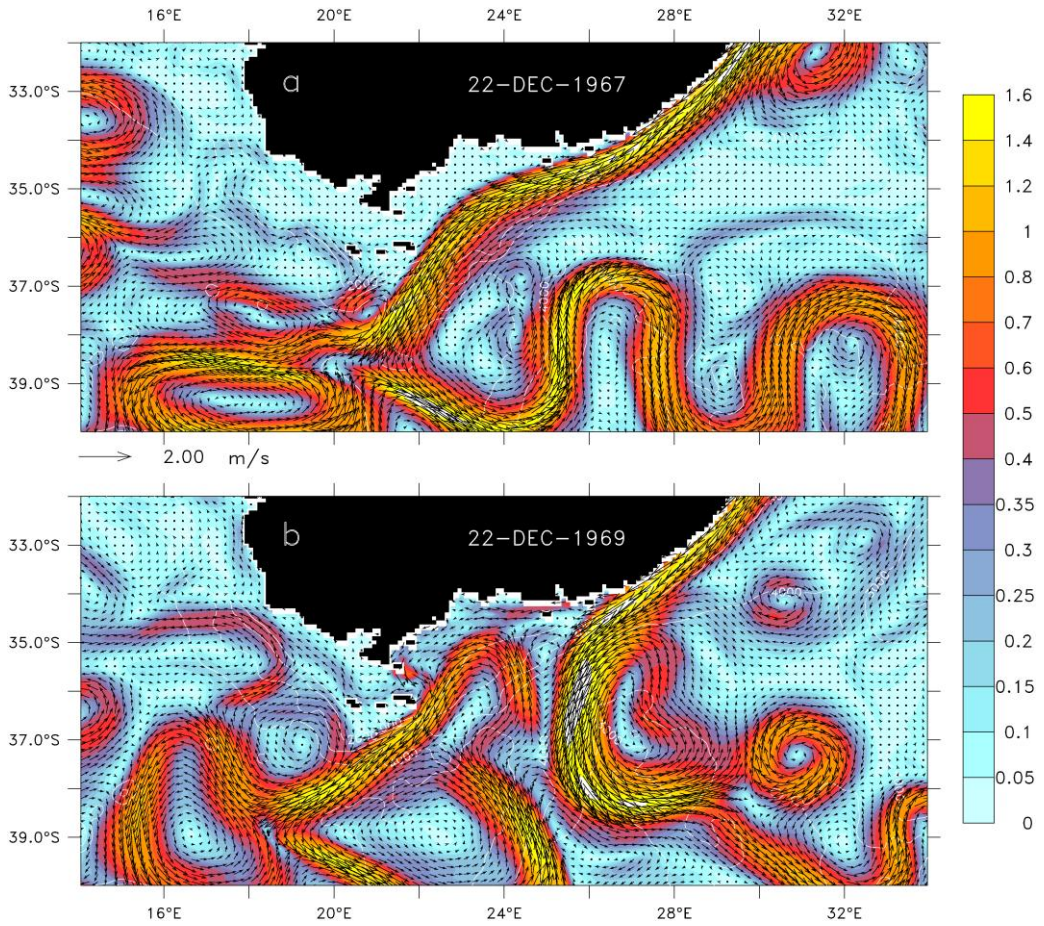

Fig. 4.2: Snapshots of the model south of Africa showing typical situations for (a) regular and (b) upstream retroflection states. Shown are speed (in m s^{-1}) and velocities (only every 2nd vector). [Adopted from ***Biastoch et al.*, 2007**]

Upstream retroflections (examples for regular and upstream retroflection are given in Fig. 4.2) of the Agulhas Current are a prominent feature of the Agulhas dynamics, effectively causing one of the largest western boundary current in the world ocean to short-cut its south-western path for about 2 - 3 months. It has been assumed that these upstream retroflections are forced by passing Natal Pulses [*Lutjeharms and van Ballegooyen*, 1988a] and that they may lead to substantial reductions in the inter-oceanic exchange [*Lutjeharms and De Ruijter*, 1996]. The time evolution of a coastal section along the African continent (Fig. 4.3) indicates that the 5 - 6 Mozambique eddies generated per year are a necessary condition for the generation of Natal Pulses; however, this is not a sufficient condition since only 2 - 5 Natal Pulses per year appear in the same period. Furthermore, only large Natal Pulses, causing a displacement of the core of the Agulhas Current by more than 400 km offshore, in combination with a northward extension of the meander of the Agulhas Return Current are able to cause upstream retroflections. Such instances are rare (about 1 - 2 per year in this example). Similar numbers can be gathered from observations (here not shown), although a one-by-one comparison is difficult to perform due to limitations in the observational data base and would require a dedicated along-track study [*Schouten et al.*, 2002]. Fig. 4.3b shows the almost complete absence of Natal Pulses in a sensitivity experiment without Mozambique eddies (AG01-S). Some single Pulses (e.g. in 1971) were generated by eddies from further offshore, but these are too weak and therefore do not cause any upstream retroflections.

However, the upstream retroflections are found to have a negligible effect on net inter-ocean exchange (Fig. 4.2, Tab. 4.1), thus not supporting previous hypotheses arguing for a large-scale relevance of these events [*Lutjeharms and De Ruijter*, 1996]. The model result that upstream retroflections do not significantly change the magnitude of inter-oceanic volume flux does not imply that mesoscale upstream control mechanisms are unimportant for a proper description of the Agulhas leakage. Although simulating a similar number of Agulhas rings, those in the sensitivity experiment without Mozambique eddies show uncharacteristic regularity in time and space (Fig. 2.8 and Fig. 4.4). As a result the ring paths are much more constrained in the South Atlantic, like "pearls on a string", a behavior that is typical for coarse-resolution (and sometimes even high-resolution) models [*Barnier et al.*, 2006] or more limited studies [*Speich et al.*, 2006]. This may influence the representation of the time-dependent part of the Agulhas leakage and might favor target regions where Agulhas rings finally end up, releasing their anomalous loads of heat and salt erroneously for a proper representation of the thermohaline circulation.

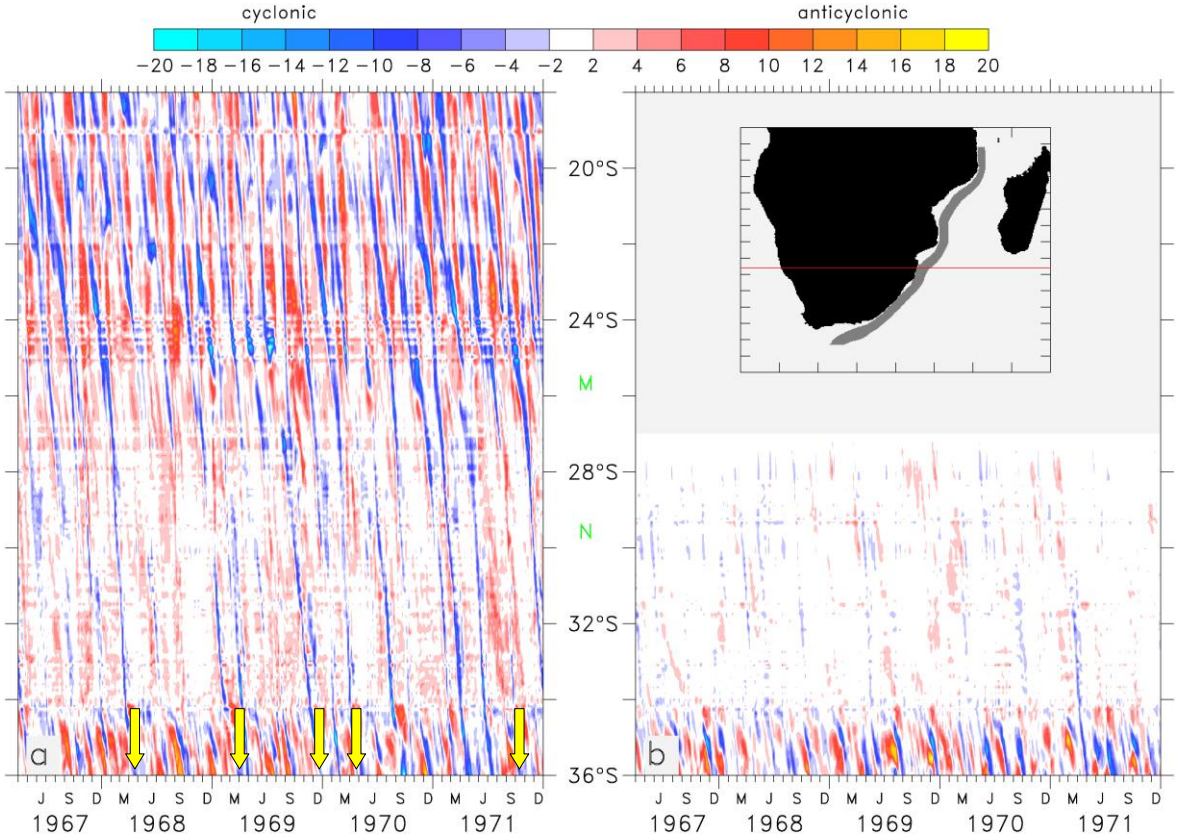

Fig. 4.3: Propagation of upstream perturbations along the African Coast. Shown are Hovmoeller plots of relative vorticity anomalies at 100 m depth for **(a)** reference (AG01-R) and **(b)** sensitivity experiment (AG01-S), the latter not including the Mozambique Channel in the high-resolution nest. The anomalies (in 10^{-6} s^{-1}) were defined relative to the 1962 - 1971 mean and zonally averaged in a section along the African coast. Early retroflections are marked by yellow arrows. (This coastal-following section, shown in the inlet figure, was defined by speeds greater than 0.3 m s^{-1} in the 10-yr mean in the Mozambique Channel and in the Agulhas Current. The area not covered by the sensitivity experiment is marked light gray and by the line in the inlet figure. Bights of Maputo (M) and Natal (N) are marked in green.). [Adopted from ***Biastoch et al., 2007***]

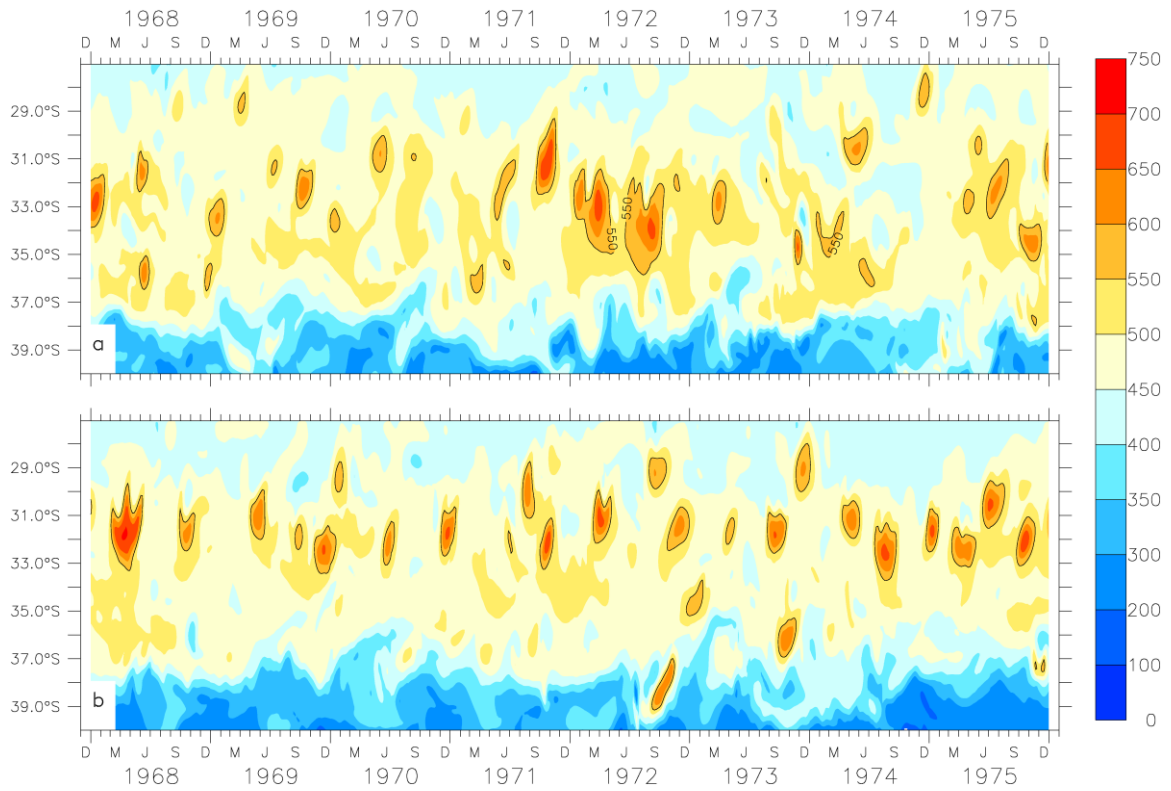

Fig. 4.4: Eddy structures in the Cape Basin. Shown are time series of depth of 10° isotherm (in m) along 5°E for **(a)** reference (AG01-R) and **(b)** sensitivity experiment (AG01-S) not including Mozambique eddies. This depth (in m) is a good indicator for Agulhas Rings crossing this longitude. [Adopted from ***Biastoch et al.*, 2007**]

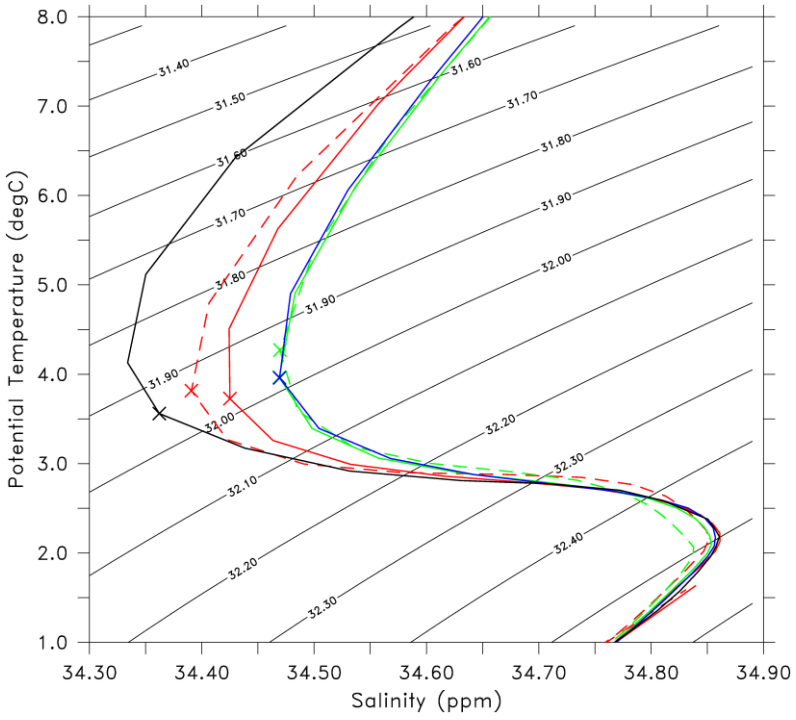

Fig. 4.5: Water mass characteristics in the Cape Basin. T/S diagram averaged over 10°W - 15°E and 40°S - 25°S for the initial conditions [***Conkright et al.*, 2002**] (black), the coarse resolution base model without Agulhas nest (ORCA05) at the end of the 20-year spin-up (year 1958, blue), the reference model (AG01-R, averaged over years 1968 - 1972 (red solid) and 2000 - 2004 (red dashed)), and ORCA05 (green solid and dashed). Values at 1000 m depth are indicated with crosses. Contoured are isolines of σ_1. [Adopted from [***Biastoch et al.*, 2007**]]

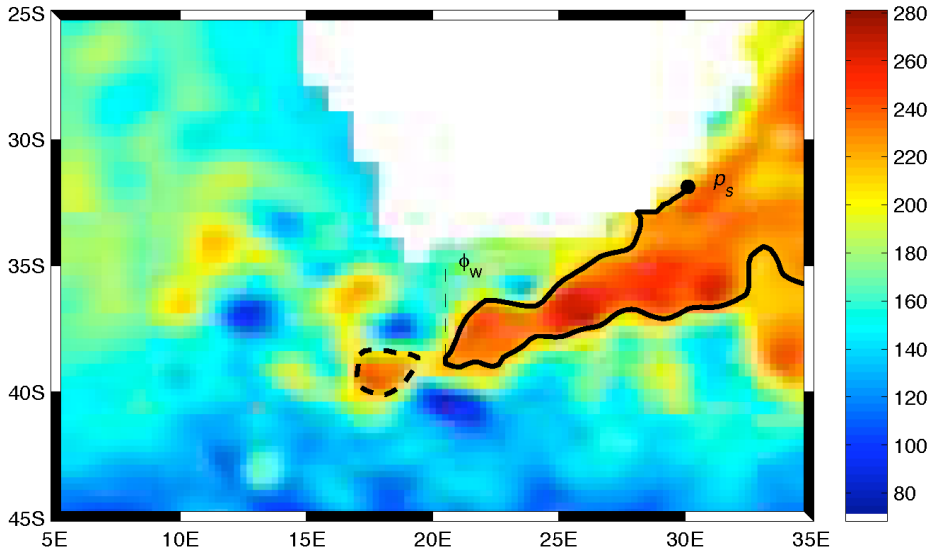

Fig. 4.6: Schematic for determining the retroflection longitude for ALI. Snapshot of dynamic topography (in cm) on July 25, 2007 from the Aviso data. The thick black line is the Agulhas Current path C_A, starting at point p_s, as detected by the algorithm. The dashed closed contour is the associated ring found by the ring detection algorithm,. The westward extension, defined by the algorithm, is indicated by ϕ_w. [Adopted from ***van Sebille et al.*, 2008**]

An analysis of water mass properties in the Cape Basin (Fig. 4.5) indicates the discrepancy between observations and the global model (note that its deep T/S characteristics (green lines) do strongly differ from the observed, climatological state (black)); the deficit is characteristic of coarse-resolution models linked to a typical problem of current climate models where intermediate water masses in the South Atlantic tend to become eroded, constructing deficits in the formation of deep water in the subpolar North Atlantic [*Banks et al.*, 2007]. In contrast the high-resolution model, initialized with the same end state of the spinup (blue line) of the coarse-resolution model, has acted to shift the water mass properties (red solid to red-dashed lines) towards a more realistic water-mass structure (black).

A more precise quantification than demonstrated earlier in this chapter is only possible in the virtual reality of a numerical model. However, for a monitoring effort of the inter-annual variability of Agulhas leakage an index that could be easily obtained from observations would be a perfect choice. Van Sebille derived an "Agulhas Leakage Index" (ALI) [*van Sebille et al.*, 2008] by using the dynamical consistency of ocean models. The basic concept is to relate the longitude at which the retroflection of the Agulhas Current takes place (i.e., actually shedding Agulhas rings) with the interoceanic transport. Such a relation can be derived from ocean models and applied to satellite observations to convert its retroflection longitudes to a leakage number in Sverdrup.

The basic procedure is pictured in Fig. 4.6: Composite satellite altimetry maps are used to calculate geostrophic velocities. At 32°E the point p_s with highest southward velocity is selected and tracked as a counter-clockwise contour representing the path of the Agulhas Current (C_A). Special conditions make sure that only those contours are followed that represent a proper retroflection. South of Africa the westernmost extension of C_A (ϕ_w in Fig.

4.6) is taken as the input for the index. To demonstrate its robustness over a wide range of leakages this quantity was obtained from three different models: The global model (ORCA05, without the Agulhas nest) and the high-resolution Agulhas nest (AG01) of this study, and the operational 1/8° global Navy Coastal Ocean Model (NCOM) [*Barron et al.*, 2006]. A linear relation between the retroflection longitude and the time-varying interoceanic transport was established. As outlined earlier in this chapter this interoceanic transport was obtained by annual releases of virtual floats and measured by integrating their transports across the GoodHOPE line [*Ansorge et al.*, 2005] in the Cape Basin (i.e., clearly westward of the retroflection). Although all three models revealed strong differences in the simulation of interoceanic transport (with a mean leakage of 16.5 ± 5.1 Sv in AG01, 32.3 ± 6.9 Sv in ORCA05, 2.7 ± 1.1 Sv in NCOM), all solutions exhibit a linear relation between the two quantities. A significant correlation over all models was found, whereby the retroflection longitude leads the interocean flux by 75 days (correlation coefficient R = -0.85). The time lag can broadly be understood if assuming a mean Agulhas ring translation speeds of 5.2 km day^{-1} [*Schouten et al.*, 2000] which corresponds to 95 days over the typical distance between retroflection and the GoodHOPE line.

Based on these model solutions we can thus conclude that the ALI does represent a useful first-order estimate of the interocean flux; it slightly overestimates the transports in AG01 (Fig. 4.7a), underestimating them in ORCA05. If applied to the Aviso satellite altimetry data it results in an estimated leakage of 11.9 ± 3.3 Sv. Not surprisingly this value is close to the interoceanic transport obtained in AG01 consistent with its substantially improved performance in representing the correct longitude of retroflection. It should be mentioned that

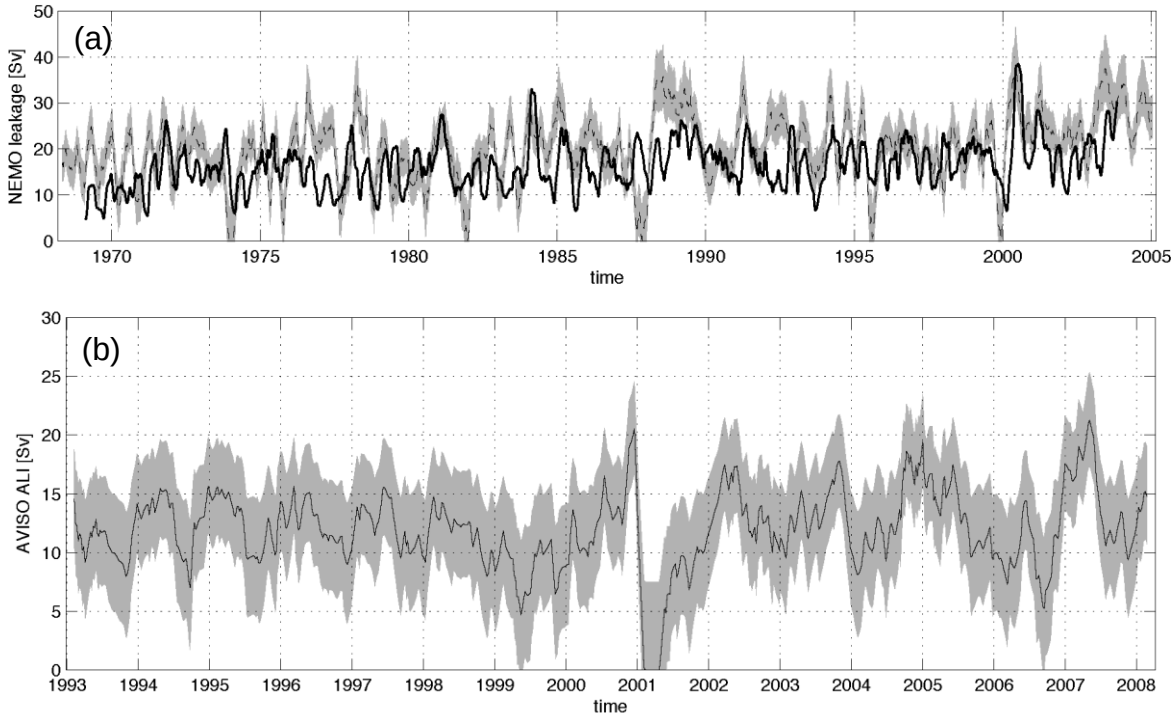

Fig. 4.7: Agulhas leakage as revealed by the ALI (a) Measured Agulhas leakage (solid) and the estimated leake from the ALI (dashed, with gray area as 95% confidence interval) for AG01, **(b)** Estimated leakage from ALI for Aviso altimetry data. [Adopted from ***van Sebille et al.*, 2008**]

the ALI from observations clearly shows a reported upstream retroflection in year 2001 [*de Ruijter et al.*, 2004], thus giving a handle on the transient effect of such extreme case on the interoceanic transport.

More generally, the analyses of this chapter demonstrated that a proper estimation of the interoceanic transport from Eulerian observations is a difficult task. Even in the dynamically consistent framework of a numerical model one has to rely on Lagrangian analysis due to the dominance of mesoscale eddies and recirculation features. The eddies, however, are an important constituent and have to be explicitly simulated for a correct determination of the leakage. A proper quantification of the eddying flow regime from observations strongly relies on the availability of a good coverage in time and space. In this respect satellite data are the best choice, probably supported and tuned by monitoring arrays such as the GoodHOPE line [*Ansorge et al.*, 2005].

5. The Influence of the Mesoscale Agulhas Leakage on the Atlantic Meridional Overturning Circulation

After evaluating the general importance of the mesoscale processes in the Agulhas region and the effects due to the upstream perturbations, this chapter demonstrates the relevance of the mesoscale Agulhas dynamics for the large-scale circulation, in particular the meridional overturning circulation (MOC) in the Atlantic Ocean (Fig. 5.1).

To assess the effect of mesoscale processes in the Agulhas leakage the novel scheme which adopts a two-way nested model is considered. More specifically, the following approach is used: Firstly, it starts using the global ocean-sea-ice model with a grid resolution of nominal 1/2° (ORCA05) that reasonably captures the different processes of deep-water formation due to the thermohaline and wind forcing and its effect on the variability of the MOC, but that does not resolve mesoscale processes. In a second configuration (AG01), the resolution is substantially refined (to 1/10°) in the Agulhas regime in this model by adopting the "two-way nesting" scheme. The high-resolution nest provides a realistic simulation of the mesoscale dynamics of the Agulhas retroflection (as shown in the previous chapters). The nest feds back to the global model at all time scales [*Debreu et al.*, 2008] so that the global circulation is able to respond to the mesoscale dynamics introduced by this limited region. Comparison of the two model simulations, the one hosting an Agulhas nest (AG01) and the one without (ORCA05), thus provides us an effective means to identify the dynamical impact of the mesoscale Agulhas dynamics on the basin-scale MOC.

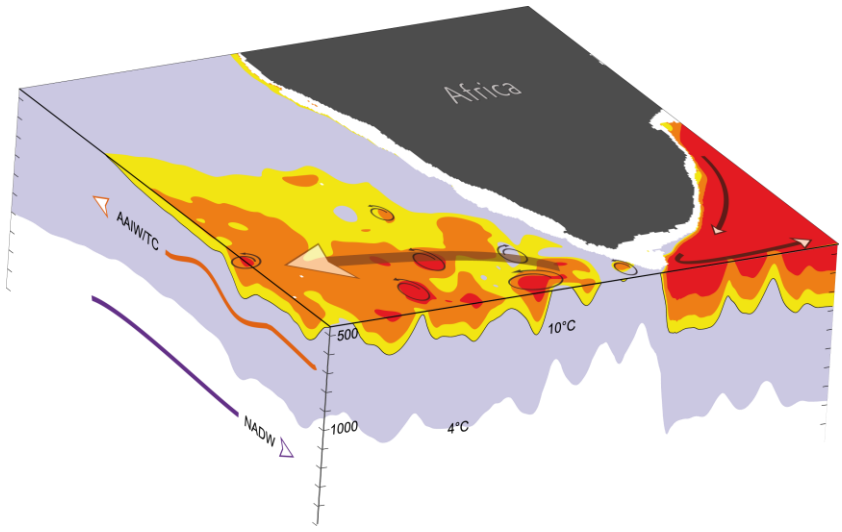

Fig. 5.1: Schematic of the embedding of the Agulhas system in the large-scale circulation. The figure shows an idealized snapshot (5-day mean around 15-Sep-2004) of the model with temperature volumes 4-10°C (blue), 10-11°C (yellow), 11-12.5°C (orange) and >12.5 °C (red). The upper interface is at 450 m since this is the depth with the largest contrast between the Indian and Atlantic Ocean. Circulation features as the Agulhas Current and Return Current, Agulhas rings are marked as black arrows. The grey arrow in the Cape Basin indicates the general drift of Agulhas rings (shown by circled arrows). The upper (Antarctic Intermediate Water and Thermocline Water) and lower (North Atlantic Deep Water) limbs of the meridional overturning circulation are shown as orange and blue arrows. [Adopted from ***Biastoch et al.*, 2008c**]

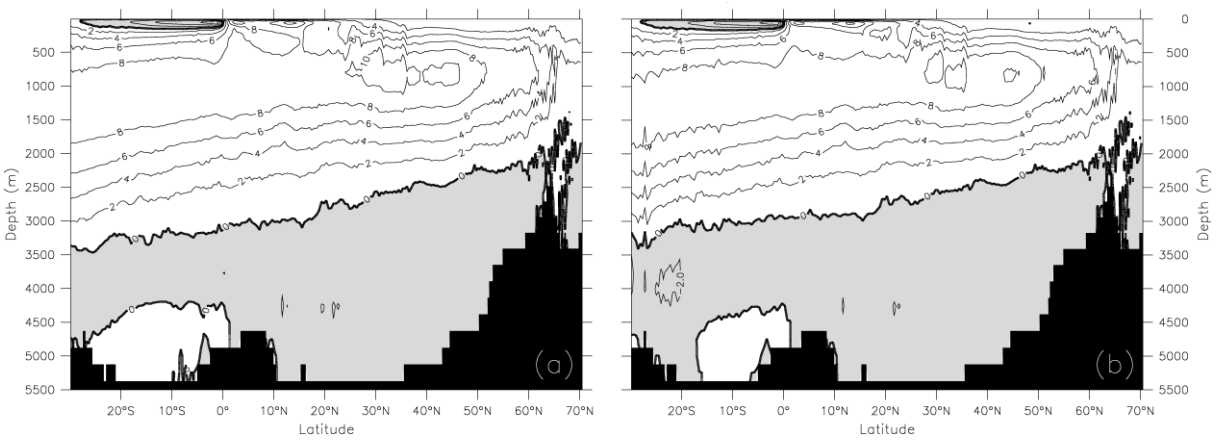

Fig. 5.2: Time-mean meridional overturning streamfunction in the simulated Atlantic sector (a) without (ORCA05) and **(b)** with (AG01) high-resolution Agulhas nest (Data are in Sv, averaged over the period 1980 - 2004; white background indicates clockwise flow, i.e. the North Atlantic Deep Water cell, gray background indicates anti-clockwise). [Adopted from ***Biastoch et al.*, 2008c**]

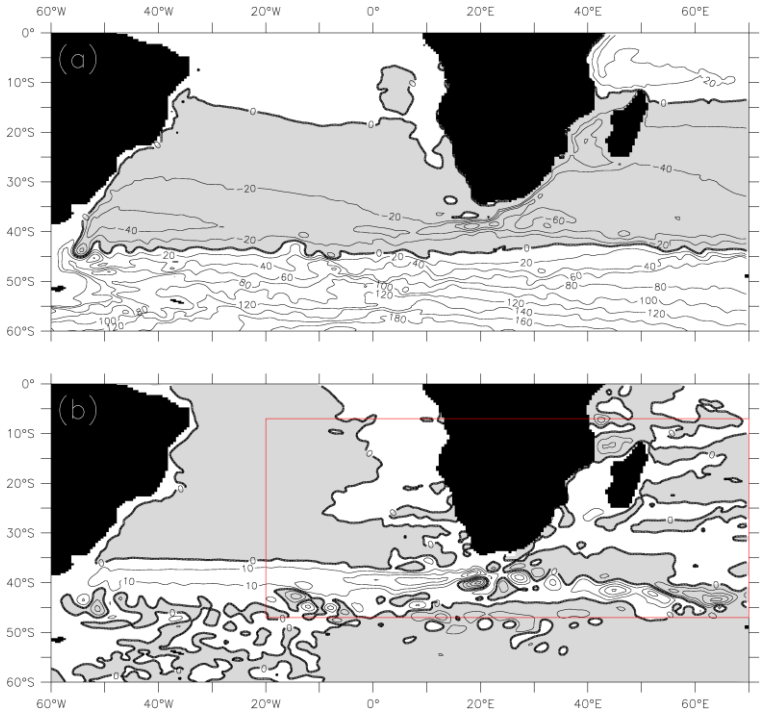

Fig. 5.3: Effect of the mesoscale Agulhas circulation on the horizontal gyre circulation. (a) Barotropic streamfunction (contour interval 20 Sv) in the global coarse resolution model without the high-resolution Agulhas nest (gray background indicates the anti-cyclonic gyre circulation, e.g. the subtropical super-gyre in the South Atlantic and Indian Ocean). **(b)** Difference (contour interval 10 Sv, positive values do have a white background) due to the high-resolution Agulhas nest (marked by the red box). All data are averaged over the period 1980 - 2004. [Adopted from ***Biastoch et al.*, 2008c**]

The introduction of the high-resolution Agulhas nest has little effect on the time-mean MOC transport; differences are, quite surprisingly, less than a Sv (Fig. 5.2) despite the large difference in the mean interoceanic transport from the Indian Ocean to the Atlantic with realistic 12 Sv in AG01 and 21.5 Sv in ORCA05 (see previous chapter). The difference of 9.5 Sv has to be attributed to the horizontal gyre circulation in the South Atlantic, where the high-resolution Agulhas nest causes a reduction and shrinking of the subtropical super-gyre in the

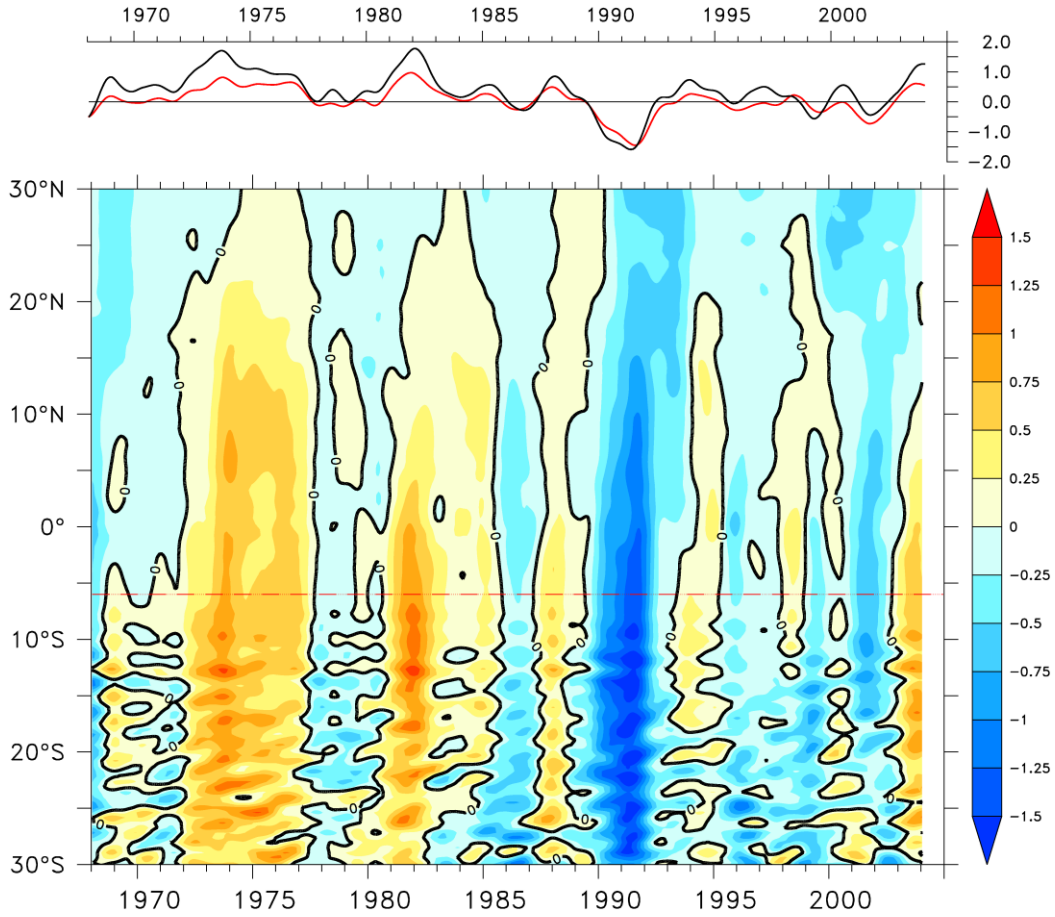

Fig. 5.4: Low-pass filtered Agulhas-induced MOC anomalies. The Hovmoeller diagram (lower panel) shows the difference of the Atlantic MOC (at 1000 m depth, in Sv) between model experiments with (AG01) and without high-resolution Agulhas nest (ORCA05). The upper panel compares the (low-pass filtered) time series of the MOC anomalies (red) at 6°S (dashed red line in lower panel) with the corresponding anomalies of the North Brazil Current (in Sv) at this latitude (black). [Adopted from ***Biastoch et al.*, 2008c**]

South Atlantic and Indian Ocean (Fig. 5.3). As a direct consequence this would imply that even a perfect knowledge of the interoceanic transport would not lead to an improved understanding of the upper limb of the MOC.

However, there is a marked difference in the MOC variability (Fig. 5.4): an isolation of the MOC variability induced by the mesoscale fluctuations in the Agulhas (i.e., the "Agulhas-induced MOC anomalies" by comparing the experiments with and without the Agulhas nest) illustrates an effect on inter-annual to decadal time scales. The clear temporal structure and meridional coherence of the Agulhas-induced MOC anomalies is remarkable: anomalies of more than ± 1.5 Sv emerge at 30°S, rapidly propagating towards the equator, with only slight damping. In the northern hemisphere the anomalies then gradually fade; at 20°N amplitudes are below 0.5 Sv. The anomalies propagate from 30°S into the northern hemisphere within one month, similar to the boundary wave processes that have been discussed in previous model studies [*Johnson and Marshall*, 2002, *Getzlaff et al.*, 2005]. The speed of the MOC anomalies is about 1 - 2 orders of magnitude faster than the usual translational speed of Agulhas rings which is a few cm s^{-1} [*Garzoli et al.*, 1999]. It furthermore has to be noticed that the modeled Agulhas rings are moving roughly in a zonal direction, projecting onto Rossby wave signals at the western boundary of the high-resolution nest at 20°W. This solution thus suggests a prime role of wave processes along the western boundary of the Atlantic Ocean in the rapid

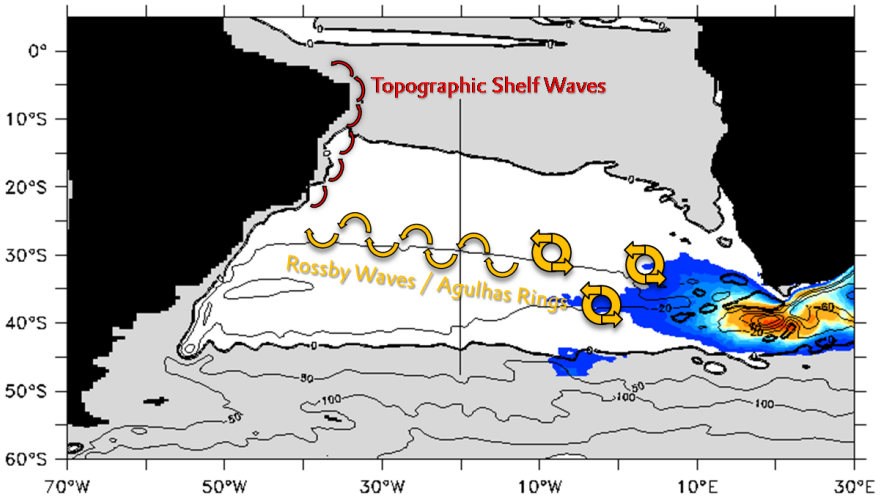

Fig. 5.5: Illustration of the wave processes conveying Agulhas-induced anomalies in the upper limb of the MOC. The contour lines depict the time-mean barotropic streamfunction, indicating the anti-cyclonic (white area) subtropical gyre in the South Atlantic, the color information shows the time-mean eddy kinetic energy. The arrows give an illustration of the dynamic processes transporting anomalies originating in the Agulhas across the South Atlantic (yellow) and along the continental slope of South America (red). [Adopted from ***Biastoch et al.*, 2008c**]

communication of the signal (Fig. 5.5), a mechanism that was theoretically described in idealized model studies [*van Sebille and van Leeuwen*, 2007].

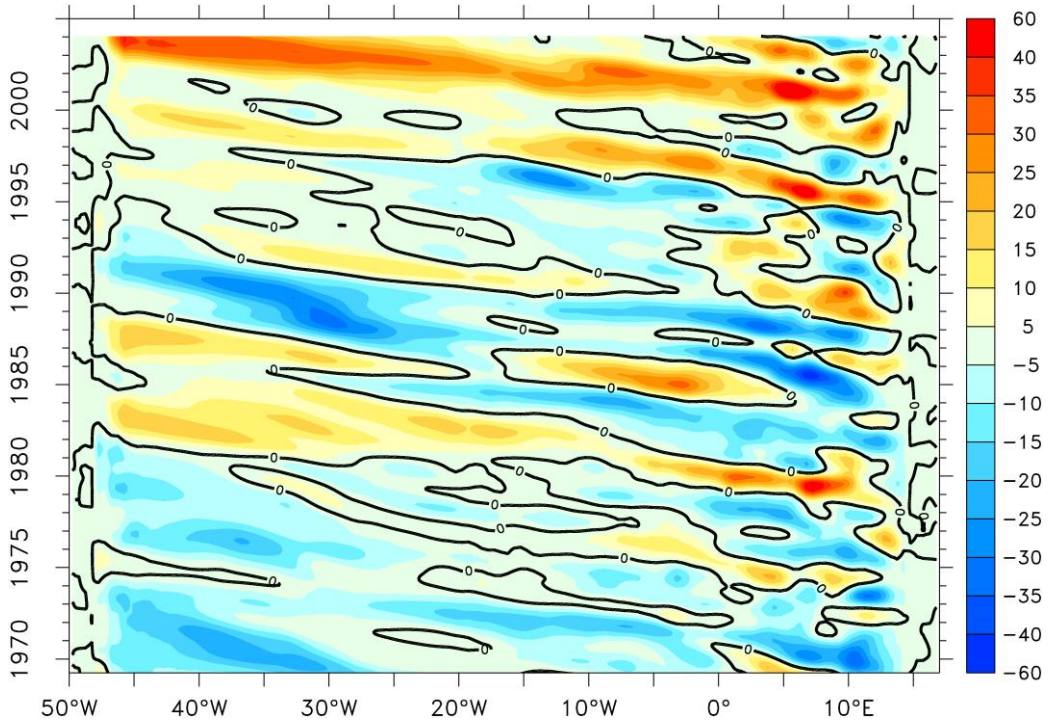

Fig. 5.6: Decadal modulation of mesoscale variability by the Agulhas nest. Hovmoeller diagram of the difference (in cm) of the 10°C-isotherm depth at 30°S between the global model runs with and without high-resolution Agulhas nest. [Adopted from ***Biastoch et al.*, 2008c**]

Agulhas rings are the dominating vehicle of the inter-basin exchange into the Cape Basin off the west coast of South Africa. They can be reasonably traced by the depth of the 10°C isotherm [*van Aken et al.*, 2003] where the anti-cyclonic rotation sense of a ring causes depressions in the isothermal surfaces. The evolution of this quantity along 30°S at full temporal resolution (here not shown) indicates translation speeds of about 6 cm s^{-1}, in good agreement with observations of Agulhas rings [*van Aken et al.*, 2003]. These signals do reveal a decadal modulation (Fig. 5.6) which is also evident in the sea surface height, in good comparison with the observational record (here not shown). The modulation has a similar temporal characteristic as the Agulhas-induced MOC signal, suggesting a projection of the zonally-propagating, meridional velocity anomalies onto the zonally-integrated MOC transport in this latitude range. Further north, the MOC variability signal is mainly concentrated at the western boundary, shown by a comparison of the MOC transport anomalies with the transport anomalies of the North Brazil Current (Fig. 5.4).

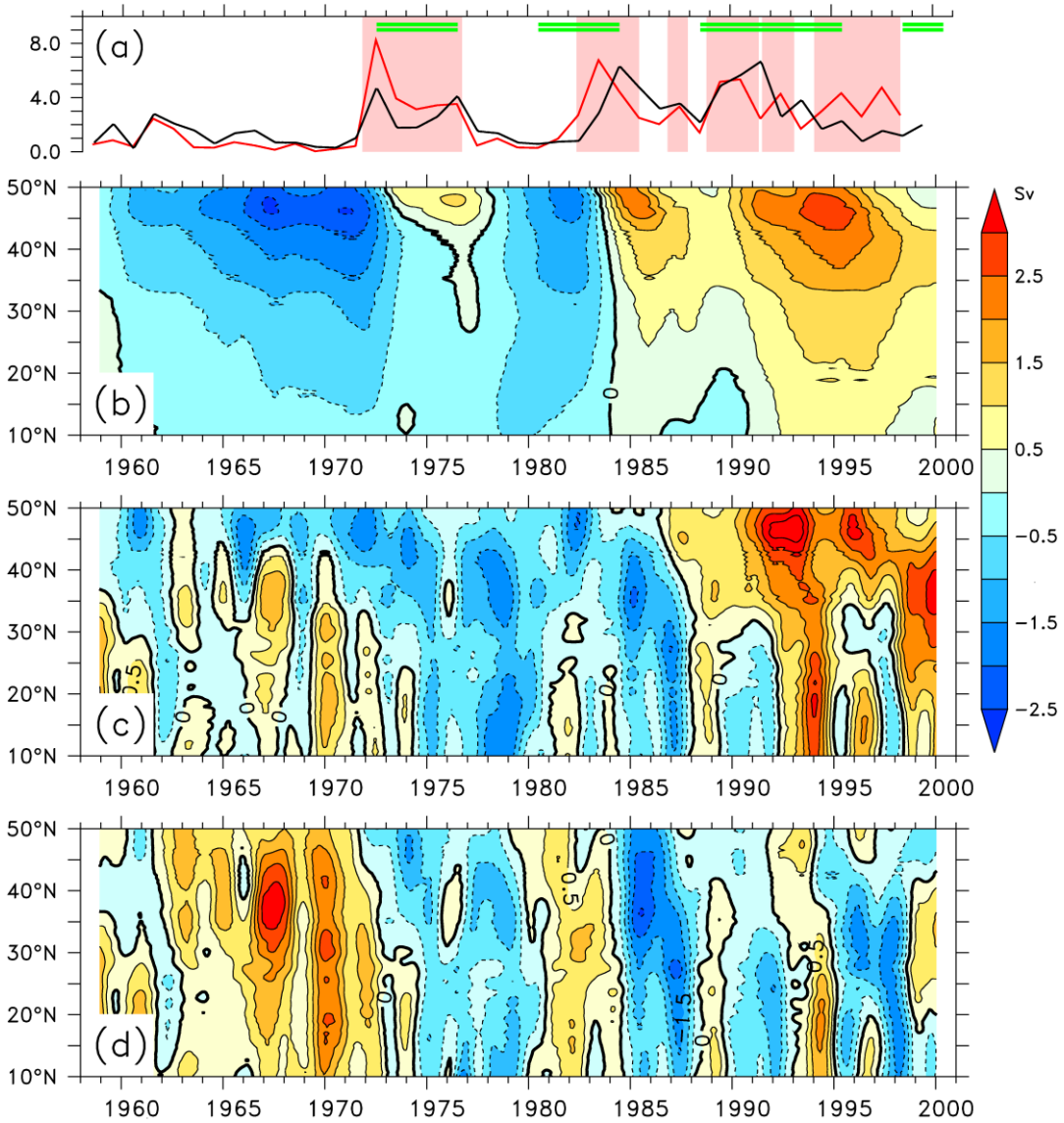

Fig. 5.7: Propagation of MOC anomalies in the North Atlantic (a) Labrador Sea Water (LSW) formation rate (defined by the increase of LSW volume during wintertime convection, in Sv) for Exp. REF (black) and HEAT+SALT (red, shaded are values above 2.5 Sv), indicated by green lines are phases of positive NAO; and Hovmoeller diagrams depicting the meridional propagation of MOC anomalies (defined by the streamfunction at 1000 m depth) for **(b)** HEAT+SALT, **(c)** REF and **(d)** WIND. [Adopted from ***Biastoch et al.*, 2008b**]

How significant are the Agulhas-induced MOC anomalies and what is their relative importance compared to the decadal MOC signals, originating from the subpolar North Atlantic? While changes in the dense overflow at the Greenland-Scotland Ridge appeared to have comparatively minors effects in the last decades [*Beismann and Barnier*, 2004, *Latif et al.*, 2006] MOC changes due to modifications in the formation of LSW were identified in model studies as basin-scale signals on decadal time scales [*Böning et al.*, 2006]. All previous studies have suggested that variability in the sub-arctic thermohaline forcing cause mid-latitude MOC changes on the order of 1 - 2 Sv. As demonstrated by the present simulations, an MOC signal of the same order can be caused by Agulhas anomalies.

To identify the contribution of different forcing mechanism on the inter-annual – decadal variability of the Atlantic MOC a suite of sensitivity experiments has been performed with the global base model (ORCA05). Building on previous studies with coarse [*Eden and Willebrand*, 2001] and medium-resolved [*Getzlaff et al.*, 2005] Atlantic models the present sequence of experiments helps to elucidate the relative effects of the variability in wind and thermohaline forcing. The reference experiment under CORE forcing (REF[4]) was complemented by a perturbation experiment (HEAT+SALT) in which the inter-annually varying forcing for 1958 - 2001 was artificially restricted to the thermohaline fluxes, whereas the climatological (repeated-year) CORE forcing was used for the wind stress forcing. Similar experiments were performed where only the heat flux forcing (HEAT) or the wind forcing (WIND) was used inter-annually. It is quite obvious that NAO-related onsets of increased Labrador Sea Water (LSW) production (Fig. 5.7a) are followed by positive MOC anomalies at the southern edge of the subpolar gyre (near 45°N) with a delay of about 1 - 2 years, then

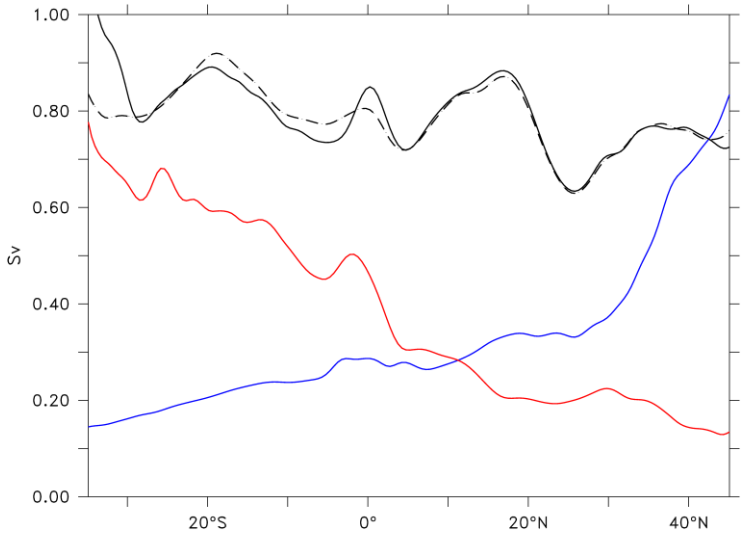

Fig. 5.8: Attribution of inter-annual MOC variability to different mechanisms. All curves represent the standard deviation of the low-pass filtered NADW cell strength as a function of latitude, obtained from different experiments: global coarse-resolution model without (ORCA05, dashed) and with Agulhas nest (AG01, black), and the standard deviation of the MOC difference of both experiments, prescribing the effect of the Agulhas-induced MOC anomalies (red), and by subpolar deep water formation events (blue). The latter is estimated by the sensitivity experiment (HEAT). [Adopted from ***Biastoch et al.*, 2008c**]

[4] Note that this configuration differs in some parameterization choices from those used to host the Agulhas model. The largest modification is the use of an eddy parameterization [*Gent and McWilliams*, 1990]. These differences are of minor consequence for the present analysis.

rapidly communicating southward (Fig. 5.7b). By superimposing the effect of wind-driven circulation variability the clear relation to the convection variability disappears (Fig. 5.7c). The prominent decadal signal governing the buoyancy-forced MOC anomalies is now masked by a stronger, higher-frequency signal. Accordingly, the meridionally-coherent structure of the former is replaced by wind-driven MOC anomalies with maximum amplitudes at varying latitudes, sometimes of a more local character, sometimes spanning a larger latitudinal extent.

An intriguing result of this set of experiments is that the total MOC variability (in REF) can to a high degree be explained by linearly superimposing the individual, buoyancy- and wind-forced MOC anomalies [*Biastoch et al.*, 2008b]. This is a remarkable property given the inherently nonlinear nature of large-scale oceanic flows and has important ramifications for the interpretation of the nature of observed MOC variability in the subtropical – mid-latitude Atlantic.

What is the relative impact of these contributions? A summary depiction of the various influence factors is provided in Fig. 5.8, showing the standard deviation of the inter-annual MOC strength as a function of latitude. In the experiments with (dashed black curve) and without the Agulhas nest (solid black), the variability is similar, mainly dominated by local wind variability (cf. Fig. 5.7). While this signal is characterized by MOC anomalies on relatively short (intra-seasonal – inter-annual) time scales and little meridional coherence, an isolation of the signals propagating from the north (blue, Exp. HEAT) and from the south (red, Agulhas-induced) contribute to basin-scale variations (Fig. 5.9). It is obvious that the signal introduced by subpolar deep water formation is reduced even more rapidly, so that (and because of the different meridional latitudes of both source regions) both effects have a similar strength in and south of the tropical North Atlantic.

The variability of the inter-hemispheric transport of deep-water is therefore a combination of effects from the north as well as the south. Even at the prominent latitude of 26°N where actual MOC observations are being taken [*Cunningham et al.*, 2007, *Kanzow et al.*, 2006, *Kanzow et al.*, 2007] the influence of Agulhas rings is significant and not negligible compared to the effects of sub-arctic origin previous studies have been concentrated on.

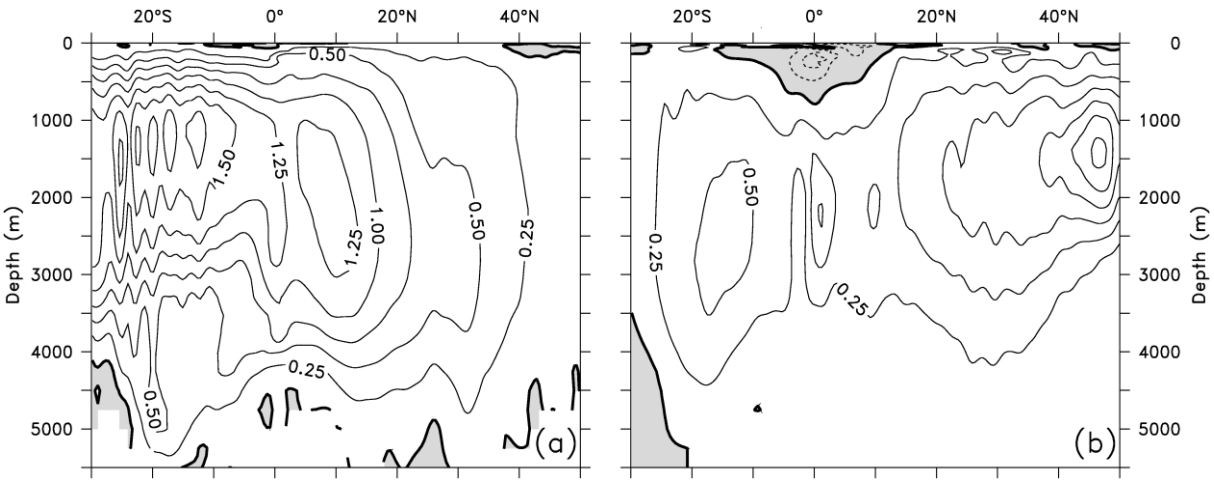

Fig. 5.9: Basin-scale signal of mesoscale Agulhas-induced and deep water formation related anomalies. Overturning differences (in Sv) **(a)** ORCA05 – AG01 (1973-1975 average minus 1990-1992 average, see **Fig. 5.4**), **(b)** ORCA05 HEAT (1976 minus 1972, see **Fig. 5.7**b).

6. Summary and Outlook

The goal of this thesis was to study the role of the mesoscale processes in the Agulhas leakage and its impact on the Atlantic meridional overturning circulation (MOC). A requirement for this was to set up an ocean model that simulates all known elements of the greater Agulhas system down to the mesoscale and that is connected to the rest of the world ocean. To fulfill both requirements a high-resolution Agulhas grid was nested into a global coarse-resolution model using an innovative "two-way" nesting approach. It was demonstrated that the combination of both grids is not only an effective compromise between high resolution and global domain, but the only means to identify the feedback of the mesoscale Agulhas dynamics on the large-scale circulation.

The model is based on a framework of ocean models within the DRAKKAR collaboration building upon the latest developments of the European model system NEMO. It was set up utilizing state-of-the-art numerical developments such as partial cells, advanced advection schemes or consistent atmospheric data sets, all shown to be essential for a proper simulation of the Agulhas system. The resulting simulation was verified to be consistent with the current knowledge of the Agulhas dynamics and existing observations in this region; it simulates a proper global ocean circulation but also realistic details of the mesoscale flow features around the southern tip of Africa.

What has been learnt by this study? Every single analysis presented here demonstrated the overall dominance of mesoscale processes in the greater Agulhas region. In the South East Madagascar Current offshore eddies do lead to different modes of the current extension, one favoring cyclonic flow into the Mozambique Channel, the other anticyclonic eddies drifting towards southwest. Eddies generated in the central Mozambique Channel introduce strong perturbations into the western boundary current systems off the African coast by triggering Natal Pulses. These are causing offshore displacements of the Agulhas Current leading to strong changes in the volume transport of the Agulhas Current and eventually to upstream retroflections of the current back into the Indian Ocean. Due to the barotropic nature of the interplay with Mozambique eddies and Natal Pulses the Agulhas Undercurrent is also affected and exhibits strong fluctuations similar to the observed ones. This raised the question what portion of the Agulhas Undercurrent is a coherent flow throughout the South Indian Ocean and what portion is virtually generated by passing Natal Pulses.

It is evident that the upstream perturbations have a substantial effect on the mesoscale dynamics in the Agulhas retroflection area. The comparison of the reference model with the sensitivity experiment not including the Mozambique Channel at high resolution inevitably demonstrated that they are not only triggering the shedding of Agulhas rings but also represent a main contribution to the vast range of eddy structures in the Cape Basin and beyond. However, the existence of upstream perturbations does not alter the net interocean exchange from the Indian Ocean to the Atlantic, the Agulhas leakage.

The magnitude of the Agulhas leakage was found, however, to be strongly dependent on the representation of Agulhas rings and other associated mesoscale processes in the retroflection area; more specifically, it was found to be unrealistically large in the coarse-

resolution case. However, in the time-mean the bulk of this difference is modifying the horizontal circulation of the subtropical super-gyre rather than the meridional overturning circulation (MOC) of the Atlantic Ocean. An isolation of the effect of the mesoscale Agulhas dynamics, on the other hand, demonstrated that it acts as the source of decadal-scale undulations in thermocline depth, a dynamical signal carried across the South Atlantic by Rossby waves and into the North Atlantic by wave processes along the American continental slope.

The resulting decadal signal in MOC transport gradually diminishes from south to north, but has an amplitude in the tropical Atlantic of comparable magnitude to the effect of sub-arctic deep water formation processes discussed in previous studies. This suggests that a proper representation of the mesoscale processes in the Agulhas regime is thus vital for the correct interpretation of meridional transport changes across the equator, and even at mid-latitudes in the North Atlantic where major MOC monitoring efforts have been established.

How can the nested model configuration be used to further expand the knowledge of the dynamics in the greater Agulhas regions and its impact on the large-scale circulation? An important issue is the response of the Agulhas circulation and its interocean leakage to atmospheric changes. An analysis of the variability of the South East Madagascar Current revealed a correlation with climate indices [*Siedler et al.*, 2008], in particular with the Indian Ocean Dipole index [*Saji et al.*, 1999]. It will be interesting to see if such linkages also exist for the other components of the current system, e.g., the transport through the Mozambique Channel, the Agulhas Current or its leakage into the South Atlantic. An isolation of the atmospherically driven variability from the variability internally generated in the model would be possible by additional, dedicated model realizations probing different variations on inter-annual to decadal time scales. Towards this goal, a set of corresponding experiments is planned that will utilize some variants of the original CORE forcing data, such as the DRAKKAR Forcing Data Set #3 [*Brodeau et al.*, 2007] or the newly developed version 2 of the CORE data set [*Large and Yeager*, 2008].

One particular question stated in the introduction, the possible effect of changing wind stress patterns on the Agulhas leakage and the MOC has not been addressed so far. In this study the main focus was rather on the mesoscale variability in the Agulhas system and its dynamical causes for inter-annual – decadal variations of the interocean leakage. An investigation of effects of, e.g., a southward migration of the mid-latitude westerlies as expected from climate scenarios (IPCC), requires several decadal experiments since the fast signal propagation found due to Agulhas rings will certainly be complemented by advective signals effectively transporting heat and salt towards the subpolar North Atlantic. In order to unravel dynamic and thermodynamic mechanisms, it is planned to run experiments with artificially modified wind pattern, motivated by paleo and climate change studies. Latitudinal shifts of the South Indian anticyclone will have consequences for the partitioning of the different source regions of the Agulhas Current [*Biastoch et al.*, 1999]; a shift of the subtropical front, which is under current climate conditions about 5° south of Africa, will immediately impact the degree of retroflection of the Agulhas Current, and therefore the amount of Agulhas leakage. These sensitivity experiments with artificially shifted wind fields will subsequently be complemented by runs using complete forcing from given IPCC scenarios,

providing a means to assess the effect of global climate change on an Agulhas regime with resolved eddies.

A model configuration is not carved in stone and it is important to identify critical model parameters that further improve solution. Apart from modifications, e.g. in the viscosity schemes and its coefficients that affect details of the western boundary current structure, an important consideration is to modify the size of the high-resolution nest. Demonstrated by the success of the sensitivity experiment without the Mozambique eddies this aids to further isolate certain dynamical elements. Since the model has been shown to underestimate the intensity of mesoscale eddies east of Madagascar a first step should include an extension of the nest towards Australia. This could include the eddies spawned into the South Indian Ocean by instabilities of the Leeuwin Current [*Fang and Morrow*, 2003], and thus a possible, remote effect adding to the upstream perturbations of the Agulhas system.

Overall, the study added to the quantitative understanding of the Agulhas system as a key region of the global circulation and helped to unravel the nature and consequences of the interactions between the mesoscale and the mean flow. From a technical point of view it was shown that the combination of a global coarse-resolution base model and a high-resolution grid, "two-way" nested by the AGRIF approach, provides a powerful and flexible tool for the study of regional structures and their interplay with the global circulation.

Acknowledgments

First of all I gratefully thank my mentor Prof. Claus Böning for long-term support during all stages of my work and lots of good discussions.

With his optimistic attitude Prof. Johann Lutjeharms had good influence on this analysis; it was great to host him in Kiel.

I also thank several IFM-GEOMAR and international colleagues for various discussions and support: Joachim Dengg, Markus Scheinert, Gerold Siedler, Lisa Beal, Erik van Sebille, Gurvan Madec, Bernard Barnier, Anne-Marie Treguier, to name just a few.

This is a modeling work and I gratefully thank the NEMO, DRAKKAR, AGRIF and Ariane system teams for their technical support. Especially Jean-Marc Molines and Rachid Benshila gave significant input to get the configuration going. Erik Behrens prepared the title figure and the movie.

The experiments have been integrated at the High Performance Computing Center Stuttgart (HLRS), the German High Performance Computing Centre for Climate- and Earth System Research Hamburg (DKRZ) and the Computing Centre at Kiel University. Thanks also for the long-term support by the IFM-GEOMAR Computing Centre.

Thanks to my parents for laying solid grounds. But, most of all, to Martina, Bjarne and Amelie – what would I be without you? Thanks for your patience with me during the final stage of this thesis.

Literature

[*Alvarez-Garcia et al.*, 2008] Alvarez-Garcia, F., M. Latif, and A. Biastoch, On multidecadal and quasi-decadal North Atlantic Variability. *J. Climate*, *21*, in press, 2008.

[*Ansorge et al.*, 2005] Ansorge, I., S. Speich, J. Lutjeharms, G. Goni, C. Rautenbach, P. Froneman, M. Rouault, and S. Garzoli, Monitoring the oceanic flow between Africa and Antarctica: Report of the first GoodHope cruise. *S. Afr. J. Sci.*, *101*(1-2), 29–35, 2005.

[*Ansorge and Lutjeharms*, 2007] Ansorge, I. J., and J. Lutjeharms, The cetacean environment off southern Africa, in *The Whales and Dolphins of the Southern African Subregion*, edited by P. Best and P. Folkens, pp. 5–13, Cambridge University Press, Cambridge, 2007.

[*Arakawa and Hsu*, 1990] Arakawa, A., and Y.-J. G. Hsu, Energy Conserving and Potential-Enstrophy Dissipating Schemes for the Shallow Water Equations. *Mon. Wea. Rev.*, *118*, 1960–1969, 1990.

[*Arakawa and Lamb*, 1981] Arakawa, A., and V. R. Lamb, A potential enstrophy and energy conserving scheme for the shallow water equations. *Mon. Wea. Rev.*, *109*, 18–36, 1981.

[*Arhan et al.*, 2003] Arhan, M., H. Mercier, and Y. Park, On the deep water circulation of the eastern South Atlantic Ocean. *Deep–Sea Res. I*, 50(7), 889–916, 2003.

[*Backeberg et al.*, 2008] Backeberg, B., J. Johannessen, L. Bertino, and C. Reason, The greater Agulhas Current system: An integrated study of its mesoscale variability. *J. Operational Oceanogr.*, *1*, 29–44, 2008.

[*Banks et al.*, 2007] Banks, H., S. Stark, and A. Keen, The Adjustment of the Coupled Climate Model HadGEM1 toward Equilibrium and the Impact on Global Climate. *J. Climate*, *20*(23), 5815–5826, 2007.

[*Barnier et al.*, 2006] Barnier, B., G. Madec, T. Penduff, J.-M. Molines, A.-M. Treguier, A. Beckmann, A. Biastoch, C. Böning, J. Dengg, J. Gulev, S. Le Sommer, E. Remy, C. Talandier, S. Theetten, and M. Maltrud, Impact of partial steps and momentum advection schemes in a global ocean circulation model at eddy permitting resolution. *Ocean Dynamics*, *56*, doi: 10.1007/s10236–006–0082–1, 2006.

[*Barron et al.*, 2006] Barron, C., A. Kara, P. Martin, R. Rhodes, and L. Smedstad, Formulation, implementation and amination of vertical coordinate choices in the Global Navy Coastal Ocean Model (NCOM). *Ocean Modelling*, *11*(3-4), 347–375, 2006.

[*Beal and Bryden*, 1999] Beal, L., and H. Bryden, The velocity and vorticity structure of the Agulhas Current at 32S. *J. Geophys. Res.*, *104*, 5151–5176, 1999.

[*Beal et al.*, 2006] Beal, L., T. Chereskin, Y. Lenn, and S. Elipot, The Sources and Mixing Characteristics of the Agulhas Current. *J. Phys. Oceanogr.*, *36*(11), 2060–2074, 2006.

[*Beal and Bryden*, 1997] Beal, L. M., and H. L. Bryden, Observations of an Agulhas Undercurrent. *Deep–Sea Res.*, *44*, 1715–1724, 1997.

[*Beismann and Barnier*, 2004] Beismann, J.-O., and B. Barnier, Variability of the meridional overturning circulation of the North Atlantic: sensitivity to overflows of dense water masses. *Ocean Dynamics*, *54*, doi: 10.1007/s10236–003–0088–x, 2004.

[*Béranger et al.*, 2006] Béranger, K., B. Barnier, S. Gulev, and M. Crépon, Comparing 20 years of precipitation estimates from different sources over the world ocean. *Ocean Dynamics*, *56*(2), 104–138, 2006.

[*Biastoch*, 1998] Biastoch, A., Zirkulation und Dynamik in der Agulhasregion anhand eines numerischen Modells, Ph.D. thesis, Berichte aus dem Institut für Meereskunde Nr. 301, Kiel, 1998.

[*Biastoch et al.*, 2008a] Biastoch, A., L. Beal, J. R. E. Lutjeharms, and T. G. D. Casal, Variability and coherence of the Agulhas Undercurrent in a high-resolution ocean general circulation model. Submitted to *J. Phys. Oceanogr, 2008a.*

[*Biastoch et al.*, 2008b] Biastoch, A., C. W. Böning, J. Getzlaff, J.-M. Molines, and G. Madec, Causes of interannual-decadal variability in the meridional overturning circulation of the mid-latitude North Atlantic Ocean. *J. Climate*, **21**, 6599-6615, *2008b.*

[*Biastoch et al.*, 2008c] Biastoch, A., C. W. Böning, and J. R. E. Lutjeharms, Agulhas leakage dynamics affects decadal variability in Atlantic overturning circulation. *Nature*, **456**, 489-492, *2008c.*

[*Biastoch et al.*, 2007] Biastoch, A., C. W. Böning, J. R. E. Lutjeharms, and M. Scheinert, Mesoscale perturbations control inter-ocean change south of Africa. *Geophys. Res. Lett.*, **35**, L20602, *2008.*

[*Biastoch and Krauss*, 1999] Biastoch, A., and W. Krauss, The role of mesoscale eddies in the source regions of the Agulhas Current. *J. Phys. Oceanogr.*, *29*, 2303–2317, 1999.

[*Biastoch et al.*, 1999] Biastoch, A., C. J. C. Reason, J. R. E. Lutjeharms, and O. Boebel, The importance of flow in the Mozambique Channel to seasonality in the greater Agulhas Current system. *Geophys. Res. Lett.*, *26*, 3321–3324, 1999.

[*Blanke et al.*, 1999] Blanke, B., M. Arhan, G. Madec, and S. Roche, Warm Water Paths in the Equatorial Atlantic as Diagnosed with a General Circulation Model. *J. Phys. Oceanogr.*, *29*(11), 2753–2768, 1999.

[*Blanke and Delecluise*, 1993] Blanke, B., and P. Delecluise, Variability of the Tropical Atlantic Ocean Simulated by a General Circulation Model with Two Different Mixed-Layer Physics. *J. Phys. Oceanogr.*, *23*, 1363–1388, 1993.

[*Boebel et al.*, 2003] Boebel, O., J. Lutjeharms, C. Schmid, W. Zenk, T. Rossby, and C. Barron, The Cape Cauldron: a regime of turbulent inter-ocean change. *Deep–Sea Res. II*, *50*, 57–86, 2003.

[*Böning et al.*, 2006] Böning, C. W., M. Scheinert, J. Dengg, A. Biastoch, and A. Funk, Decadal variability of subpolar gyre transport and its reverberation in the North Atlantic overturning. *Geophys. Res. Lett.*, *33*, doi: 2006GL026906RR, 2006.

[*Boudra and de Ruijter*, 1986] Boudra, D. B., and W. P. M. de Ruijter, The wind-driven circulation of the South Atlantic-Indian Ocean – II. periments using a multi-layer numerical model. *Deep–Sea Res.*, *33*, 447–482, 1986.

[*Brodeau et al.*, 2007] Brodeau, L., B. Barnier, T. Penduff, A.-M. Treguier, and S. Gulev, An ERA-40 based atmospheric forcing for global ocean circulation models. *Ocean Modelling*, , *submitted, 2007.*

[*Bryden et al.*, 2005a] Bryden, H., L. Beal, and L. Duncan, Structure and Transport of the Agulhas Current and Its Temporal Variability. *Journal of Oceanography*, *61*(3), 479–492, 2005a.

[*Bryden et al.*, 2005b] Bryden, H., H. R. Longworth, and S. A. Cunningham, Slowing of the Atlantic meridional overturning circulation at 25N. *Nature*, *438*, 655–657, 2005b.

[*Byrne et al.*, 1995] Byrne, D. A., A. L. Gordon, and W. F. Haxby, Agulhas Eddies: A synoptic view using Geosat ERM data. *J. Phys. Oceanogr.*, *25*, 902–917, 1995.

[*Cai*, 2006] Cai, W., Antarctic ozone depletion causes an intensification of the Southern Ocean super-gyre circulation. *Geophys. Res. Lett.*, *33*(3), 2006.

[*Chanut et al.*, 2008] Chanut, J., B. Barnier, L. Debreu, W. Large, L. Debreu, T. Penduff, J.-M. Molines, and P. Mathiot, Mesoscale eddies in the Labrador Sea and their contribution to convection and re-stratification. *J. Phys. Oceanogr.*, , *doi: 10.1175/2008JPO3485.1, 2008.*

[*Chapman et al.*, 2003] Chapman, P., S. Marco, R. Davis, and A. Coward, Flow at intermediate depths around Madagascar based on ALACE float trajectories. *Deep–Sea Res. II*, *50*(12-13), 1957–1986, 2003.

[*Chelton et al.*, 2007] Chelton, D., M. Schlax, R. Samelson, and R. de Szoeke, Global observations of large oceanic eddies. *Geophys. Res. Lett.*, *34*, 2007.

[*Chelton et al.*, 1998] Chelton, D. B., R. A. DeSzoeke, M. G. Schlax, K. E. Naggar, and N. Siwertz, Geographical Variability of the First Baroclinic Rossby Radius of Deformation. *J. Phys. Oceanogr.*, *28*, 433–460, 1998.

[*Conkright et al.*, 2002] Conkright, M., J. Antonov, O. Baranova, T. Boyer, H. Garcia, F. Gelfeld, D. Johnson, R. Locarnini, P. Murphy, T. O'Brien, I. Smolyar, and C. Stephens, World Ocean Database 2001, Volume 1: Introduction, *NOAA Atlas NESDIS 42, U.S. Government Printing Office 13*, NOAA, Washington, D.C., 2002. 167 pp.

[*Coward and de Cuevas*, 2005] Coward, A., and B. de Cuevas, The OCCAM 66 level model: model description, physics, initial conditions and ternal forcing, *internal document 99*, Southampton Oceanography Centre, Southampton, UK, 2005.

[*Cunningham et al.*, 2007] Cunningham, S., T. Kanzow, D. Rayner, M. Baringer, W. Johns, J. Marotzke, H. Longworth, E. Grant, J. Hirschi, L. Beal, C. Meinen, and J. Marotzke, Temporal Variability of the Atlantic Meridional Overturning Circulation at 26.5 N. *Science*, *317*(5840), 935, 2007.

[*Dai and Trenberth*, 2002] Dai, A., and K. Trenberth, Estimates of Freshwater Discharge from Continents: Latitudinal and Seasonal Variations. *Journal of Hydrometeorology*, *3*(6), 660–687, 2002.

[*de Ruijter et al.*, 2004] de Ruijter, W., H. Aken, E. Beier, J. Lutjeharms, R. Matano, and M. Schouten, Eddies and dipoles around South Madagascar: formation, pathways and large-scale impact. *Deep–Sea Res. I*, *51*(3), 383–400, 2004.

[*de Ruijter et al.*, 2002] de Ruijter, W., H. Ridderinkhof, J. Lutjeharms, M. Schouten, and C. Veth, Observations of the flow in the Mozambique Channel. *Geophys. Res. Lett.*, *29*(10), 140–1, 2002.

[*de Ruijter*, 1982] de Ruijter, W. P. M., Asymptotic analysis of the Agulhas and Brasil Current systems. *J. Phys. Oceanogr.*, *12*, 361–373, 1982.

[*de Ruijter et al.*, 1999a] de Ruijter, W. P. M., A. Biastoch, S. S. Drijfhout, J. R. E. Lutjeharms, R. Matano, T. Pichevin, P. J. van Leeuwen, and W. Weijer, Indian-Atlantic Inter-Ocean change: Dynamics, Estimation and Impact. *J. Geophys. Res.*, *104*, 20,885–20,910, 1999a.

[*de Ruijter et al.*, 1999b] de Ruijter, W. P. M., P. J. van Leeuwen, and J. R. E. Lutjeharms, Generation and evolution of Natal Pulses, solitary meanders in the Agulhas Current. *J. Phys. Oceanogr.*, *29*, 3043–3055, 1999b.

[*DeBoyer Montegut et al.*, 2007] DeBoyer Montegut, C., J. Vialard, S. Shenoi, D. Shankar, F. Durand, C. Ethe, and G. Madec, Simulated seasonal and interannual variability of mixed layer heat budget in the northern Indian Ocean. *J. Climate*, *20*(13), 3249–3268p, 2007.

[*Debreu et al.*, 2008] Debreu, L., C. Vouland, and E. Blayo, AGRIF: Adaptive grid refinement in Fortran. *Computers and Geosciences*, *34*(1), 8–13, 2008.

[*Donohue et al.*, 2000] Donohue, K., E. Firing, and L. Beal, Comparison of three velocity sections of the Agulhas Current and Agulhas Undercurrent. *J. Geophys. Res.*, *105*, 28, 2000.

[*Donohue and Toole*, 2003] Donohue, K., and J. Toole, A near-synoptic survey of the Southwest Indian Ocean. *Deep–Sea Res. II*, *50*(12-13), 1893–1931, 2003.

[*Eden and Willebrand*, 2001] Eden, C., and J. Willebrand, Mechanism of interannual to decadal variability of the North Atlantic circulation. *J. Climate*, *14*, 2266–2280, 2001.

[*Fang and Morrow*, 2003] Fang, F., and R. Morrow, Evolution, movement and decay of warm-core Leeuwin Current eddies. *Deep–Sea Res. II*, *50*(12-13), 2245–2261, 2003.

[*Fichefet and Morales Maqueda*, 1999] Fichefet, T., and M. A. Morales Maqueda, Modelling the influence of snow accumulation and snow-ice formation on the seasonal cycle of the Antarctic sea-ice cover. *Climate Dynamics*, *15*, 251–268, 1999.

[*Flores et al.*, 1999] Flores, J.-A., R. Gersonde, and F. J. Sierro, Pleistocene fluctuations in the Agulhas Current Retroflection based on calcareous plankton record. *Marine Micropaleontology*, *37*, 1–22, 1999.

[*Fox and Maskell*, 1996] Fox, A. D., and S. J. Maskell, A nested primitive equation model of the Iceland-Faeroe front. *J. Geophys. Res.*, *101*, 18259–18278, 1996.

[*Friocourt et al.*, 2005] Friocourt, Y., S. Drijfhout, B. Blanke, and S. Speich, Water Mass port from Drake Passage to the Atlantic, Indian, and Pacific Oceans: A Lagrangian Model Analysis. *J. Phys. Oceanogr.*, *35*(7), 1206–1222, 2005.

[*Garzoli et al.*, 1999] Garzoli, S. L., P. L. Richardson, C. M. Duncombe Rae, D. M. Fratantoni, G. J. Goni, and A. J. Roubicek, Three Agulhas Rings Observed During the Benguela Current periment. *J. Geophys. Res.*, *104*, 20,971–20,986, 1999.

[*Gent and McWilliams*, 1990] Gent, P. R., and J. McWilliams, Isopycnal mixing in ocean circulation models. *J. Phys. Oceanogr.*, *20*, 150–155, 1990.

[*Getzlaff et al.*, 2005] Getzlaff, J., C. W. Böning, C. Eden, and A. Biastoch, Signal propagation in the North Atlantic overturning. *Geophys. Res. Lett.*, *32*, doi:10.1029/2004GL021002, 2005.

[*Gordon*, 2003] Gordon, A. L., Oceanography: The brawniest retroflection. *Nature*, *421*, 904–905, 2003.

[*Gordon and Haxby*, 1990] Gordon, A. L., and W. F. Haxby, Agulhas Eddies invade the South Atlantic: Evidence from Geosat altimeter and shipboard conductivity-temperature-depth survey. *J. Geophys. Res.*, *95*, 3117–3125, 1990.

[*Gordon et al.*, 1987] Gordon, A. L., J. R. E. Lutjeharms, and M. L. Gründlingh, Stratification and Circulation at the Agulhas Retroflection. *Deep–Sea Res.*, *34*, 565–599, 1987.

[*Griffies et al.*, 2007] Griffies, S., A. Biastoch, C. W. Böning, F. Bryan, G. Danabasoglu, E. Chassignet, M. England, R. Gerdes, H. Haak, R. W. Hallberg, W. Hazeleger, J. Jungclaus, , W. G. Large, G. Madec, A. Pirani, B. L. Samuels, M. Scheinert, A. S. Gupta, C. A. Severijns, H. L. Simons, A. M. Treguier, M. Winton, S. Yeager, and J. Yin, Coordinated Ocean-ice Reference periments (COREs). *Ocean Modelling*, *submitted, 2007*.

[*Howard and Prell*, 1992] Howard, W. R., and W. L. Prell, Late quarternary surface circulation of the southern Indian Ocean and its relationship to orbital variations. *Paleooceanogr.*, *7*, 79–117, 1992.

[*Jakobsson et al.*, 2000] Jakobsson, M., N. Cherkis, J. Woodward, R. Macnab, and B. Coakley, New grid of Arctic bathymetry aids scientists and mapmakers. *Eos, Trans. Amer. Geophys. Union*, *81*(9), 89, 2000.

[*Johnson and Marshall*, 2002] Johnson, H. L., and D. P. Marshall, Localization of abrupt change in the North Atlantic thermohaline circulation. *Geophys. Res. Lett.*, *29*, 7–1, 2002.

[*Jouanno et al.*, 2008] Jouanno, J., J. Sheinbaum, B. Barnier, J. Molines, L. Debreu, and F. Lemarié, The mesoscale variability in the Caribbean Sea. Part I: Simulations and characteristics with an embedded model. *Ocean Modelling*, *, doi:10.1016/j.ocemod.2008.04.002, 2008*.

[*Kalnay et al.*, 1996] Kalnay, E., M. Kanamitsu, R. Kistler, W. Collins, D. Deaven, L. Gandin, M. Iredell, S. Saha, G. White, J. Woollen, Y. Zhu, M. Chelliah, W. Ebiszusaki, W. Higgins, J.

Janowiak, K. Mo, C. Ropelewski, J. Whang, A. Leetmaa, R. Reynolds, R. Jenne, and D. Joseph, The NCEP/NCAR 40-years reanalysis project. *Bull. Amer. Meteor. Soc.*, *77*, 437–471, 1996.

[*Kantha and Clayson*, 2000] Kantha, L., and C. Clayson, *Numerical Models of Oceans and Oceanic Processes*. Academic Press, 2000.

[*Kanzow et al.*, 2007] Kanzow, T., S. Cunningham, D. Rayner, J. Hirschi, W. Johns, M. Baringer, H. Bryden, L. Beal, C. Meinen, and J. Marotzke, Observed Flow Compensation Associated with the MOC at 26.5 N in the Atlantic. *Science*, *317*(5840), 938, 2007.

[*Kanzow et al.*, 2006] Kanzow, T., U. Send, W. Zenk, A. Chave, and M. Rhein, Monitoring the integrated deep meridional flow in the tropical North Atlantic: Long-term performance of a geostrophic array. *Deep–Sea Res. I*, *53*(3), 528–546, 2006.

[*Käse et al.*, 2003] Käse, R. H., J. B. Girton, and T. B. Sanford, Structure and variability of the Denmark Strait Overflow: Model and Observations. *J. Geophys. Res.*, *108*, 3181, doi:10.1029/2002JC001548, 2003.

[*Keenlyside et al.*, 2008] Keenlyside, N., M. Latif, J. Jungclaus, L. Kornblueh, and E. Roeckner, Advancing decadal-scale climate prediction in the North Atlantic sector. *Nature*, *453*(7191), 84–8, 2008.

[*Killworth et al.*, 2000] Killworth, P., D. Smeed, and A. Nurser, The Effects on Ocean Models of Relaxation toward Observations at the Surface. *J. Phys. Oceanogr.*, *30*(1), 160–174, 2000.

[*Knorr and Lohmann*, 2003] Knorr, G., and G. Lohmann, Southern Ocean origin for the resumption of Atlantic thermohaline circulation during deglaciation. *Nature*, *424*(6948), 532–6, 2003.

[*Lachkar et al.*, 2007] Lachkar, Z., J. Orr, J. Dutay, and P. Delecluse, Effects of mesoscale eddies on global ocean distributions of CFC-11, CO 2, and Delta 14 C. *Ocean Sci.*, *3*(4), 461–482, 2007.

[*Large and Yeager*, 2007] Large, W. G., and S. Yeager, Global means and seasonal to decadal variability of air-sea fluxes. *J. Climate, submitted, 2007.*

[*Large and Yeager*, 2008] Large, W. G., and S. Yeager, The global climatology of an interannually varying air-sea flux data set. *Climate Dynamics, submitted, 2008.*

[*Large and Yeager*, 2004] Large, W. G., and S. G. Yeager, Diurnal to decadal global forcing for ocean and sea-ice models: the data sets and flux climatologies, *NCAR Technical Note NCAR/TN-460+STR*, NCAR, 2004.

[*Latif et al.*, 2007] Latif, M., C. Böning, J. Willebrand, A. Biastoch, F. Alvarez-Garcia, N. Keenlyside, and H. Pohlmann, Decadal to Multidecadal Variability of the Atlantic MOC: Mechanisms and Predictability. *GEOPHYSICAL MONOGRAPH-AMERICAN GEOPHYSICAL UNION*, *173*, 149, 2007.

[*Latif et al.*, 2006] Latif, M., C. Böning, J. Willebrand, A. Biastoch, J. Dengg, N. Keenlyside, G. Madec, and U. Schweckendiek, Is the thermohaline circulation changing? *J. Climate*, , *4631–4637, 2006.*

[*Le Sommer et al.*, 2008] Le Sommer, J., T. Penduff, S. Theetten, G. Madec, and B. Barnier, How momentum advection schemes influence current-topography interactions at eddy-permitting resolution. *Ocean Modelling*, *22*, in press, 2008.

[*Legg et al.*, 2006] Legg, S., R. Hallberg, and J. Girton, Comparison of entrainment in overflows simulated by z-coordinate, isopycnal and non-hydrostatic models. *Ocean Modelling*, *11*(1-2), 69–97, 2006.

[*Lübbecke et al.*, 2008] Lübbecke, J., C. Böning, and A. Biastoch, Variability in the subtropical-tropical cells and its effect on near-surface temperature of the equatorial Pacific: a model study. *Ocean Sci.*, *4*, 73–88, 2008.

[*Lutjeharms and van Ballegooyen*, 1988a] Lutjeharms, J., and R. van Ballegooyen, Anomalous Upstream Retroflection in the Agulhas Current. *Science*, *240*(4860), 1770–1770, 1988a.

[*Lutjeharms*, 1988] Lutjeharms, J. R. E., Remote sensing corroboration of retroflection of the East Madagascar Current. *Deep–Sea Res.*, *35*, 2045–2050, 1988.

[*Lutjeharms*, 2006] Lutjeharms, J. R. E., *The Agulhas Current*, 329 pp. Springer, 2006.

[*Lutjeharms and Ansorge*, 1997] Lutjeharms, J. R. E., and I. J. Ansorge, The Agulhas Return Current. *J. Mar. Syst.*, *30*, 115–138, 1997.

[*Lutjeharms et al.*, 1981] Lutjeharms, J. R. E., N. D. Bang, and C. P. Duncan, Characteristics of the currents east and south of Madagascar. *Deep–Sea Res.*, *28*, 879–899, 1981.

[*Lutjeharms and De Ruijter*, 1996] Lutjeharms, J. R. E., and W. P. M. De Ruijter, The influence of the Agulhas Current on the adjacent coastal ocean: possible impacts of climate change. *J. Mar. Systems*, *7*, 321–336, 1996.

[*Lutjeharms and Roberts*, 1988] Lutjeharms, J. R. E., and H. R. Roberts, The Natal Pulse: an treme transient on the Agulhas Current. *J. Geophys. Res.*, *93*, 631–645, 1988.

[*Lutjeharms and van Ballegooyen*, 1988b] Lutjeharms, J. R. E., and R. C. van Ballegooyen, The retroflection of the Agulhas Current. *J. Phys. Oceanogr.*, *18*, 1570–1583, 1988b.

[*Lutjeharms and Webb*, 1995] Lutjeharms, J. R. E., and D. J. Webb, Modelling the Agulhas Current system with FRAM (Fine Resolution Antarctic Model). *Deep–Sea Res.*, *42*, 523–551, 1995.

[*Madec*, 2006] Madec, G., NEMO ocean engine, *Tech. rep. 27*, Note du Pole de modelisation, Institut Pierre Simon Laplace (IPSL), France, 2006.

[*Madec et al.*, 1998] Madec, G., P. Delecluse, M. Imbard, and C. Levy, OPA 8 Ocean General Circulation Model-Reference Manual, *Tech. rep.*, LODYC/IPSL Note 11, 1998.

[*Madec et al.*, 1999] Madec, G., P. Delecluse, M. Imbard, and C. Levy, OPA 8.1 Ocean General Circulation Model Reference Manual, *Tech. rep.*, Institut Pierre Simon Laplace des Sciences de l'Environment Global, 1999.

[*Madec and Imbard*, 1996] Madec, G., and M. Imbard, A global ocean mesh to overcome the North Pole singularity. *Climate Dynamics*, *12*, 381–388, 1996.

[*Maltrud and McClean*, 2005] Maltrud, M. E., and J. McClean, An eddy resolving global 1/10 deg ocean simulation. *Ocean Modelling*, *8*, 31–54, 2005.

[*Marsh et al.*, 2007] Marsh, R., W. Hazeleger, A. Yool, and E. Rohling, Stability of the Thermohaline Circulation under millennial CO2 forcing and two alternative controls on Atlantic salinity. *Geophys. Res. Lett.*, *34*(3), 2007.

[*Martnez-Méndez et al.*, 2007] Martnez-Méndez, G., R. Zahn, I. Hall, L. Pena, and I. Cacho, 345,000-year-long multi-proxy records off South Africa document variable contributions of Northern versus Southern Component Water to the Deep South Atlantic. *Earth and Planetary Science Letters*, , *2007*.

[*Matano and Beier*, 2003] Matano, R., and E. Beier, A kinematic analysis of the Indian/Atlantic interocean change. *Deep–Sea Res. II*, *50*(1), 229–249, 2003.

[*Matano et al.*, 2008] Matano, R., E. Beier, and P. Strub, The seasonal variability of the circulation in the South Indian Ocean: Model and observations. *J. Mar. Res.*, , *doi:10.1016/j.jmarsys.2008.01.007, 2008*.

[*Matano*, 1996] Matano, R. P., A Numerical Study of the Agulhas Retroflection: The Role of Bottom Topography. *J. Phys. Oceanogr.*, *26*, 2267–2279, 1996.

[*Matano et al.*, 2002] Matano, R. P., E. J. Beier, and P. T. Strub, Large-scale Forcing of the Agulhas Variability: The Seasonal Cycle. *J. Phys. Oceanogr.*, *32*, 1228–1241, 2002.

[*Mathiot*, 2005] Mathiot, P., Interactions ocean glace de mer en Antarctique, Ph.D. thesis, Rapport de Master 2 STUE de la Universite Joseph Fourier de Grenoble. realise au LEGI et au LGGE, Grenoble, 2005.

[*Matsumoto et al.*, 2004] Matsumoto, K., H. Sasaki, T. Kagimoto, N. Komoro, A. Ishida, Y. Sasai, T. Miyama, T. Motoi, H. Mitsudera, K. Takahashi, H. Sakuma, and T. Yamagata, A fifty-year eddy-resolving simulation of the world ocean: preliminary outcomes of OFES (OGCM for the Earth Simulator). *J. Earth Simulator*, *1*, 35–56, 2004.

[*Meehl et al.*, 2007] Meehl, G., T. Stocker, W. Collins, P. Friedlingstein, A. Gaye, J. Gregory, A. Kitoh, R. Knutti, J. Murphy, A. Noda, S. Raper, I. Watterson, A. Weaver, and Z.-C. Zhao, Global Climate Projections, pp. 747–846, Cambridge University Press, Cambridge, United Kingdom and New York, NY, USA, 2007.

[*Meijers et al.*, 2007] Meijers, A., N. Bindoff, and J. Roberts, On the total, mean, and eddy heat and freshwater transports in the southern hemisphere of a 1/8Â° x 1/8 Â° global ocean model. *J. Phys. Oceanogr.*, *37*(2), 277–295, 2007.

[*Nauw et al.*, 2008] Nauw, J., H. van Aken, J. Lutjeharms, W. de Ruijter, and A. Webb, Observations in the southern East Madagascar Current and undercurrent system. *J. Geophys. Res., in press, 2008.*

[*New et al.*, 2007] New, A., S. Alderson, D. Smeed, and K. Stansfield, On the circulation of water masses across the Mascarene Plateau in the South Indian Ocean. *Deep–Sea Res. I*, *54*(1), 42–74, 2007.

[*Olson and Evans*, 1986] Olson, D. B., and R. H. Evans, Rings of the Agulhas Current. *Deep–Sea Res.*, *33*, 27–42, 1986.

[*Palastanga et al.*, 2007] Palastanga, V., P. van Leeuwen, M. Schouten, and W. De Ruijter, Flow structure and variability in the subtropical Indian Ocean: Instability of the South Indian Ocean Countercurrent. *J. Geophys. Res.*, *112*, doi:10.1029/2005JC003395, 2007.

[*Peeters et al.*, 2004] Peeters, F. J. C., R. Acheson, G.-J. A. Brummer, W. P. M. de Ruijter, G. G. Ganssen, R. R. Schneider, E. Ufkes, and D. Kroon, Vigorous change between Indian and Atlantic Ocean at the end of the last five glacial periods. *Nature*, *400*, 661–665, 2004.

[*Penduff et al.*, 2002] Penduff, T., B. Barnier, M. Kerbiriou, and J. Verron, How Topographic Smoothing Contributes to Differences between the Eddy Flows Simulated by Sigma-and Geopotential-Coordinate Models. *J. Phys. Oceanogr.*, *32*(1), 122–137, 2002.

[*Penven et al.*, 2006] Penven, P., J. Lutjeharms, and P. Florenchie, Madagascar: A pacemaker for the Agulhas Current system? *Geophys. Res. Lett.*, *33*, 2006.

[*Penven et al.*, 2001] Penven, P., J. R. E. Lutjeharms, P. Marchesiello, C. Roy, and S. J. Weeks, Generation of cyclonic eddies by the Agulhas Current in the lee of the Agulhas Bank. *Geophys. Res. Lett.*, *27*, 1055–1058, 2001.

[*Quartly et al.*, 2006] Quartly, G., J. Buck, M. Srokosz, and A. Coward, Eddies around Madagascar: The retroflection re-considered. *J. Mar. Res.*, *63*(3-4), 115–129, 2006.

[*Rau et al.*, 2002] Rau, A., J. Rogers, J. Lutjeharms, J. Giraudeau, J. Lee-Thorp, M. Chen, and C. Waelbroeck, A 450-kyr record of hydrological conditions on the western Agulhas Bank Slope, south of Africa. *Marine Geology*, *180*(1), 183–201, 2002.

[*Reason et al.*, 2003] Reason, C., J. Lutjeharms, J. Hermes, A. Biastoch, and R. Roman, Inter-ocean fluxes south of Africa in an eddy-permitting model. *Deep–Sea Res. II*, *50*(1), 281–298, 2003.

[*Richardson*, 2007] Richardson, P., Agulhas leakage into the Atlantic estimated with subsurface floats and surface drifters. *Deep–Sea Res. I*, *54*(8), 1361–1389, 2007.

[*Rio et al.*, 2005] Rio, M. H., P. Schaeffer, F. Hernandez, and J.-M. Lemoine, The estimation of the ocean Mean Dynamic Topography through the combination of altimetric data, in-situ measurements and GRACE geoid: From global to regional studies. in *Proceedings of the GOCINA international workshop*, p. 6 pp., Luxembourg, 2005.

[*Roullet and Madec*, 2000] Roullet, G., and G. Madec, Salt conservation, free surface, and varying levels: A new formulation for ocean general circulation models. *J. Geophys. Res.*, *105*(C10), 23927–23942, 2000.

[*Russell et al.*, 2006] Russell, J., R. Stouffer, and K. Dixon, Intercomparison of the Southern Ocean Circulations in IPCC Coupled Model Control Simulations. *Journal of Climate*, *19*(18), 4560–4575, 2006.

[*Saji et al.*, 1999] Saji, N., B. Goswami, P. Vinayachandran, and T. Yamagata, A dipole mode in the tropical Indian Ocean. *Nature*, *401*(6751), 360–3, 1999.

[*Scheinert*, 2008] Scheinert, M., Causes and Impacts of Northern North Atlantic Freshening, Ph.D. thesis, Leibniz-Institut für Meereswissenschaften an der Universität Kiel, 2008.

[*Schouten et al.*, 2002] Schouten, M., W. de Ruijter, and P. van Leeuwen, Upstream control of Agulhas Ring shedding. *J. Geophys. Res.*, *107*(10.1029), 2002.

[*Schouten et al.*, 2000] Schouten, M. W., W. P. M. de Ruijter, P. J. van Leeuwen, and J. R. E. Lutjeharms, Translation, decay and splitting of Agulhas rings in the south-eastern Atlantic Ocean. *J. Geophys. Res.*, *105*, 21,913–21.925, 2000.

[*Schouten et al.*, 2003] Schouten, M. W., W. P. M. de Ruijter, P. J. van Leeuwen, and H. Ridderinkhof, Eddies and variability in the Mozambique Channel. *Deep–Sea Res. II*, *50*, 1987–2004, 2003.

[*Siedler et al.*, 2008] Siedler, G., M. Rouault, A. Biastoch, B. Backeberg, C. Reason, and J. Lutjeharms, Modes of the southern tension of the East Madagascar Current. *J. Geophys. Res.*, *submitted, 2008.*

[*Siedler et al.*, 2006] Siedler, G., M. Rouault, and J. Lutjeharms, Structure and origin of the subtropical South Indian Ocean Countercurrent. *Geophys. Res. Lett.*, *33*, doi:10.1029/2006GL027399, 2006.

[*Smith and Sandwell*, 1997] Smith, W., and D. Sandwell, Global Sea Floor Topography from Satellite Altimetry and Ship Depth Soundings. *Science*, *277*(5334), 1956, 1997.

[*Speich et al.*, 2002] Speich, S., B. Blanke, P. de Vries, S. Drijfhout, K. Doos, A. Ganachaud, and R. Marsh, Tasman leakage- A new route in the global ocean conveyor belt. *Geophys. Res. Lett.*, *29*(10), 55–1, 2002.

[*Speich et al.*, 2001] Speich, S., B. Blanke, and G. Madec, Warm and cold water routes of an OGCM thermohaline conveyor belt. *Geophys. Res. Lett.*, *28*(2), 311–314, 2001.

[*Speich et al.*, 2006] Speich, S., J. Lutjeharms, P. Penven, and B. Blanke, Role of bathymetry in Agulhas Current configuration and behaviour. *Geophys. Res. Lett.*, *33*, 2006.

[*Steele et al.*, 2001] Steele, M., R. Morfley, and W. Ermold, PHC: A global ocean hydrography with a high-quality Arctic Ocean. *J. Climate*, *14*, 2079–2087, 2001.

[*Stevens*, 1990] Stevens, D. P., On open boundary conditions for three dimensional primitive equation ocean circulation models. *Geophys. Astrophys. Fluid Dyn.*, *51*, 103–133, 1990.

[*Stocker et al.*, 2001] Stocker, T. F., G. K. C. Clarke, H. Le Treut, R. S. Lindzen, V. P. Meleshko, R. K. Mugura, T. N. Palmer, R. T. Pierrehumbert, P. J. Sellers, K. E. Trenberth, and J. Willebrand, Physical Climate Processes and Feedbacks, in *Climate Change 2001: The Scientific Basis. Contribution of Working Group I to the Third Assessment Report of the Intergovernmental Panel on Climate Change*, edited by J. T. Houghton, Y. Ding, D. J. Griggs, M. Noguer, P. J. van der Linden, X. Dai, K. Maskell and C. A. Johnson, Cambridge University Press, 2001.

[*The DRAKKAR Group*, 2007] The DRAKKAR Group, Eddy-Permitting Ocean Circulation Hindcasts of Past Decades. *Clivar Exchanges*, *12*, 8–10, 2007.

[*Tréguier*, 1992] Tréguier, A., Kinetic energy analysis of an eddy resolving, primitive equation North Atlantic model. *J. Geophys. Res.*, *97*, 687–701, 1992.

[*Treguier et al.*, 2003] Treguier, A., O. Boebel, B. Barnier, and G. Madec, Agulhas eddy fluxes in a 1/6Â° Atlantic model. *Deep–Sea Res. II*, *50*(1), 251–280, 2003.

[*van Aken et al.*, 2003] van Aken, H., A. van Velthoven, C. Veth, W. de Ruijter, P. van Leeuwen, S. Drijfhout, C. Whittle, and M. Rouault, Observations of a young Agulhasring, Astrid, during MARE in March 2000. *Deep–Sea Res. II*, *50*, 167–195, 2003.

[*van Leeuwen and Lutjeharms*, 2000] van Leeuwen, P. J. de Ruijter, W. P. M., and J. R. E. Lutjeharms, Natal pulses and the formation of Agulhas rings. *J. Geophys. Res.*, *105*, 6425–6436, 2000.

[*van Sebille et al.*, 2008] van Sebille, E., C. Barron, A. Biastoch, P. van Leeuwen, C. Vossepoel, and W. de Ruijter, An Ind for the inter-annual variability in Agulhas leakage. *J. Geophys. Res., submitted, 2008.*

[*van Sebille and van Leeuwen*, 2007] van Sebille, E., and P. van Leeuwen, Fast Northward Energy Transfer in the Atlantic due to Agulhas Rings. *J. Phys. Oceanogr.*, *37*(9), 2305–2315, 2007.

[*Webb et al.*, 1998] Webb, D., B. de Cuevas, and C. Richmond, Improved Advection Schemes for Ocean Models. *Journal of Atmospheric and Oceanic Technology*, *15*(5), 1171–1187, 1998.

[*Weijer et al.*, 1999] Weijer, W., W. P. M. de Ruijter, H. A. Dijkstra, and P. J. Van Leeuwen, Impact of Interbasin change on the Atlantic Overturning Circulation. *J. Phys. Oceanogr.*, *29*, 2266–2284, 1999.

[*Witter and Gordon*, 1999] Witter, D., and A. Gordon, Interannual variability of South Atlantic circulation from 4 years of TOP/POSEIDON satellite altimeter observations. *J. Geophys. Res.*, *104*, 20, 1999.

[*Wunsch*, 2008] Wunsch, C., Mass and volume transport variability in an eddy-filled ocean. *Nature Geoscience*, *1*(3), 165, 2008.

[*Zalesak*, 1979] Zalesak, S. T., Fully multidimensional flux corrected transport algorithms for fluids. *J. Comput. Phys.*, *31*, 1979.